Université de Montréal

Toxicité, transfert et gestion subcellulaire de l'yttrium (Y) chez trois organismes d'eau douce

par Pierre-Yves Cardon

Département de sciences biologiques
Faculté des arts et des sciences

Thèse présentée
en vue de l'obtention du grade de Philosophiae Doctor (Ph. D)
en sciences biologiques

Novembre 2018

Résumé

Les métaux inclus dans le groupe des éléments de Terres Rares (ETR), ressource essentielle à l'électrification des transports et à la production d'énergie éolienne, entre autres, pourraient être exploités au Canada dans un futur proche. Cette exploitation minière, associée à leur utilisation industrielle croissante, serait susceptible d'entraîner une contamination en ETR des milieux aquatiques dulcicoles. Il convient donc d'évaluer le danger associé à ces métaux pour ces écosystèmes. L'yttrium (Y) est parmi les quatre ETR les plus abondants, le seul faisant parti du groupe dit des ETR lourds. Il est aussi celui dont la toxicité a le moins fait l'objet d'études à ce jour. Pourtant, de premières études suggèrent des écarts de toxicité significatifs entre les ETR lourds et les ETR légers. Cette thèse vise par conséquent à évaluer en laboratoire la toxicité et le transfert trophique de l'Y en relation avec son fractionnement subcellulaire chez trois organismes dulcicoles : *Daphnia magna*, *Chironomus riparius* et *Oncorhynchus mykiss*.

L'étude de la distribution intracellulaire des métaux ouvre des voies prometteuses en écotoxicologie. Cependant, suivant l'organisme considéré et la méthode d'homogénéisation utilisée, le protocole de fractionnement peut conduire à une séparation erronée des différentes composantes subcellulaires. Le premier volet de cette thèse vise de ce fait à optimiser, à l'aide d'essais enzymatiques, le protocole de fractionnement pour nos trois organismes. Quel que soit le protocole appliqué, des écarts importants ont été observés entre les fractions véritablement séparées et validées durant nos essais et celles prédites dans la littérature en absence de vérification. Ce volet de la thèse se conclut sur l'établissement de protocole de fractionnement adaptée à chacun de nos organismes et sur la recommandation de préférer l'utilisation de fraction validées aux fractions prédites dans toutes études de fractionnement subcellulaire des métaux.

La toxicité chronique de l'Y est évaluée dans le deuxième volet de la thèse à travers des bioessais exposant nos trois organismes à des concentrations sub-létales en Y. Seule l'espèce benthique, *C. riparius*, a présenté des signes de toxicité pour des concentrations d'exposition proches de celles relevées en milieu naturel. Par ailleurs, différentes stratégies de régulation subcellulaire de l'Y ont été mises en évidence entre chaque organisme. *D. magna*

par exemple, en accumulant très majoritairement l'Y dans ses fractions détoxiquées, était capable de bioaccumuler des quantités d'Y par masse de tissu jusqu'à cent fois plus élevées que les deux autres organismes.

Le troisième volet de la thèse examine le potentiel de transfert trophique de l'Y. Des expériences d'exposition de *O. mykiss* soit à des daphnies soit à une eau préalablement enrichie en Y ont ainsi été réalisées et comparées. Comme prédit à la vue du fractionnement subcellulaire de cet élément chez *D. magna,* le transfert trophique de l'Y s'est avéré très faible durant nos essais. Au niveau des tissus, ce métal se distribuait dans l'ordre suivant chez *O. mykiss* : intestin > branchies > foie > muscle. Toutefois, à l'inverse des autres organes, aucun phénomène de dépuration n'était mesuré dans le foie. Le volet conclut sur l'importance de cet organe dans l'étude de la toxicité des ETR.

Cette thèse contribue à perfectionner la méthode de fractionnement subcellulaire des métaux et les interprétations qui lui sont liées. Elle confirme l'intérêt de ce type d'analyse dans la compréhension des mécanismes liés à la toxicité et au transfert des métaux. Enfin, à travers l'estimation de seuils de toxicité pour l'Y et de son potentiel de transfert trophique, cette thèse contribue à l'évaluation du risque induit par l'Y sur les écosystèmes dulcicoles.

Mots-clefs : Terres Rares, Yttrium, Écotoxicologie, Bioessais, Transfert trophique, Fractionnement subcellulaire, *Daphnia magna*, *Chironomus riparius*, *Oncorhynchus mykiss.*

Abstract

Metals included in the Rare Earth Elements (REE) group, a key resource in green energy technologies, may soon be exploited in Canada. This, combined with their increasing industrial use, could lead to contamination of freshwater ecosystems by these metals. REE risk assessment is therefore of emerging concern. Yttrium (Y) is the only heavy REE amongst the four most abundant REE. It is also the one that has been the subject of the least toxicity studies even though previous studies have shown a higher toxicity for heavy REE than for light REE. Hence, this thesis aims to evaluate in the laboratory the toxicity and trophic transfer of Y, in relation to its subcellular fractionation, in three freshwater organisms: *Daphnia magna*, *Chironomus riparius* and *Oncorhynchus mykiss*.

Analysis of metal subcellular distribution provides promising insights in ecotoxicology. Nonetheless, depending on the organism and the homogenisation step chosen, the fractionation protocol may lead to an erroneous separation of the different subcellular components. Thus, the first part of this thesis optimizes the fractionation protocol for our three organisms. Regardless of the protocol used, we observed significant gaps between predicted fractions in literature and fractions validated in our trials. This section concludes with the establishment of fractionation protocols adapted to each of our organisms and the recommendation to use validated fractions instead of predicted ones in future subcellular fractionation studies.

The chronic sublethal toxicity of Y was assessed in the second part of this thesis through bioassays on our three organisms. *C. riparius*, the benthic species, was the only one presenting adverse effects at exposure levels close to those already reported in natural ecosystems. In addition, we observed different subcellular Y management strategies for each organism. For instance, *D. magna*, by accumulating Y mainly in its detoxified fractions, was able to bioaccumulate up to 100 times more Y than the other two organisms.

The last part of this thesis investigates the trophic transfer potential of Y. Experiments consisting in the exposure of trouts either to Y-spiked daphnids or Y-spiked water were performed. As predicted from Y subcellular partitioning in *D. magna*, Y trophic transfer was low in our trials. Inside *O. mykiss*, Y was distributed following this order:

guts > gills > liver > muscle. However, unlike other organs, the liver was the only one for which no Y-depuration was measured. We concluded on the importance of the liver in REE toxicity analysis.

This thesis contributes to optimize metal subcellular fractionation method and data produced by this approach. It shows the importance of understanding the mechanisms behind metal toxicity and its transfer in the food chain. Finally, by measuring Y toxicity thresholds and Y trophic transfer potential, this thesis contributes to the risk assessment of Y on freshwater ecosystems.

Keywords: Rare earth, Yttrium, Ecotoxicology, Bioassays, Trophic transfer, Subcellular fractionation, *Daphnia magna*, *Chironomus riparius*, *Oncorhynchus mykiss*

Table des matières

Liste des tableaux

INTRODUCTION

CHAPITRE 1

CHAPITRE 2

CHAPITRE 3

Liste des figures

INTRODUCTION

CHAPITRE 1

CHAPITRE 2

Liste des abréviations

Les caractères en italique indiquent les termes en anglais

APHO : Acid Phosphatase

$CaCO_3$: Carbonate de calcium

***CCO** : Cytochrome C Oxidase*

Ce : Cerium

CE_{50} : Concentration Efficace mediane

CL_{50} : Concentration Létales médiane

CE_{10} : Concentration Efficace sur 10% de la population

CMAT : Concentration Maximale Acceptable de Toxique

CMEO/*LOEC* : Concentration Minimale produisant un effet observé/*Lowest Observable Effect Concentration*

***CS** : Citrate Synthase*

CSEO/*NOEC* : Concentration Sans Effet Observé/*No Observable Effect Concentration*

CVAC : Critère pour la Vie Aquatique Chronique

Dy : Dysprosium

dw : dried weight

e.g. : exempli gracia

ETR/*REE* : Élément de Terre rare/*Rare Earth Element*

***FCC** : Fluid Catalytic Cracking*

Gd : Gadolinum

***HDP** : Heat Denaturated Proteins*

***HSP** : Heat Stable Proteins*

***ICP-MS** : Inductively Coupled Plasma -Mass Spectrometry*

i.e. : Id est

La : Lanthane

***LDH** : Lactate Dehydrogenase*

Ln : Lanthanide

Lu : Lutétium

***MDF** : Metal Detoxified Fractions*

***MPC** : Maximum Permissible Concentration*

***MRG** : Metal-Rich Granule*

***MSF** : Metal Sensitive Fractions*

Mt : Millions de tonnes

MT : Métallothionéine

Nd : Neodyme

***PNEC** : Predicted No Effect Concentration*

Pr : Praseodyme

***TAM** : Trophically Available Metal*

***ww** : wet weight*

Y : Yttrium

Remerciements

Ce projet de thèse n'aurait pas pu voir le jour sans la collaboration entre trois organismes, l'université de Montréal, le CEAEQ de Québec et l'INRS-ETE. Je tiens tout d'abord à remercier ces trois institutions de m'avoir accueilli et de m'avoir fourni tout au long de ces années le soutien nécessaire à la réalisation de ce projet.

Merci à Marc Amyot mon directeur, de m'avoir accueilli dans son équipe et de m'avoir donné l'opportunité de réaliser cette thèse. Merci pour ses conseils, pour m'avoir toujours apporté l'aide nécessaire, pour avoir su trouver les bons collaborateurs pour mon projet, et pour s'être toujours montré disponible quand j'en avais besoin. Merci à toute l'équipe du laboratoire Amyot de m'avoir accueilli et pour mes 6 premiers mois passés à Montréal.

Au sein du CEAEQ, je souhaiterais dire un grand merci à toute l'équipe de la division de l'écotoxicologie et de l'évaluation du risque pour leurs encouragements et leurs conseils. Merci à Louis Martel de m'avoir accueilli dans son équipe. Merci à Gaëlle pour sa bienveillance et pour sa disponibilité à chacune de mes questions. Merci à Nathalie pour notre collaboration dans le CA et le CO du Chapitre Saint-Laurent. Merci à Mélanie pour son aide précieuse en statistique. Merci aussi à toute l'équipe de la division biologie et microbiologie pour m'avoir formé sur les bioessais, pour m'avoir apporté leur aide dans leur mise en place et pour leur patience face à mon incapacité à me souvenir de la localisation de l'ensemble du matériel. En espérant n'oublier personne, merci à Cathy, Daniel, Étienne, Karine, Lorraine, Nancy, Nicole, Nicole et Sophie. Un merci tout particulier à leur chef, Nicolas pour son soutien indéfectible, pour son écoute dans mes moments de doute et pour nous avoir cédé son appartement à Sarah et à moi. Enfin merci à l'équipe de la division des contaminants inorganiques. Un merci tout particulier à Julie et à Steeve, pour les analyses en terres rares et pour leur aide.

À l'INRS ETE j'aimerais en premier lieu remercier mon co-directeur Claude Fortin de m'avoir intégré dans son équipe. Merci pour tous ses conseils et pour la clarté de ses explications. Je remercie aussi tous ses étudiants du bureau 5328 pour leur amitié.

Je souhaiterais associer à ces remerciements Antoine Caron et Maikel Rosabal pour m'avoir initié au fractionnement subcellulaire et aux essais enzymatiques. Merci à eux pour être resté jusqu'au bout dans ce projet et pour m'avoir apporté leur aide et conseil tout au long

de ces années. Aussi, un grand merci à Antoine pour son investissement dans l'optimisation du protocole de fractionnement.

Merci à l'ensemble des stagiaires qui ont apporté leur aide à ce projet : Diane, Tiphaine, Xavier, et Olivier (dans l'ordre d'apparition), merci !

Merci au CRSNG et au réseau mine de savoir pour leur support financier.

Enfin merci à Sarah sans qui je n'aurais jamais pu achever mon doctorat. Merci pour ta patience face à mon humeur lugubre après une énième expérience ratée, ta compréhension lorsque je n'arrivais plus à me sortir la tête de la thèse, tes encouragements quand j'avais envie d'abandonner, ton sens de l'humour sans égal, ton amour malgré ma maladresse, ton soutien dans tous mes projets mêmes les plus idiots, ta tendresse de tous les jours, ton tajine de kefta, et encore beaucoup de choses.

Avant-propos

Le marché des éléments de terres rares (ETR) est en plein essor. Leur nécessité dans les nouvelles technologies comme les énergies vertes en font des métaux de premier plan. Conséquence directe, de premiers cas de milieux aquatiques contaminés en ETR d'origine anthropique commencent à être reportés. Pour autant, nos connaissances du risque induit par ces métaux sur ces écosystèmes restent limitées. Cette thèse vise à répondre à cette problématique en améliorant notre compréhension du potentiel de toxicité et de transfert d'un ETR, l'Y, à la vue de sa distribution subcellulaire chez les organismes. Au travers de ce projet, l'intérêt, les limites et les perspectives d'amélioration de l'analyse du fractionnement subcellulaire des métaux sont discutés.

Introduction

Les éléments de terres rares (ETR)

Les terres rares ou Éléments de Terres Rares (ETR) sont un ensemble de métaux comprenant les éléments du groupe des lanthanides, le scandium (Sc) et l'yttrium (Y). À contresens de ce que leur nom semble indiquer, les ETR sont plutôt abondants dans la croûte terrestre. Ainsi, l'Y et le cérium (Ce) sont présents en moyenne à 33 et 66 ppm respectivement, ce qui est supérieur aux concentrations en cuivre (Cu), 60 ppm, et en cobalt (Co), 25 ppm (Hedrick, 1995; Lide, 2003). En vérité, la prétendue rareté des ETR trouve son explication dans leur forte dispersion. En effet, seuls trois minéraux parmi 200 répertoriés comme contenant des ETR (Gupta et Krishnamurthy, 2005) présentent des concentrations suffisantes en ces métaux pour rendre leur exploitation rentable. Les principales sources pour ces métaux sont les minéraux de bastnaesite, un minéral fluorocarbonatée ($Ln(CO_3)F$) contenant principalement des ETR légers associés à la carbonatite, les minéraux de monazite, et ceux de xenotime, deux minéraux contenant du phosphate. Tous les ETR existent naturellement sous forme stable à l'exception du prométhium qui est un élément radioactif synthétique (Greenwood et Earnshaw, 1997; Jordens et al., 2013).

Les terres rares forment un groupe très homogène dans ses propriétés physico-chimiques. Cette analogie serait due à la particularité des ETR qui, contrairement aux autres éléments du tableau périodique, montre une diminution de leur rayon ionique plus leur numéro atomique est élevé. Ce phénomène appelé "contraction lanthanidique" (Gupta et Krishnamurti, 2005), rend ces derniers très proches les uns des autres dans leurs propriétés physico-chimiques, mais surtout explique qu'ils soient interchangeables dans la plupart des minéraux et qu'il demeure en conséquence très difficile de les séparer (Gupta et Krishnamurti, 2005).

Tableau I. Classification des ETR

Lanthane	La	ETR légers Groupe du Lanthane	ETR légers réduits
Cerium	Ce		
Praseodyme	Pr		
Neodyme	Nd		
Promethium	Pm		
Samarium	Sm		
Europium	Eu		ETR du milieu
Gadolinium	Gd	ETR Lourds Groupe de l'Yttrium	
Terbium	Tb		
Dysprosium	Dy		
Holmium	Ho		ETR lourds réduits
Erbium	Er		
Thulium	Tm		
Ytterbium	Yb		
Lutetium	Lu		
Yttrium	Y		
Scandium	Sc		

Les ETR sont généralement classés en deux groupes (Tableau I):

- Le groupe du cérium appelé aussi groupe des ETR légers qui comprend les lanthanides du lanthane à l'europium dans le tableau périodique.
- Le groupe de l'yttrium nommé aussi groupe des ETR lourds qui comprend les lanthanides du gadolinium à l'ytterbium ainsi que l'yttrium.

En plus de ces deux premiers groupes, certains auteurs différencient aussi le groupe des ETR du milieu de cette série (Ferrat et al., 2011) qui comprend l'Eu, le Gd, le Tb, et le Dy. Le scandium fait partie des ETR lourds mais est régulièrement mis à l'écart des autres ETR dans les publications.

Applications et demande mondiale en ETR

Les propriétés optiques et magnétiques des ETR en font une ressource de premier plan dans le domaine des nouvelles technologies. Ainsi ils entrent dans la composition d'aimant permanent à haute énergie (Dent, 2012), de phosphate constituant les écrans haute définition (Humphries, 2013), d'agent d'alliage pour certains métaux (Paulick et Machacek, 2017), et trouvent de nombreuses applications dans le secteur de

l'électrification et des énergies vertes (turbine des éoliennes, voitures hybrides, ampoules basse consommation, etc.).

D'autres usages, moins connus, ayant un impact direct sur les organismes et les écosystèmes leurs sont aussi attribués :

- Depuis les années 1970, des engrais à base d'ETR sont vendus en Chine (Hu et al., 2004). L'étendue des surfaces agricoles amendées à l'aide de ces métaux dépasse aujourd'hui les 10 millions d'hectares.
- Dans l'élevage, les terres rares sont utilisées en tant que complément alimentaire (He et al., 2001; He et al., 2010; Redling, 2006) ou encore comme une alternative aux antibiotiques (Thacker, 2013).
- En médecine le Gd est utilisé en imagerie médicale (Xie et al., 2014) et l'ingestion de carbonate de La peut être prescrite comme traitement dans les cas d'hyperphosphatémie chez les patients de maladies de reins chroniques (Martin et al., 2011).
- Sous forme de benthonite, le La est utilisé pour faire précipiter le phosphore des lacs et possiblement limiter ainsi le phénomène d'eutrophisation (Lürling et Tolman, 2010).

Les réserves mondiales en ETR sont actuellement estimées à 165 millions de tonnes réparties entre 30 pays (Paulick et Machacek, 2017). La Chine fournit toutefois encore plus de 85 % de la demande mondiale en ETR et garde le quasi-monopole pour cette ressource (Paulick et Machacek, 2017). Néanmoins, après avoir atteint un maximum autour de 70 000 tonnes d'ETR en 2005 (Morrison et Tang, 2012), la Chine a depuis décidé de restreindre ses exportations ne leur accordant plus, en moyenne, que 30 000 tonnes depuis 2008. Pourtant la demande mondiale pour ces métaux n'a cessé de s'accroître ces dernières années. Alonso et al. (2012) estiment d'ailleurs que certains d'entre eux pourraient voir leur demande augmenter jusqu'à 2600% d'ici 2035. Cette situation a conduit au lancement de nombreux projets d'exploration et d'exploitation de gisement d'ETR à travers le monde comme au Canada. Ainsi entre 2010 entre 2015, suite au lancement d'importantes campagnes d'exploration, les ressources connues en oxide d'ETR dans ce pays sont passés de 4 à 38 Mt (Paulick et Machacek, 2017). Par ailleurs,

plusieurs projets localisés au Québec, sont en cours de développement et pourraient être finalisés dans les prochaines années (Figure 1).

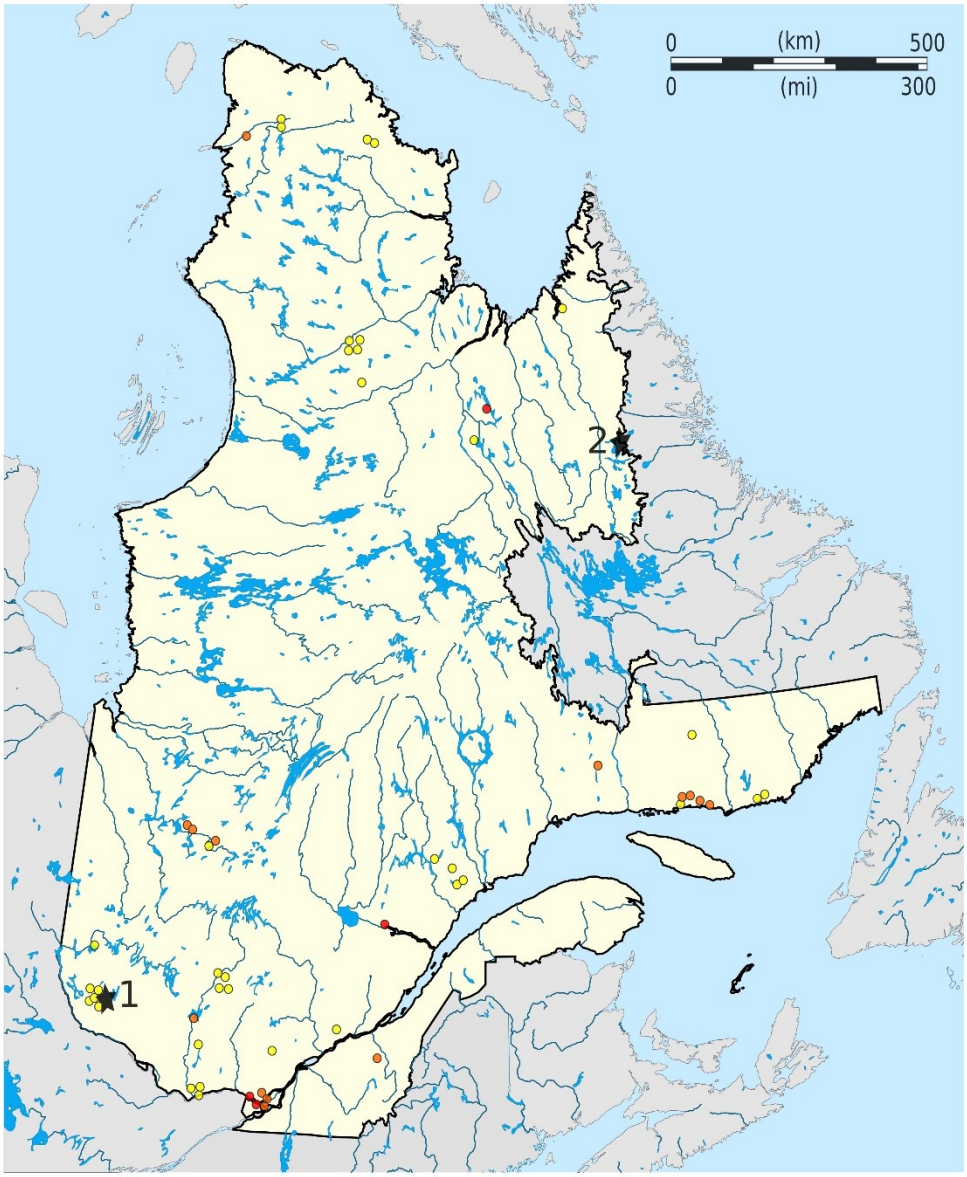

Figure 1. Carte des projets miniers, gîtes et indices d'ETR au Québec (AEMQ, 2016)*

***https://mern.gouv.qc.ca/mines/industrie/metaux/metaux-exploration-terres-rares.jsp**

Les ETR dans l'environnement

Les ETR forment tous un cation trivalent fréquemment noté Ln^{3+}. Néanmoins, le Ce peut apparaître sous la forme Ln^{4+} et l'Eu sous forme divalente Ln^{2+} (Aide et Aide, 2012). Ils appartiennent tous aux métaux du groupe A, dits des accepteurs "durs" ou chercheurs d'oxygène. Ainsi, les ETR présentent une forte affinité pour les ligands contenant de l'oxygène, en particulier les phosphates et les carbonates avec qui ils forment des complexes stables. Cependant, leur affinité pour les sulfates reste plus limitée (Nieboer and Richardson, 1980), la complexation des ETR avec ces ligands n'étant significative que pour des pH très faibles, pH<4 (Tang et Johannesson, 2003)

Les carbonates d'ETR et les complexes formés entre la matière organique et ces métaux sont les espèces dominantes des ETR en solution (Sneller et al., 2000). Ces derniers présentent aussi une forte affinité pour les argiles (Babula et al., 2008). Enfin, la solubilité des ETR est très faible. À titre d'exemple, les constantes de solubilité des formes d'ETR-phosphate s'échelonnent autour de 10^{-25} mol L^{-1} (Liu et Byrne, 1997). Cette faible solubilité des ETR explique que ces derniers se retrouvent principalement retenus dans les sédiments (Sneller et al., 2000). Ainsi, Weltje (2002) observe que 99% des ETR présents dans les milieux aquatiques sont soit liés à la matière en suspension soit aux sédiments. Les concentrations dissoutes en ETR dans ces environnements sont donc souvent très faibles, s'échelonnant par exemple de 2,9 à 714 ng L^{-1} pour le Ce et de 0,04 à 7 ng L^{-1} pour le Lu (Ng and Smith, 2011). En laboratoire, El-Akl et al. (2015) observaient que seulement 30% du métal restait sous forme véritablement dissoute à pH 7. Celui-ci était majoritairement présent sous formes de colloïdes et ce en présence ou en absence de matière organique naturelle (MON).

Risques liés aux ETR dans l'environnement

Contamination en ETR d'origine anthropique

Les nombreux usages des ETR, leur faible recyclage ainsi que l'activité minière qui leur est liée entrainent que de premiers cas de contamination en ETR d'origine anthropique d'écosystèmes aquatiques ont été rapportés (Gwenzi et al., 2018).

Le Rhin, un fleuve qui traverse la Suisse, l'Autriche, la France, l'Allemagne, les Pays-Bas, la Belgique, le Luxembourg et le Liechtenstein, voit par exemple ses concentrations en Gd augmenter de façon importante depuis 2001 (Sneller et al., 2000; Kulaksız et Bau, 2011). Parallèlement, entre 1993 et 2013 les concentrations en Gd dans la baie de San Francisco ont été multipliées par dix (Hatje et al., 2016), en lien avec l'utilisation importante de cet ETR en imagerie de résonance magnétique dans les hôpitaux et son rejet par leurs effluents. De plus, les concentrations en La dissous dans l'eau du Rhin sont deux fois plus importantes que les concentrations liées au contexte géologique de la zone considérée (Kulaksız et Bau, 2011). Une des sources majeures de cette contamination serait l'usine de production de catalyseur pour craquage catalytique en lit fluidisée (en anglais FCC: Fluid Calalytic Cracking) (Merschel et Bau, 2015). En Chine au niveau de la rivière Jaune dans la région de Bayan Obo, où se situe l'un des principaux gisements en terres rares, les concentrations en ETR dans l'eau et les sédiments sont environ 200 fois supérieures à celles mesurées en moyenne dans les autres rivières au Nord du Pays (Liang et al., 2014).

Dans la province de Copperbelt en république démocratique du Congo, les sédiments de deux rivières proches de zones d'activité minière intensive sont classés comme extrêmement pollués en ETR (Atibu et al., 2016). Toujours en Afrique, dans le Sud-Ouest du Nigeria une contamination au Ce des nappes phréatiques de l'état du Lagos a été rapportée (Ayedun et al., 2017).

Enfin, la mesure d'un enrichissement en ETR léger dans les sédiments d'un estuaire au Brésil a été mise en relation avec l'utilisation des engrais phosphatés enrichis en ETR dans cette région (Sanders et al., 2013).

La toxicité des ETR

Si les preuves d'une contamination des écosystèmes par les ETR se multiplient, force est de constater que les études sur les effets toxiques des ETR restent rares. Plusieurs tendances ont déjà été rapportées cependant.

La toxicité des ETR serait négativement corrélée à la dureté des milieux. Une toxicité de l'ensemble des ETR (estimée par les concentrations létales médianes Cl_{50}) deux à dix fois plus élevée dans une eau douce (18 mg L^{-1} de $CaCO_3$) que dans de l'eau

du robinet (124 mg L^{-1} de $CaCO_3$) a été ainsi mesurée lors de tests sur *Hyalella azteca* (Borgmann et al., 2005). De la même manière, le La montrait une toxicité de l'ordre de 30 fois plus importante sur *Daphnia carinata* dans une eau douce (22 mg L^{-1} de $CaCO_3$) que dans une eau dure (160 mg L^{-1} de $CaCO_3$) (Barry et Meehan, 2000). Enfin, cette diminution de toxicité a aussi été mesurée lors de bioessais exposant des individus de *Daphnia pulex* et de *H. azteca* au Dy (Vukov et al., 2016). Dans cette dernière étude, les auteurs ajoutent que si l'apport de calcium dans le milieu d'exposition induisait bien une diminution de la toxicité du Dy pour *H. azteca,* l'ajout de magnésium seul ne conduisait pas à ce résultat.

Les ETR peuvent tous présenter un effet d'hormèse. Ainsi, une exposition à de faibles doses de ces métaux induirait des effets bénéfiques pour les organismes (Calabrese, 2005). L'application d'engrais à base d'ETR conduit par exemple à une augmentation moyenne de la productivité de 5 à 15% pour une centaine d'espèces cultivées (Hu et al., 2004). De la même manière, l'utilisation de compléments alimentaires enrichis en ETR permet des gains de poids et de croissance significatifs pour plusieurs espèces d'élevage (bœuf, porc, poule, etc.) (He et al., 2010). Une stimulation de l'activité métabolique d'une bactérie *Vibrio fisheri* suite à son exposition à de faibles concentrations de 11 ETR, de l'ordre de 2 µM, a aussi été relevée (Welte, 2002). Ce phénomène mesuré pour la majorité des ETR sur de nombreux organismes, a conduit Agathokleous et al. (2018) à suggérer l'inclusion de cet effet d'hormèse lors des évaluations de risque pour le La.

Enfin, les ETR ne semblent pas induire une forte toxicité sur les organismes pélagique dulcicole d'une manière générale. Les seuils de toxicité estimés dans la majorité des publications se situent à des concentrations en ETR 100 à 1000 fois plus élevées que les concentrations mesurées en milieu naturel (Tableau II). Toutefois, au regard du faible nombre d'études réalisé sur la toxicité des ETR accumulés dans les sédiments sur les communautés benthiques, il reste impossible de statuer sur leur toxicité depuis cette matrice. De surcroit, une majorité des études analysant la toxicité des ETR considèrent les ETR légers, comme le La et le Ce, mais n'incluent pas les ETR lourds.

Tableau II. Seuils de toxicité en ETR chez des organismes dulcicoles. Les concentrations seuils correspondent à des valeurs (N) nominales, (D) dissoutes ou (T) totales. Le ^{m} indique l'ajout d'une solution tampon d'acide 3-morpholino-1-propanesulfonique durant le test

Espèces	ETR	Forme de l'ETR	Dureté de l'eau (mg $CaCO_3$ L^{-1})	pH	Temp (°C)	Test	[ETR] (μgL^{-1})	Références
Skeletonema costatum	Lanthanides (seuls ou en mélanges) Y Sc	Chlorure ou Nitrate $Y(NO_3)_3$ $ScCl_3$		8	25	CL_{50} (72 h)	4000-5000 (N)	Tai et al., 2010
Chlorella vulgaris	Ce	$Ce(NO_3)_3$			37	CSEO (24 h) CMEO (24 h) CE_{50} (24 h)	224 (T) 308 (T) 2158 (T)	Evseeva et al., 2010
Raphidocelis subcapitata	Ce Gd Lu	$CeCl_3$ $GdCl_3$ $LuCl_3$			23	CE_{50} (72 h)	6317 (D) 2219 (D) 2079 (D)	González et al., 2015
Daphnia carinata	La	$LaCl_3$	98 160 22	7,8 7,5	20	CL_{50} (48 h) CL_{50} (24 h) CL_{50} (48 h) CMEO (14 j) CL_{50} (24 h) CL_{50} (48 h)	49 (T) 1232 (T) 1180 (T) 39 (T) 485 (T) 43 (T)	Barry et Meehan, 2000
Daphnia magna	Ce, Gd et Lu (seuls)	Chlorure	252		25	CE_{50} (48 h)	>6400 (N)	González et al., 2015
	Ce	$Ce(NO_3)_3$	252	7,8	20	CL_{50} (24 h) CL_{50} (48 h) CSEO (21 j) CMEO (21 j)	2298 (D) 1694 (D) 50-200 (D) 101-401 (D)	Ma et al., 2016
	La	$La(NO_3)_3$	88	7,6	20	CMEO (14 j)	100 (N)	Lürling et Tolman, 2010
Daphnia pulex	Dy					CL_{50} (48 h)	487 (D)	Vukov et al., 2016

*D'autres études, citées entres autres dans Sneller (2000) et dans Ng et Smith. (2011), déterminant des seuils de toxicité pour les ETR ont été publiées. Toutefois la langue utilisée ne nous permettant pas d'en vérifier la pertinence, elles n'ont pas été intégrées au tableau.

Espèces	ETR	Forme de l'ETR	Dureté de l'eau (mg $CaCO_3$ L^{-1})	pH	Temp (°C)	Test	[ETR] (μgL^{-1})	Références
Ceriodaphnia dubia	La	Lixiviat de benthonite	Eau douce synthétique	7	25	CE_{50} (48 h)	80 (D)	NICNAS, 2001
			Eau miliQ	7			40 (D)	
		$LaCl_3$	40-48	7			5000 (N)	
Hydra attenuata	Er	Nanoparticule	130	6-6,8	20-24	CE_{50} (96 h)	440-4 400	Blaise et Gagné, 2008
	Ho						44-440	
	Sm						430-4 300	
Thamnocephalus platyurus	Ce		-	7,4	25	CL_{50} (24 h)	4 069 767	
	Er			6-6,8			> 44 000	
	Ho						> 44 000	
	Sm						> 43 000	
Hyalella azteca	Dy		84.9	6,9	-	CL_{50} (96 h)	127 (D)	Vukov et al., 2016
			812	6,8[m]			1284 (D)	
			78	7,8			341 (D)	
			131	7,7			341 (D)	
			237	7,7			455 (D)	
			84	7,8[m]			228 (D)	
			78	8,0[m]			228 (D)	

*D'autres études, citées entres autres dans Sneller (2000) et dans Ng et Smith. (2011), déterminant des seuils de toxicité pour les ETR ont été publiées. Toutefois la langue utilisée ne nous permettant pas d'en vérifier la pertinence, elles n'ont pas été intégrées au tableau.

Espèces	ETR	Forme de l'ETR	Dureté de l'eau (mg $CaCO_3$ L^{-1})	pH	Temp (°C)	Test	[ETR] (μgL^{-1})	Références
Hyalella azteca	La	Oxyde	124	7,2-9,0	24-25	CL_{50} (7 j)	1665 (N)	Borgmann et al., 2005
	Ce						651 (N)	
	Dy						897 (N)	
	Er						929 (N)	
	Eu						717 (N)	
	Gd						599 (N)	
	Ho						755 (N)	
	Lu						1054 (N)	
	Nd						511 (N)	
	Pr						441 (N)	
	Sm						846 (N)	
	Tb						693 (N)	
	Tm						739 (N)	
	Yb						278 (N)	
	Y						549 (N)	
	La		18	6,4-8,7			18 (D)	
	Ce						32 (D)	
	Dy						162 (D)	
	Er						191 (D)	
	Eu						112 (D)	
	Gd						150 (D)	
	Ho						143 (D)	
	Lu						29 (D)	
	Nd						55 (D)	
	Pr						35 (D)	
	Sm						74 (D)	
	Tb						84 (D)	
	Tm						0.01 (D)	
	Yb						69 (D)	
	Y						66 (D)	

*D'autres études, citées entres autres dans Sneller (2000) et dans Ng et Smith. (2011), déterminant des seuils de toxicité pour les ETR ont été publiées. Toutefois la langue utilisée ne nous permettant pas d'en vérifier la pertinence, elles n'ont pas été intégrées au tableau.

Espèces	ETR	Forme de l'ETR	Dureté de l'eau (mg $CaCO_3$ L^{-1})	pH	Temp (°C)	Test	[ETR] (μgL^{-1})	Références
Melanotaenia duboulayi	La	Chlorure	84.9	6.9	-	CSEO (96 h)	127 (D)	Stauber, 2000
	La	Benthonite enrichie en La	40 à 48	6,5-8,1	23-25	CSEO (96 h)	<600 (D)	NICNAS, 2001
Oncorhynchus mykiss	La		128	7,1-8,4	15	CSEO (96 h)	>63 270	Watson-leung, 2009
Danio rerio	Ce	Nanoparticule	209	7,4	28	CE_{10} (72 h)	162 791	Hoecke et al., 2009
Gobiocypris rarus	La	$LaCl_3$		6,3	23	CL_{50} (96 h)	1920	Hua et al., 2017

*D'autres études, citées entres autres dans Sneller (2000) et dans Ng et Smith. (2011), déterminant des seuils de toxicité pour les ETR ont été publiées. Toutefois la langue utilisée ne nous permettant pas d'en vérifier la pertinence, elles n'ont pas été intégrées au tableau.

L'Yttrium (Y) et les ETR lourds

L'Y avec le Ce, le La et le Nd est l'un des quatre ETR les plus abondants. Contrairement aux trois autres ETR, l'Y fait partie des ETR dits lourds (Tableau III). Ses principales propriétés sont données dans le tableau 2.

Numéro atomique	Nombre de masse	Valence	Point de fusion (°C)	Point d'ébullition (°C)	Densité à 20°C (g/cm^3)	Rayon atomique (Å)
39	88,9	+3	1522	3345	4,47	1,8

Tableau III. Propriétés physiques de l'Y (Lide, 2003)

Sur l'ensemble de la littérature portant sur la toxicologie des ETR en eau douce, l'Y et le Nd sont de ces quatre ETR principaux, ceux les moins étudiés. Pourtant, tout comme le La et le Ce, l'Y entre dans la composition de nombreuses technologies de nouvelle génération comme la fibre optique, les superconducteurs ou encore dans les ampoules et les lasers de nouvelle génération (Lobinger et al., 2005; Eliseeva et Bünzli, 2011; Gwenzi et al., 2018). Une contamination des milieux aquatiques en Y d'origine anthropique apparaît de ce fait probable. Par ailleurs, des différences notables ont été mesurées entre la toxicité des ETR légers et ceux, comme l'Y, dits lourds dans la littérature.

Ainsi certaines études concluaient que les ETR lourds apparaissaient plus toxiques que les ETR légers. Weltje (2002) observait par exemple que la toxicité des ETR sur la bactérie *Vibrio fischeri* était corrélée avec leur masse atomique. Ainsi, le Lu était l'élément le plus toxique pour la bactérie alors que le La était celui présentant la toxicité la plus faible. Cette même tendance était constatée par González et al. (2015), lors de tests d'exposition en ETR réalisés à la fois sur *Vibrio fischeri* et aussi sur une algue (*Raphidocelis subcapitata*). Cette tendance n'était cependant pas retrouvée chez les autres organismes testés comme les invertébrés *Daphnia magna*, *Heteocypris incongruens*, *Brachionus calyciflorus* et *Hydra attenuata* qui d'une manière générale présentaient la même sensibilité quel que soit l'ETR auquel ils étaient exposés.

Une tendance inverse était néanmoins estimée par Borgmann et al. (2005) qui mesuraient en moyenne une toxicité plus forte pour les ETR légers que pour les ETR lourds sur *H. azteca*, à l'exception du Lu. Cette étude contrairement aux deux précédentes (Weltje, 2002; Gonzalez et al., 2015), incluait l'Y. Il présentait une toxicité comparable à celle des ETR légers et en moyenne deux fois plus forte que celle des autres ETR lourds (Tableau II).

Méthode d'évaluation du risque lié aux ETR

Norme de rejets des ETR dans l'environnement

Actuellement, le manque d'informations et d'études de toxicité viables est un obstacle à l'établissement de norme de rejet en ETR et de la mise en place de seuil de toxicité pour ces éléments. Herrmann et al. (2016) ont néanmoins tenté d'établir ces valeurs pour le La dans l'eau et les sédiments. En se basant sur les recommandations faites dans le document d'orientation technique (European Commission, 2003) et sur les résultats des différentes études répertoriées dans leur revue, Herrmann et al. (2016) ont estimé une PNEC (concentration prédite comme sans effet) pour le La de 4 $\mu g\ L^{-1}$ dans l'eau et de 5 $mg\ kg^{-1}$ pour les sédiments. Les auteurs affinent ces seuils en appliquant une approche par risques ajoutés, approche qui tient compte des concentrations naturelles propres au site considéré. Ainsi, la concentration maximale en La permise (MPC) en appliquant cette approche est de 36,9 $mg\ kg^{-1}$ pour les sédiments, car cette matrice présente des concentrations en La naturellement importante. La MPC pour l'eau est égale à la PNEC donnée précédemment. Les auteurs indiquent cependant que cette valeur pourrait être plus élevée pour des sites aux eaux naturellement riches en La.

Plusieurs années auparavant, Sneller (2000) avec les données existantes à ce moment avait déjà essayé de fixer des MPC pour les ETR. Ainsi, il estimait des MPC en eau douce allant de 1,8 $\mu g\ L^{-1}$ pour le Nd à 22 $\mu g\ L^{-1}$ pour le Ce. Pour les sédiments, en se basant sur les équilibres de partitionnement, l'auteur fixait des MPC s'échelonnant entre 1,4 $g\ kg^{-1}$ pour l'Y et 19 $g\ kg^{-1}$ pour le Ce.

En plus de ces valeurs seuils pour les milieux aquatiques, une étude de Li et al. (2013) estiment que les ETR sont dangereux pour la santé humaine à partir d'une dose journalière de 100-110 $\mu g\ kg^{-1}$.

Les bioessais; *Daphnia magna, Oncorhynchus mykiss et Chironomus riparius*

Comme indiqué précédemment, l'une des causes de l'absence de norme de rejet en ETR et de l'établissement de seuil de toxicité pour ces éléments par les gouvernements est le manque d'études de toxicité réalisées sur les ETR. Au Québec, le CVAC (Critère de qualité pour la protection de la Vie Aquatique Chronique) qui correspond à « la concentration la plus élevée d'une substance qui ne produira aucun effet sur les organismes aquatiques » (MDDEFP, 2013) constitue un de ces seuils. Pour le calculer trois méthodologies sont proposées (MENVIQ, 1990b). Les deux premières préconisées intègrent dans le calcul les valeurs de toxicité chronique (CMEO et CMAT pour la première et CE_{50} ou CL_{50} pour la seconde) mesurées pour au moins une espèce d'eau douce des six familles suivantes : Salmonidés, Cyprinidés, Daphnidés, de la famille des macroinvertébrés benthiques, et d'une famille d'invertébrés et d'Osteichtes non incluses dans les précédentes familles indiquées. La troisième méthode ne nécessite pour sa part au minimum qu'une valeur de toxicité (CE_{50} ou CL_{50}) mesurée sur une espèce de la famille des Daphnidés et une mesurée sur une espèce de poisson (Truite arc-en-ciel, Crapet arlequin ou Méné tête-de-boule).

Ainsi quel que soit la méthode choisie, la réalisation de tests de toxicité chronique sur une espèce de la famille des Daphnidés et d'un poisson de la famille des Salmonidés ou des Cyprinidés est recommandée pour le calcul du CVAC. D'autre part, la mise au point de critère de qualité pour les sédiments d'eau douce au Québec s'appuie aussi sur les résultats de bioessais réalisés sur des espèces benthiques (MDDELCC, 2016), les trois espèces recommandées étant *H. azteca, Chironomus dilutus*, et *C. riparius* (EC et MDDEP, 2007).

À partir de ces recommandations et afin d'évaluer au mieux le risque lié à l'Y sur les organismes d'eau douce, les trois espèces sélectionnées durant ce projet de thèse sont *D. magna*, *C. riparius* et *O. mykiss*. Leur cycle de vie et leurs caractéristiques sont présentés ci-dessous.

Daphnia magna

La grande daphnie*, Daphnia magna* est un microcrustacé de l'ordre des Cladocères vivant dans les écosystèmes dulcicoles de zones tempérées. Les néonates de *D. magna* atteignent leur maturité sexuelle au bout de 7 jours en moyenne pour une taille comprise entre 5 et 6 mm. Les daphnies sont des organismes filtreurs se nourrissant de microorganismes (phytoplancton, bactérie, détritus organiques, etc.). Leur alimentation est assurée par le mouvement de le leurs pattes thoraciques ciliés (Figure 2) qui créent en permanence un courant d'eau. Celui-ci permet l'acheminement des particules nutritives en suspension dans leur gouttière thoracique jusqu'à leur bouche.

D. magna est un organisme parthénogénétique qui présente usuellement une reproduction asexuée. Ainsi une femelle adulte va pouvoir produire une portée de 10 à 30 néonates femelles génétiquement identiques tous les 3 à 4 jours, en parallèle de ses mues, jusqu'à la fin de sa vie. Toutefois, lorsque les conditions environnementales sont défavorables, *D. magna* peut se reproduire de manière sexuée. Dans ce cas, des mâles vont être mis au monde. Ces derniers vont fertiliser les femelles qui vont ainsi produire un ou deux œufs de résistance, appelés éphippies. Les éphippies expulsées dans le milieu n'éclosent seulement que lorsque les conditions redeviennent favorables permettant ainsi aux populations de *D. magna* de perdurer. À 25°C, la durée de vie de *D. magna* est en moyenne de 40 jours.

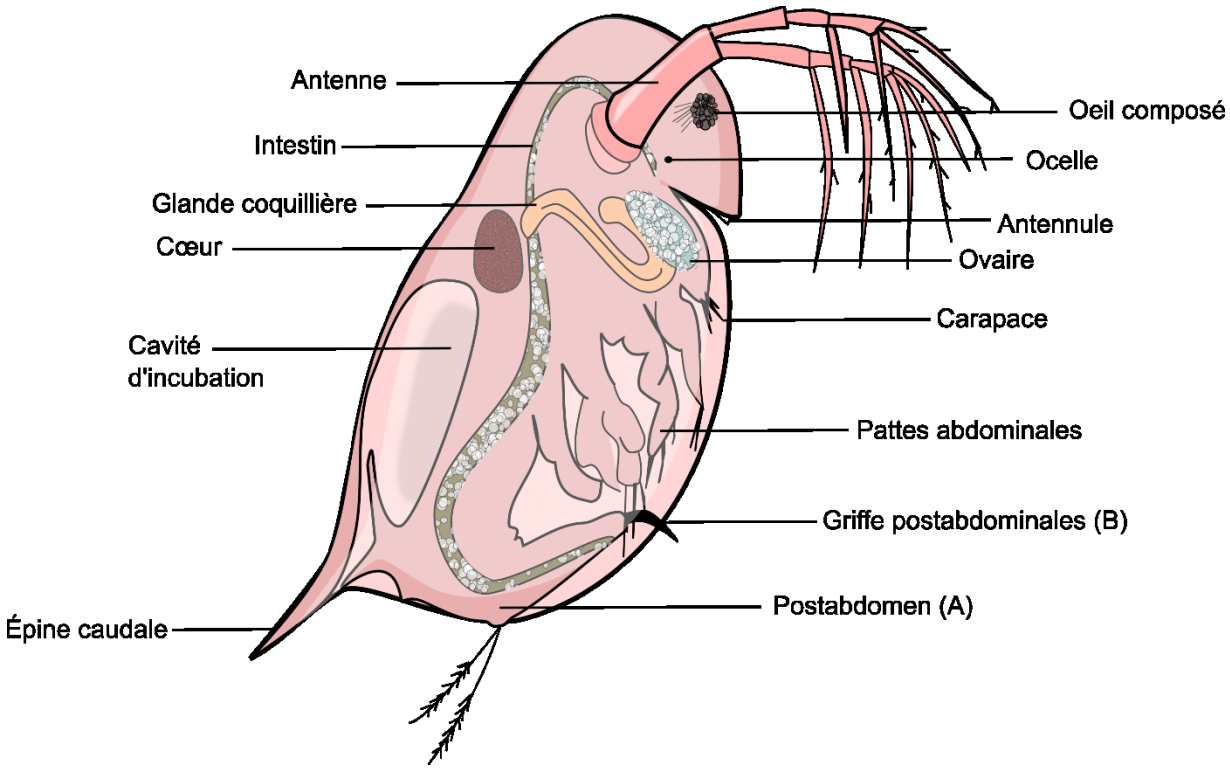

Figure 2. Anatomie d'une femelle de *D. magna* (EPA, 1985)

Le principal bioessai réalisé sur *D. magna* correspond à un test de toxicité aigüe de 48 heures prenant comme variable biologique la perte de mobilité de cet organisme (CEAEQ, 2011). Un test visant à mesurer l'effet chronique d'une substance sur la reproduction de *D. magna* sur 21 jours, même s'il est moins utilisé dans les règlementations, est aussi régulièrement réalisé dans les études écotoxicologiques (ISO 10706, 2000).

Chironomus riparius

La mouche arlequin, *Chironomus riparius* est un insecte de l'ordre des Diptères appartenant à la famille des Chironomidés présent aussi bien dans les milieux dulcicoles lotiques que lenthiques européens et nord-américains. La larve de *C. riparius* se développe dans les dix premiers centimètres des sédiments ce qui en fait un organisme benthique. Au sein du sédiment, il forme des tubes et se nourrit de la matière organique et des microorganismes qui le composent. La figure 3 présente l'anatomie des larves de *C. riparius*.

Le cycle de vie de *C. riparius* comprend quatre stades : œuf, larve, pupe, et adulte. Chaque stade dure entre 4 et 7 jours, pour un cycle de vie totale s'étirant de 15 à 30 jours et

une durée de vie des adultes comprise entre 4 et 11 jours. La larve de *C. riparius* mesure 1 à 2 mm à son premier stade et atteint en moyenne 16 mm à son dernier stade larvaire (4^{e} instar).

Deux bioessais sont communément réalisés à l'aide de *C. riparius* pour déterminer la toxicité des sédiments (NF XP T90-339-1, 2004). Le premier estime la survie et la croissance de l'organisme après 7 jours d'exposition à un contaminant alors que le second vise à mesurer l'impact d'une exposition de 28 jours sur la survie et le taux d'émergence des larves de *C. riparius*.

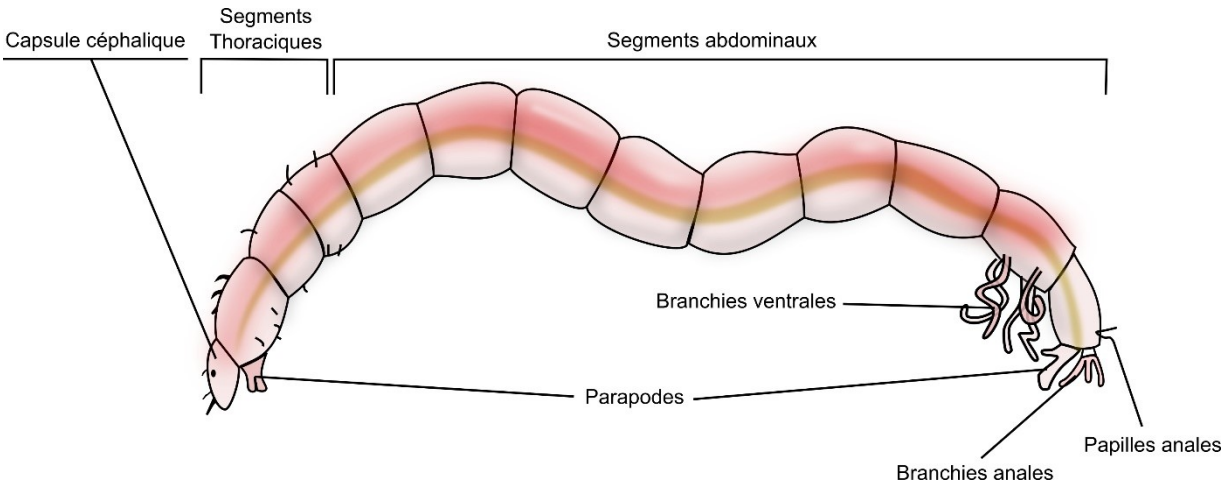

Figure 3. Anatomie de la larve de *C. riparius* (NF XP T90-339-1, 2004)

Oncorhynchus mykiss

La truite arc-en-ciel, *Oncorhynchus mykiss*, est un téléostéen, ou poisson osseux de la famille des Salmonidés. C'est un organisme dulcicole originaire d'Amérique du Nord mais aussi présent en Europe. Préférant les rivières peu profondes aux courants modérés, bien oxygénées, et fraîches (son préférendum est à 10-15°C), cette espèce peut néanmoins être observée dans une variété d'autres habitats jusqu'aux lacs dans la mesure où ces derniers présentent une végétation assez dense avec un substrat de gravier. En effet, *O. mykiss* est une espèce carnivore qui se nourrit principalement au niveau des substrats du fond des cours d'eau. Néanmoins son régime alimentaire varie selon son âge, sa taille et son habitat. Les alevins consommeront principalement du zooplancton, et incluront en grandissant dans leur régime des larves d'insectes, des insectes, des crustacés pour finalement consommer d'autres

poissons à leur stade adulte. La truite arc-en-ciel atteint sa maturité sexuelle entre 3 et 5 ans pour une taille moyenne entre 30 et 45 cm. Son anatomie est détaillée dans la Figure 4.

Comme *D. magna*, deux bioessais, impliquant la truite arc-en-ciel, ont été développés et normés afin d'évaluer les toxicités aigüe et chronique d'une substance (ISO 10229, 1994). Le premier évalue le taux de survie des truites après une exposition de 96 heures. Le second détermine le toxicité chronique de la substance sur la croissance de la truite au bout de 14 jours et de 28 jours d'exposition.

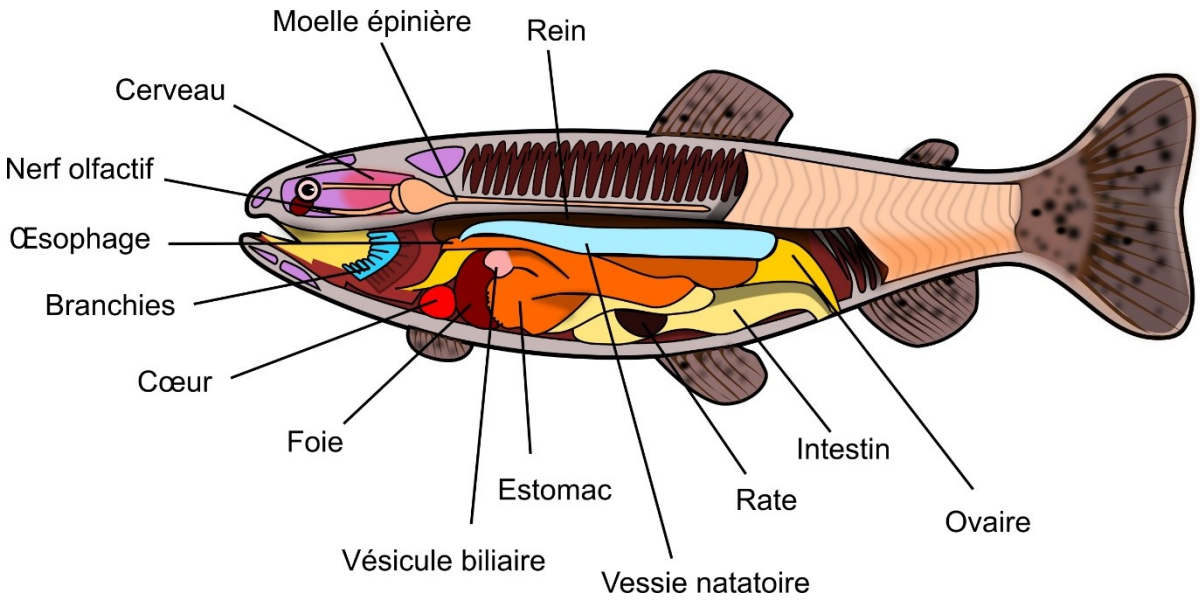

Figure 4. Anatomie de *O. mykiss* (source : Association des pisciculteurs de la région Nord)

Le transfert trophique des ETR

Les ETR dans les réseaux trophiques

Les ETR se concentrant principalement dans les sédiments des milieux aquatiques, les organismes benthiques seraient donc les plus exposés à ces contaminants. Une étude des concentrations en ETR accumulées par dix espèces de poisson vivant dans un réservoir de l'état de Washington (Mayfield et Fairbrother, 2015) concluait que les espèces benthiques (le Meunier à grande écailles et le Meunier rouge) accumulaient significativement plus d'ETR que les autres espèces. De la même manière, l'analyse des réseaux trophiques de 14 lacs tempérés canadiens révélait des concentrations maximales en ETR pour les invertébrés

benthiques non-prédateurs (Amyot et al., 2017). Dans cette étude, les concentrations en ETR dans le zooplancton, bien qu'en moyenne plus faibles, ne différaient néanmoins pas significativement de celles des invertébrés benthiques. Le zooplancton serait donc aussi un compartiment important d'accumulation des ETR dans les réseaux trophiques. Ce constat se confirmait dans les réseaux trophiques de huit lacs arctiques de l'Est Canadien où les concentrations moyennes maximales en ETR étaient mesurées dans le zooplancton pélagique (MacMillan et al., 2017). Par ailleurs, en laboratoire, les concentrations en ETR accumulés à la fin d'essais en microcosmes chez quatre organismes à quatre ETR (La, Ce, Sa et Y) se distribuaient dans l'ordre suivant : phytoplancton > zooplancton > espèce benthique > poisson (Yang et al., 1999).

Ainsi, si les invertébrés benthiques sont effectivement les plus exposés aux ETR, les organismes zooplanctoniques et phytoplanctoniques apparaissent aussi comme des compartiments importants d'accumulation des ETR dans les réseaux trophiques.

Le potentiel de transfert trophique des ETRs

Pour certains métaux, la nourriture peut être l'une des principales voies de contamination pour les organismes. Ces métaux peuvent alors conduire à des phénomènes de bioamplification, c'est-à-dire une accumulation progressive des métaux tout au long de la chaîne trophique, et provoquer *in fine* des effets délétères chez les espèces, telles que les superprédateurs, situées en haut de celle-ci. Bien que le mercure apparaît comme l'élément dont le caractère bioamplifiable est le plus connu et le plus référencé (Bowles et al., 2001; Zhang et al., 2012; Økelsrud et al., 2016), d'autres éléments entrainent ce phénomène. Ainsi, Croteau et al. (2005) observaient que dans le delta de la baie de San Francisco, les concentrations en cadmium accumulées étaient multipliées par 15 entre les proies et les prédateurs que ce soit pour des invertébrés se nourrissant d'algues épiphytes ou dans le cas de poissons piscivores. Dans une autre étude Campbell et al. (2005) mettaient en lumière une corrélation significative positive entre les valeurs de $\delta^{15}N$, indicateur de la position trophique des organismes, et les concentrations en césium et en rubidium mesurées sur des poissons d'eau douce du lac Érié et de lacs arctiques. Ce constat suggère aussi un phénomène de bioamplification pour ces deux éléments. Dernier exemple, le sélénium présentait un facteur

de bioamplification de 1,29 dans une étude mesurant les concentrations de ce métal entre des perches (*Perca fluviatilis*) et des invertébrés pélagiques (Økelsrud et al., 2016).

Le potentiel de transfert trophique des ETR n'a pour l'instant été que très peu étudié. Dans les deux études analysant les concentrations en ETR accumulées le long de chaînes trophiques lacustres canadiennes, les concentrations les plus faibles étaient mesurées dans les organismes en bout de chaîne trophique comme les poissons (Amyot et al., 2017, MacMillan et al., 2017). Cette observation suggère une biodilution de ces éléments. Les ETR ne présenteraient de ce fait qu'un faible potentiel de transfert trophique dans les écosystèmes aquatiques. D'autre part, une très faible accumulation de ces métaux dans les tissus musculaires des vertébrés aquatiques et terrestres a été rapportée dans une majorité d'étude. Pour les poissons plus particulièrement, les ETR se distribueraient principalement dans l'ordre suivant : muscle < squelette < branchies < organes internes (Qiang et al., 1994; Hao et al., 1996). La consommation humaine en chair de poissons ne devrait donc pas être une source importante de transfert pour ces métaux.

Le fractionnement subcellulaire

Principe

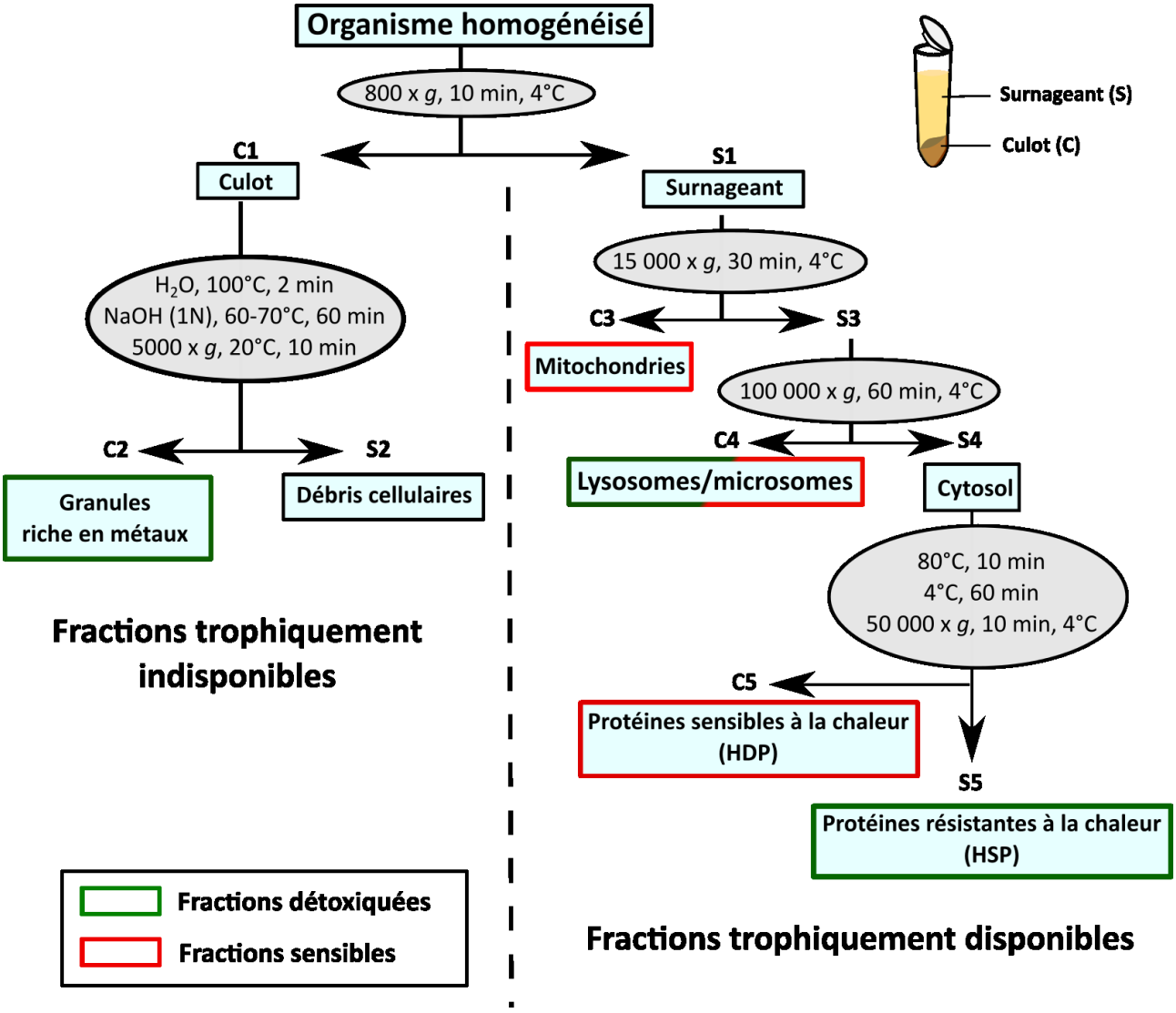

Figure 5. Protocole de fractionnement subcellulaire (Rosabal et al., 2012). Le classement proposé dans ce schéma entre fractions trophiquement disponibles et indisponibles correspond à celui décrit par Wallace and Luoma (2003)

Le fractionnement subcellulaire (Figure 5) conduit à la séparation des cellules des organismes en six fractions : les débris cellulaires, les granules riches en métaux, les mitochondries, les microsomes/lysosomes, les protéines stables à la chaleur ou HSP (*Heat Stable Protein*), et les protéines sensibles à la chaleur ou HDP (*Heat Denaturated Protein*). Cette séparation de ces composantes basées sur leurs différences de densité est réalisée à l'aide

d'une centrifugation différentielle. D'autres méthodes de séparation et d'isolation de composantes subcellulaires existent tels que l'élutriation centrifuge (Lin et al., 1985) ou encore la filtration sur membrane (Lilley et al., 1982). Néanmoins, la méthode par centrifugation différentielle présente l'avantage d'être relativement rapide et/ou de limiter les sources potentielles de contamination en métaux, comme les réactifs utilisés, lors de la séparation des différentes composantes (Lavoie et al., 2009).

L'analyse du fractionnement subcellulaire des métaux chez les organismes est une méthode qui a connu un essor en 2003 avec l'étude de Wallace et ses collaborateurs. Elle répond à deux grands objectifs (Figure 5) qui sont :

1. Étudier la distribution des métaux entre les fractions subcellulaires dites sensibles et celles dites détoxiquées.
2. Étudier cette même distribution entre les fractions supposées trophiquement disponibles chez une proie et celles qui ne le sont pas.

Fraction sensible VS fraction détoxiquée

Parmi les différentes fractions subcellulaires séparées, plusieurs présentent un intérêt tout particulier pour étudier la toxicité des métaux. Les HSP, aussi appelées *Metallothionein-Like proteins*, regroupent un ensemble de protéines de faible poids moléculaire, dont les métallothionéines (MT). Les MT jouent un rôle majeur dans la gestion des métaux au sein des cellules. Leur fonction est de se lier à ces derniers et de maintenir l'homéostasie de leur concentration sous forme "réactive" dans la cellule (Campbell et al., 2005; Cooper et al., 2013). Ainsi, il a été prouvé que la synthèse des MT chez les organismes était induite en réponse à une exposition à certains métaux (Mason et Jenkins, 1995; Langston et al., 1998; Bustamante et al., 2002; Kawagoe et al., 2005; Amiard et al., 2006) et certains auteurs utilisent la mesure des concentrations en MT comme un indicateur biochimique d'exposition à ces métaux (Couillard et al., 1995; Giguère et al., 2003; Perceval et al., 2006).

Les granules riches en métal (MRG), aussi nommée fraction résistante au NaOH, sont des concrétions de métaux liés à différents composés tels que des phosphates, des sulfures, des carbonates de calcium ou encore des protéines comme la ferritine (Hopkin, 1990; Khan et al., 2010). L'accumulation des métaux au sein de ces granules constitue un mécanisme de séquestration des métaux à l'intérieur des cellules. Bien que Mason et Nott (1981) séparaient

les granules en deux groupes suivant leur fonction et indiquaient que les granules sous forme de phosphate étaient celles liées à un mécanisme de détoxication, une majorité d'auteurs suggèrent que les MRG correspondent à une fraction détoxiquée (Bustamante et al., 2006; de Bisthoven et al., 1998; Wallace et al., 2003; Wang et Guan, 2010). Par ailleurs, plusieurs études semblent indiquer que les granules riches en métaux sont des sous-produits de la dégradation des métallothionéines par les lysosomes (Nassiri et al., 2000; Marigómez et al., 2002) et pourraient être une étape préalable à l'excrétion des métaux par les organismes. Avec la fraction contenant les métallothionéines, les granules forment le groupe des fractions détoxiquées aux métaux (MDF).

À l'inverse, certaines fractions comme celle des mitochondries et celles des protéines sensibles à la chaleur sont classées dans la catégorie des fractions sensibles aux métaux (MSF) (Wallace et al., 2003). Une accumulation de métaux dans ces fractions a pu être mise en relation avec des effets délétères sur les organismes dans plusieurs études (Campana et al., 2015; Leonard et al., 2014; Rainbow et al., 2015). Campana et al. (2015) observaient en étudiant les effets du cuivre sur deux organismes, un bivalve *Tellina deltoidalis* et un amphipode *Melita plumulosa,* que même si le bivalve présente un taux d'accumulation en cuivre beaucoup plus important que l'amphipode, la sensibilité de ces deux organismes à ce métal est très proche lorsqu'elle est mesurée en termes de quantité en cuivre accumulé dans les fractions dites sensibles. D'autres études considéraient pour leur part que la présence de métaux non essentiels dans ces fractions sensibles entraine un risque probable pour les organismes (Rosabal et al., 2015).

Évaluer la distribution de l'Y entre ces différentes fractions subcellulaires permettrait donc de comprendre et de définir la sensibilité des espèces à ce métal. À noter que cet élément formant un cation trivalent (Tableau III) et appartenant aux métaux du groupe A comme l'aluminium (Al) ou encore le Chrome (Cr) (Nieboer and Richardson, 1980), il est probable qu'une analogie entre sa distribution intracellulaire et celle de ces deux métaux soit observable. De la même manière, le rayon atomique de l'Y (Tableau III) est très proche de celui du Ca. Cette caractéristique lui confère des propriétés analogues au Ca ce qui pourrait se traduire par un schéma de distribution intracellulaire semblable entre ces deux éléments.

Fractions trophiquement disponible VS trophiquement indisponible

Au-delà de l'étude de la toxicité des métaux, le deuxième objectif attribué à l'étude de la distribution subcellulaire des métaux est lié au concept de TAM (*Trophically Available Metal*). Ce concept suggère qu'il est possible de prévoir le potentiel de transfert trophique du métal depuis une proie vers son prédateur en se basant sur la distribution subcellulaire de ce métal chez la proie, et plus particulièrement sur son accumulation dans les fractions dites trophiquement disponibles. En effet, selon certains auteurs, seules ces fractions de la cellule de la proie vont pouvoir être assimilées par le prédateur. *In extenso*, seule la portion du métal associée à ces fractions, le métal dit trophiquement disponible, chez la proie sera disponible pour le prédateur la consommant. Ainsi, aux cours d'expériences de nourrissage de larve de *Sialis velata,* un insecte de l'ordre des Mégaloptères*,* avec des proies, une larve de Diptères, *Chironomus riparius,* et un oligochète, *Tubifex tubifex*, préalablement contaminées soit en nickel (Ni), soit en thallium (Tl), ou encore en sélénium (Se) l'efficacité d'assimilation de ces métaux par le prédateur était proche de la proportion de ces derniers dans les fractions trophiquement disponibles des proies (Dumas et Hare, 2008; Dubois et Hare, 2009a). Une expérience similaire, mettant en jeu le même prédateur et les mêmes proies, mais un métal différent, le cadmium (Cd), montrait que l'efficacité d'assimilation de ce métal par le prédateur pouvait être estimée à partir des concentrations en cadmium dans les fractions trophiquement disponibles des proies, mais que pour l'une des proies, *Tubifex tubifex*, il était nécessaire de présumer que la moitié du cadmium associé aux organites n'était pas assimilée par le prédateur (Dubois et Hare, 2009b). Par ailleurs, Wallace et Lopez (1996) mesuraient une relation de 1:1 entre la proportion et la quantité de Cd accumulée dans la fraction cytosolique d'un oligochète, *Limnodrilus hoffmeisteri*, et le pourcentage de Cd assimilé par une crevette, *Palaemonetes pugio*, le consommant. Une relation similaire était obtenue pour ce même prédateur nourri cette fois avec un amphipode, *Gammarus lawrencianus*, préalablement enrichi en Cd (Seebaugh et al., 2006). À l'inverse, d'autres études indiquent qu'il est nécessaire de considérer qu'une partie des métaux issus de fractions considérées comme trophiquement indisponibles est assimilée (Rainbow et al., 2011).

Ces différentes observations ont été synthétisées par Rainbow et al. (2011) qui proposaient que le concept de TAM soit dépendant du métal, de la proie et du pouvoir digestif

du prédateur considéré. Si dans certains cas l'efficacité d'assimilation des métaux par le prédateur peut effectivement être prédite à partir de leurs concentrations dans les fractions trophiquement disponibles chez ses proies (Wallace et Luoma, 2003; Dumas et Hare, 2008; Dubois et Hare, 2009a), il est souvent nécessaire d'admettre que certaines fractions qui n'étaient pas considérées comme trophiquement disponibles le sont pourtant (Steen Redeker et al., 2007). Ainsi, plusieurs auteurs s'accordent à dire que les TAM permettent de prédire le minimum de métaux qui est disponible pour un organisme depuis ses proies (Dubois et Hare, 2009b; Rainbow et Smith, 2010). Il est à noter toutefois que d'autres auteurs concluaient à l'inverse que les TAM représentent un maximum (Seebaugh et al., 2006).

Le concept de TAM présente donc un intérêt évident pour prédire le potentiel de transfert trophique des métaux. Il nécessite néanmoins d'être approfondi pour pouvoir statuer sur sa pertinence pour chaque cas considéré comme celui des ETR.

Limites de la méthode

Il est nécessaire cependant de considérer l'efficacité de la séparation permise par le protocole de fractionnement subcellulaire tel que décrit précédemment. En effet, celui-ci se confronte à de nombreuses limites opérationnelles.

L'un des premiers objectifs du fractionnement subcellulaire est de libérer le maximum des composantes des cellules sans pour autant menacer l'intégrité de celles-ci. Or, de nombreux auteurs ont observé que l'étape d'homogénéisation réalisée au préalable de la centrifugation différentielle pouvait, suivant son intensité, la méthode utilisée et selon l'espèce fractionnée, conduire à une libération incomplète des composantes subcellulaires ou encore à la dégradation de ces dernières (Giguère et al., 2006; Lavoie et al., 2009; Rosabal et al., 2014). Dans les deux cas, les fractions séparées par la suite contiendraient une part plus ou moins importante de composantes subcellulaires différentes de celles qu'elles étaient censées contenir. D'autre part, certains auteurs suggèrent qu'un transfert des métaux depuis les HDP vers les HSP se produit lors de l'étape de dénaturation à 80°C incluse dans le protocole de fractionnement. En effet, Geffard et al. (2010) en comparant les concentrations en cadmium (Cd) associé aux HSP et aux HDP mesurées chez un amphipode selon deux méthodes de séparation observaient de grandes différences. La séparation de ces deux fractions à l'aide du traitement à la chaleur préconisé dans le protocole de fractionnement subcellulaire permettait

de conclure que le Cd était principalement associé dans le cytosol au MT alors que la séparation par exclusion chromatographique des différentes fractions cytosoliques, ne comprenant pas de choc thermique, aboutissait à la conclusion que le Cd se retrouvait majoritairement associé à des protéines autres que les MT. Ce transfert des métaux entre fractions cytosoliques, déjà suggéré par Bragigand and Berthet (2003), serait donc une autre source potentielle de chevauchement entre les différentes fractions. La majorité des études impliquant le fractionnement subcellulaire ne vérifiant pas l'efficacité de la libération et de la séparation des composantes subcellulaires de leurs organismes lors de leur fractionnement, il est essentiel de prendre en compte que les fractions subcellulaires décrites dans ces études peuvent être en partie mélangées.

Au-delà de ces limites opérationnelles, d'autres limites, liées à l'interprétation de la distribution des métaux entre les fractions, viennent s'ajouter. Si le choix d'inclure ou non certaines fractions comme les organelles dans les TAM a déjà été mentionné précédemment, le classement de certaines fractions comme détoxiquées ou non est aussi sujet à débat. En effet, bien que les lysosomes soient considérés par certains auteurs comme liés à un mécanisme de détoxication chez les organismes (Bustamante et al., 2002; Rosabal et al., 2012), ces composantes subcellulaires sont regroupées lors de leur fractionnement avec d'autres vésicules biologiques, les microsomes, qui peuvent être considérées comme des composantes subcellulaires sensibles et non détoxiquées (Giguère et al., 2006 ; Rosabal et al., 2012). De la même façon, le classement de la fraction des débris cellulaires entre ces deux catégories est complexe. Certains auteurs les incluent dans la catégorie des fractions dites sensibles (Steen Redeker et al., 2007; Casado-Martinez et al., 2012) alors que de nombreux autres indiquent qu'il est nécessaire d'interpréter les résultats d'accumulation en métal dans les débris cellulaires avec beaucoup de précautions (Cain et al., 2004; Lavoie et al., 2009; Rosabal et al., 2012; Campana et al., 2015).

Cadre conceptuel de la thèse

Chapitre 1

L'analyse du fractionnement subcellulaire de l'Y apparaît comme une méthode particulièrement intéressante pour évaluer à la fois la toxicité de cet élément et aussi son potentiel de transfert trophique chez nos trois organismes d'essais.

Toutefois, les limites opérationnelles liés au protocole de fractionnement subcellulaire pourraient conduire à une mauvaise interprétation du fractionnement de l'Y. En conséquence, le **Chapitre 1** de cette thèse visait à adapter le protocole de fractionnement subcellulaire pour chacun des trois organismes d'essais.

Différents paramètres et étapes de ce protocole (ex. : méthodes de conservation, tampon d'homogénéisation, vitesses de centrifugation, etc.), en particulier la méthode d'homogénéisation, ont été adaptés pour chaque organisme. L'objectif était de :

1) S'assurer qu'un maximum de cellules des échantillons soit lysé.
2) De minimiser la dégradation des mitochondries lors de leur libération / séparation.
3) D'obtenir une séparation efficace, en limitant les chevauchements inter-fractions, des quatre fractions suivantes : Débris, mitochondries, lysosomes / microsomes et cytosol.

Pour valider les protocoles développés, des essais enzymatiques impliquant des enzymes spécifiques de ces fractions subcellulaires ont été mis en place. Quel que soit l'organisme, le broyage au pilon Elvehjem avec une seconde étape d'homogénéisation à la sonde à ultrasons apparait comme la meilleure méthode d'homogénéisation pour atteindre notre objectif 1. Afin de réduire les chevauchements inter-fractions, la vitesse de centrifugation à chacune des étapes, en particulier pour la séparation des mitochondries, a dû être modifiée par rapport au protocole originale développé par Wallace et al. (2003). Enfin, à la vue de l'écart observé entre les fractions véritablement séparées sur l'ensemble des protocoles testés durant nos essais et celles prédites dans la littérature en absence de vérification, le concept de fraction validée a été mis au point. Ainsi, dans le cas de nos organismes, la fraction mitochondriale, par exemple, ne contiendrait que les membranes mitochondriales, la matrice mitochondriale étant récupérée avec le cytosol. Le chapitre conclue sur la nécessité d'adapter le protocole de fractionnement subcellulaire à l'organisme considéré (Cardon et al., 2018).

Chapitre 2

Les valeurs seuils de toxicité des ETR chez les organismes pélagiques disponibles dans la littérature apparaissent très élevées par rapport aux concentrations en ETR reportées à ce

jour dans les milieux naturels. Bien que la toxicité de l'Y n'a fait l'objet que de peu d'étude, il est fort probable que ce métal soit également peu toxique. Il n'est cependant pas possible de statuer sur la toxicité des ETR depuis les sédiments sur les organismes benthiques. Le faible nombre d'études réalisées sur ce sujet ne le permet pas. Pourtant, il devient urgent de fixer des seuils de toxicité pour ces métaux au regard des perspectives de pollution futur qui leur sont liées. Par ailleurs, il serait essentiel lors du développement de ces seuils d'intégrer des paramètres comme la dureté qui semble être négativement corrélée à la toxicité des ETR et donc potentiellement à celle de l'Y. *D. magna*, *O. mykiss* ainsi que *C. riparius* sont des organismes de choix pour la mise au point de ces seuils puisqu'ils sont tous les trois des organismes recommandés par le ministère de l'environnement et de la lutte contre les changements climatiques (MELCC) pour la réalisation des bioessais nécessaires à l'établissement de norme de qualité pour la préservation des écosystèmes aquatiques.

La distribution subcellulaire d'un métal au sein d'un organisme est un indice de sa toxicité et de ses mécanismes de toxicité. Une accumulation croissante de ce métal dans les MSF des cellules d'un organisme au détriment de ses MDF (concept de *spill-over*) indiquerait par exemple que la capacité de l'organisme à le détoxiquer est dépassée. L'exposition d'un organisme à une gamme de concentrations en Y incluant à la fois des concentrations avec effet toxique, comme une CMEO, et d'autres sans effet pourrait permettre d'observer ce phénomène de « *spill-over* ». D'autre part, l'analyse de la distribution d'un métal entre les MSF et les MDF des cellules d'un organisme serait révélateur de sa capacité à l'accumuler et donc de sa sensibilité à ce dernier. Si un organisme est capable de stocker des quantités en Y bien supérieures à la moyenne des autres organismes, il est probable que sa propension à accumuler ce métal dans les MDF de ses cellules soit elle aussi supérieure à celles des autres organismes. À notre connaissance la distribution subcellulaire des ETR n'a fait l'objet que de deux études à ce jour (Magnusson, 1963; Racine, 2016). Néanmoins à la vue de la distribution intracellulaire des ETR observée chez *C. reinhardti* (Racine, 2016), l'hypothèse d'une accumulation de l'Y principalement dans la fraction résistante à la soude chez nos organismes peut être émise.

Le **Chapitre 2** de cette thèse visait de ce fait à :

1) Déterminer des CMEO en Y pour chacun de nos organismes et les comparer avec les concentrations en Y et en ETR totaux rapportées dans les milieux naturels.
2) Évaluer l'influence de la dureté du milieu sur ces CMEO pour l'Y.
3) Estimer la distribution subcellulaire de l'Y le long d'une gamme d'exposition comprenant ces CMEO pour chacun de nos organismes.
4) Analyser cette distribution subcellulaire de l'Y chez nos organismes au regard des différents concepts liés à l'accumulation des métaux entre MDF et MSF.

Dans cette optique, des bioessais de toxicité chronique ont été réalisés sur chacun de nos organismes. Dans le cas de *D. magna*, ces essais ont été répétés dans des milieux de différentes duretés. À la fin des bioessais, les organismes ont été récupérés et la distribution subcellulaire de l'Y a été déterminée à l'aide des protocoles de fractionnement établis dans le Chapitre 1. Les CMEO estimées semblent indiquer que seules les espèces benthiques présenteraient un risque potentiel de toxicité aux ETR aux concentrations naturelles relevées à ce jour. En termes de fractionnement, pour les deux invertébrés la fraction résistante au NaOH apparaît comme le principal lieu de détoxication de l'Y. Cette MDF serait à l'origine de l'importante capacité d'accumulation en Y de *D. magna* par rapport aux deux autres organismes. À l'inverse aucune stratégie de détoxication subcellulaire n'a été observée dans le foie de la Truite. Enfin, quel que soit l'organisme, l'étude suggère que l'interaction de l'Y avec les membranes mitochondriales, principale MSF ciblée par ce métal, serait à l'origine de sa toxicité.

Chapitre 3

Le potentiel de transfert trophique des ETR n'a pour l'instant jamais été étudié en laboratoire. Cependant, les concentrations d'ETR mesurées le long de chaînes trophiques lacustres semblent démontrer un phénomène de biodilution. Cette observation suggèrerait un potentiel de transfert trophique faible pour l'Y, qui s'accumulerait chez les organismes aquatiques plus probablement depuis l'eau. L'analyse de la proportion en Y accumulée dans les fractions trophiquement disponibles d'organismes à la base des réseaux trophiques, comme les consommateurs primaires, pourrait permettre de valider ce faible potentiel de transfert

trophique. Les résultats de fractionnement subcellulaire de l'Y observés chez *D. magna* et *C. riparius* dans le Chapitre 2 semblent le confirmer. Il est toutefois nécessaire de valider au préalable le concept de TAM pour ce métal.

D'autre part, les résultats du Chapitre 2 indiquent une absence de détoxication subcellulaire de l'Y dans le foie de la Truite. Pourtant, la littérature suggère que cet organe est l'un des principaux sites d'accumulation des ETR chez les poissons. Il est donc probable qu'il le soit aussi pour l'Y dans le cas de *O. mykiss*. Une hypothèse serait qu'une autre stratégie de détoxication d'ordre biodynamique pourrait avoir été mis en place par cet organisme face à la contamination en Y. Il aurait pu par exemple, augmenter ses flux d'externalisation en Y au détriment de ses flux d'internalisation.

Le **Chapitre 3** de cette thèse se fixe par conséquent comme objectif :

1) De vérifier la pertinence du concept de TAM pour l'Y.

2) De comparer l'importance du transfert de l'Y depuis la nourriture par rapport à celui depuis l'eau.

3) D'évaluer la distribution de l'Y au sein de quatre organes de la truite (le foie, le muscle, l'intestin et les branchies).

4) D'analyser les mécanismes de dépuration de l'Y chez cet organisme.

Pour répondre à ces objectifs, des essais de nourrissage de *O. mykiss* avec une gamme de *D. magna* contaminées en Y ont été réalisés. Une expérience de dépuration des truites sur cinq jours a été ajoutée à la fin de ces essais. De plus, la distribution subcellulaire de l'Y chez les daphnies le long de la gamme d'exposition a été évaluée. Enfin, des expériences exposant des truites à une gamme d'eau enrichie en Y en absence de nourriture ont été réalisées. Les résultats confirment une efficacité d'assimilation de l'Y par la truite depuis *D. magna* semblable à la proportion en Y dans les TAM de *D. magna*. De plus, l'eau apparaît comme une voie d'assimilation de l'Y vers *O. mykiss* beaucoup plus importante que la nourriture dans nos conditions d'essais. Enfin, les intestins et les branchies se sont révélés être les deux principaux organes accumulant l'Y chez *O. mykiss*. Toutefois, contrairement à ces deux organes et aux muscles, aucune diminution significative en Y n'a été relevée dans le foie au cours de l'expérience de dépuration.

CHAPITRE 1. Validation enzymatique de protocoles de fractionnement subcellulaire des métaux adaptés aux organismes dulcicoles

Enzymatic validation of species-specific protocols for metal subcellular fractionation in freshwater animals

Pierre-Yves Cardon[1], Antoine Caron[1], Maikel Rosabal[2], Claude Fortin[3], and Marc Amyot[1]

[1] GRIL, Université de Montréal (UdeM), Département de sciences biologiques, Pavillon Marin-Victorin, 90 avenue Vincent-d'Indy, Montréal (Québec), Canada H3C 3J7

[2] GRIL, Université du Québec à Montréal (UQAM), Département des sciences biologiques, 141 avenue du président-Kennedy, Montréal (Québec), Canada H2X 1Y4

[3]Institut National de la Recherche Scientifique, Centre Eau Terre Environnement (INRS-ETE), 490 rue de la Couronne, Québec (Québec), Canada G1K 9A9

Published in Limnology and Oceanography: methods, 16(9), 537-555

DOI: 10.1002/lom3.10265

Abstract

The use of fractionation protocols to determine metal subcellular distribution in aquatic organisms has gained much interest over the last fifteen years, however, accurate separations among the different components of cells is challenging. Subcellular fractions separated with such an approach are operationally defined and a potentially significant difference can exist between anticipated and resulting fractions. This study customizes and validates subcellular partitioning protocols, for three different freshwater organisms representing a diversity of challenges for subcellular fractionation: *Daphnia magna*, *Chironomus riparius* and liver of *Oncorhynchus mykiss*. Several protocols involving different homogenization methods, centrifugation speeds or conservation conditions were tested, and their efficiencies were assessed using enzymatic biomarker assays.

Our work allowed us to identify critical steps to improve separations. First, for *D. magna*, a crustacean with a reinforced chitinous exoskeleton, the use of a strong homogenization method using a sonicator is necessary. Second, for both invertebrates, we observed the leaking of the mitochondrial matrix during cell fractionation, regardless of the homogenization strength and conservation conditions. Therefore, we propose that the mitochondria fraction should be referred to as the mitochondrial membrane fraction, and the cytosol fraction should be identified as the cytosol and mitochondrial matrix fraction. Third, the presence of a lipid-rich layer during *O. mykiss* liver fractionation may lead to an overlap between mitochondria and cytosol and must be considered in the protocol development. Finally, lysosomes should not be pooled with the microsomes fraction without prior validation. Overall, this study provides a benchmark for future methodological studies on similar taxa.

Introduction

Metal subcellular fractionation is an operationally-defined approach that allows the study of metal handling strategies by aquatic organisms (Wallace et al., 2003). It consists in (gently) disrupting the plasma membrane of the organisms' cells, in separating their subcellular components into fractions (i.e. cellular debris/nuclei, mitochondria, organelles and cytosol) and determining the metal content in each of them. Such an approach usually has two objectives. The first is to infer on metal subcellular detoxification processes based on metal accumulation in each fraction. It is well established that metal distribution among detoxified subcellular components (i.e metallothionein, metal-rich granules) and components considered as sensitive (i.e mitochondria, enzymes) may explain to some extent metal tolerance or sensitivity in aquatic organisms (Wallace et al., 2003; Rosabal et al., 2015). The second objective is to estimate the metal trophic transfer potential. Indeed, metal trophic availability from prey to a predator has been shown to be potentially measurable by determining the metal subcellular partitioning in preys (Wallace and Luoma, 2003; Sánchez-Marín and Beiras, 2017). Since the pioneering work of Wallace and its collaborators (Wallace et al., 2003; Wallace and Luoma, 2003), around 120 studies about metal subcellular fractionation have been published in the fields of limnology and oceanography (according to a search in Google Scholar using keywords such as "metal subcellular fractionation").

A typical fractionation scheme involves three steps, namely conservation of samples prior to analysis, homogenization, and separation of subcellular fractions (Fig. 1). For conservation, most studies use freezing at -80ºC or lower. While the homogenization step is usually performed using mechanical approaches, the separation of the subcellular components is based on their size and their density, by successive centrifugation at increasing speeds. During this last step, a mixture or overlap among subcellular fractions may occur as a result of (1) variability in size and density of fractions between organs, individuals and species, and inappropriate centrifugation speed (2) incomplete homogenization, (3) clumping of particles, or (4) damages and subsequent leakage of organelles (e.g. mitochondria, lysosomes) (De Duve, 1975; Graham and

Rickwood, 1997; Simon et al., 2005). Consequently, some customization may be required to minimize the occurrence of these artefacts.

Subcellular fractionation protocols should achieve two goals: (1) to efficiently but gently lyse cells in order to release all the subcellular components and (2) to maximize the clear separation of subcellular fractions after cell disruption (Graham and Rickwood, 1997). Most aquatic studies involving this approach follow the protocol described by Wallace et al. (2003) (Campbell et al., 2005; Geffard et al., 2010; Casado-Martinez et al., 2012). Modifications to this general protocol have been introduced by many authors (e.g. disruption method or buffer composition), but the achievement of the two goals previously described is rarely demonstrated rigorously (Giguère et al., 2006; Kamunde, 2009; Campana et al., 2015).

Validation studies are scarce and include those of Bustamante et al. (2006) and Simon et al. (2005), who controlled the accuracy of their fractionation protocol by transmission electronic microscopy, Lavoie et al. (2009) who used an electronic particle counter to estimate the cell lysis efficiency of their homogenization step and enzymatic biomarkers assays to control the separation of subcellular fractions and Rosabal et al. (2014) who validated both the cell lysis and separation efficiency of their fractionation protocol with enzymatic biomarkers assays. This type of assays is the most commonly used to assess the efficiency of subcellular fractionation methods. Its principle is to measure the activity of certain enzymes, that are located exclusively in a given subcellular component, on every separated fraction. By determining the fraction in which the majority of the activity of these enzymes is measured, we can verify in which fraction our subcellular components are located. For instance, Taylor and Maher (2012) by measuring an enrichment of the activity of two enzymes, one specific to mitochondria (Cytochrome C Oxidase) and the other to lysosomes (acid phosphatase) in their respective putative fraction, confirmed the location of these two subcellular component in the anticipated fractions after their separation. Enzymatic biomarker assays can also be used to assess the cell lysis efficicency of the homogenization step. Thus, assessment of lactate dehydrogenase (LDH) activity, an enzyme specific to cytosol, in the sample after homogenization leads some authors to conclude that a maximum of cells has been

disrupted with their protocol since a maximal LDH activity was reached on their homogenate (Seib et al., 2006; Rosabal et al., 2014).

Very few studies have systematically compared the efficiency of different fractionation protocols. Simon et al. (2005) compared the cell disruption efficiency of two homogenization methods and its consequences on uranium subcellular fractionation in visceral and gill samples of a freshwater bivalve. They concluded that the efficiency of homogenization methods was organ-specific, limiting the use of a common protocol to compare metal cellular distribution between organs and organisms. Using two green algae, Lavoie et al. (2009) showed that sonication led to a higher cell disruption rate than the use of a rotor stator homogenizer, a widely used tool for subcellular fractionation studies (Wallace et al., 2003; Geffard et al., 2010; Campana et al., 2015). Similarly, Rosabal et al. (2014) compared the efficiency of three subcellular partitioning procedures on an insect larva, *Chaoborus sp*, each of them using a different homogenization step. Moreover, enzymatic assay results showed that repeating the homogenization and the first centrifugation steps twice (the two supernatants resulting from these steps being pooled), led to a better cell disruption efficiency while maintaining the integrity of subcellular components.

We are currently faced with a paucity of comparative subcellular fractionation studies for key aquatic species of interest, and most studies do not include any validation steps. In our opinion, there is no universally applicable method for aquatic organisms. On the contrary, we propose that species specific protocols be developed to rigourously determine subcellular metal distribution among cell components.

Thus, the aim of this study is to customize the subcellular fractionation protocols for three freshwater species, *Daphnia magna*, *Chironomus riparius* and *Oncorhynchus mykiss*. These species are commonly used by government agencies for aquatic toxicity tests. In addition, since *O. mykiss* can feed on the other two organisms, they can be used to study trophic transfer of metals. They are therefore of interest both for studies on trophically available metals and for studies on the fractionation of metals between metal-sensitive subcellular components and detoxified metal subcellular components. Beyond their interest on ecotoxicology, these species have also been chosen

because they are anatomically different: *D. magna* is a pelagic microcustacean with a reinforced chitinous exoskeleton, *C. riparius* is a benthic dipteran made of soft tissues, and *O. mykiss* liver tissues are rich in lipids. Therefore, they represent a diversity of challenges for subcellular fractionation. Different homogenization methods, centrifugation speeds and preservation conditions were tested. The cell disruption efficiency and the integrity of the mitochondria achieved with the different protocols were assessed using enzymatic biomarkers. To our knowledge, it is the first study comparing and optimizing subcellular fractionation protocols between key species in ecotoxicology.

Materials and procedures

The fractionation procedure involves three main steps: the conservation, homogenization and separation steps (Fig. 1). For conservation, we tested the impact of storage at -80°C on *C. riparius* fractionation. Indeed, studies have reported mitochondrial damage even after only a few hours of freezing (Fuller et al., 1989; Gnaiger et al., 2000). Nonetheless, most studies stored their organisms at -80°C or lower prior to fractionation. Regarding homogenization, we tested different tools used to disrupt or grind organisms. Furthermore, we compared protocols with different cycles of homogenization and resuspension of debris pellets, since an enhancement of homogenization efficiency and of fraction purity with the inclusion of such additional steps has recently been observed (Ng et al., 2011; Rosabal et al., 2014). With respect to separation, we focused on maintaining mitochondria integrity during fractionation and on avoiding overlaps between subcellular components, by assessing different centrifugation speeds for the second separation step (Fig. 1). Moreover, for *O. mykiss* livers, we observed an intermediate layer on top of mitochondrial pellet. Therefore in order to improve mitochondria separation, we tested different protocols regarding whether or not to collect this layer with the surpernatant (Fig. 1). For each organism, numerous fractionation procedures were tested. Summary of all fractionation protocols tested with each organism is given in Supplementary Information SI, Table SI. However, only procedures showing the most promising results are described in detail in this section.

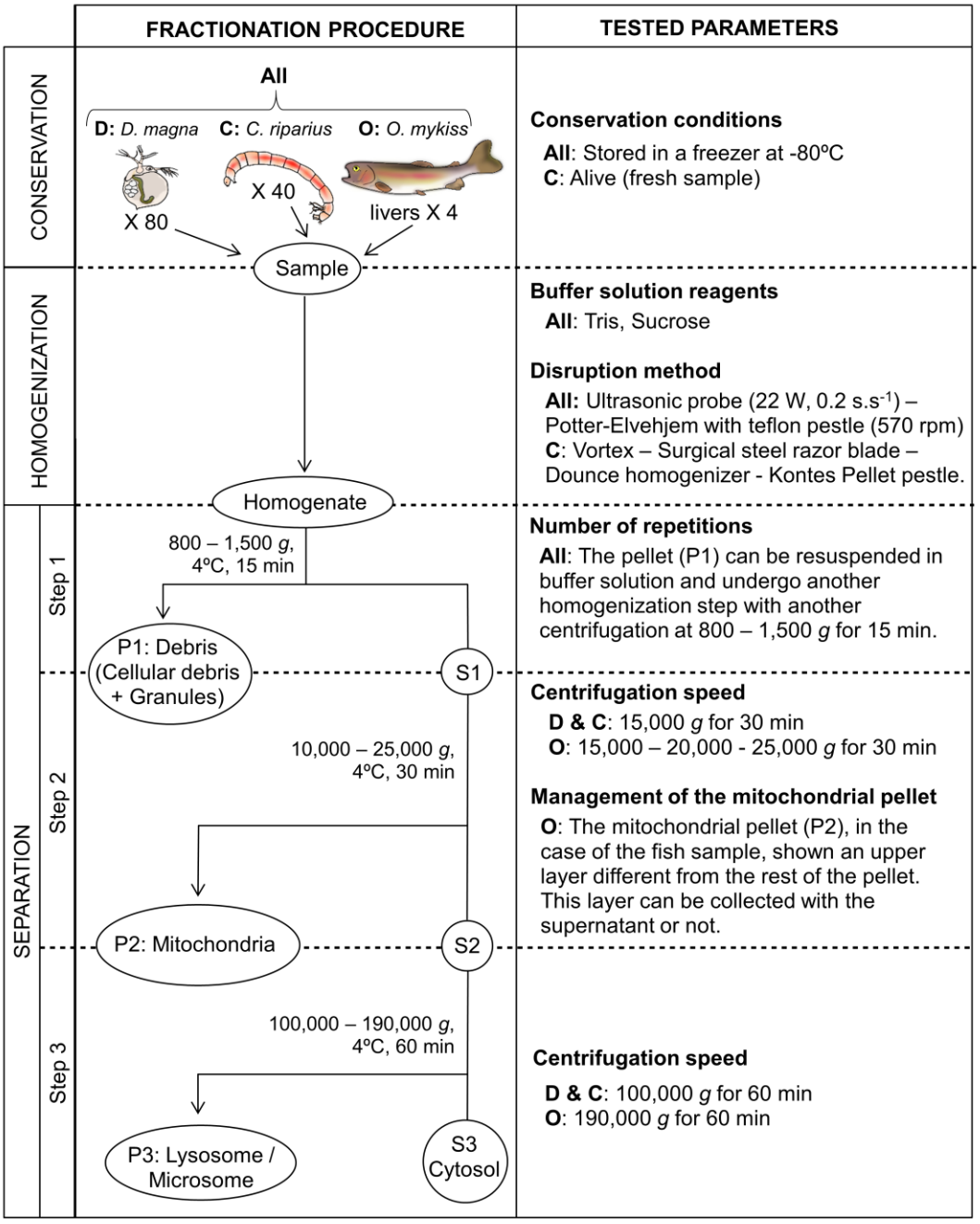

Figure 1. Subcellular fractionation procedure and its parameters subjected to a customization for each organism (P:Pellet / S:Supernatant; D: *D. magna*, C: *C. riparius*, O: *O. mykiss*).

Organisms and breeding conditions

D. magna and *C. riparius* were provided by the *Centre d'Expertise en Analyse Environnementale du Québec* (CEAEQ, Quebec City, QC, Canada). *O. mykiss* individuals were purchased from the *pisciculture des Arpents Verts* (Ste-Edwidge, QC, Canada) and were acclimated to laboratory conditions for at least 3 weeks prior to use. Before use, breeding water consisted of municipal drinking water that had been treated with activated carbon and aerated at least 24 hours to remove chlorine and chlorinated compounds from the water and to reach oxygen saturation. During the breeding period, aeration and a photoperiod of 16:8 h light:dark were maintained.

D. magna neonates less than 24-h old were bred at 21 ± 1°C by batches of 300 in 15 L polypropylene (PP) containers for one week. At the end of the breeding period, *D. magna* were transferred for 4 h in breeding water free of food to reduce their gut content.

Instars of *C. riparius* less than 48-h old were bred at 21 ± 1°C by batches of 30 individuals for 10 days in 500 mL polypropylene (PP) containers with 70 mg of an autoclaved artificial sediment made of 250-500 µm silica sand (30% dw), 106-250 µm silica sand (69.85% dw) and $CaCO_3$ (0.15% dw) and 460 mL of breeding water as recommended by SPE 1/RM/32 (1997). At the end of the breeding period, individuals were transferred for 24 h in breeding water free of food to reduce their gut content.

Three hundred 15-days old *O. mykiss* were bred in a 500-L tank at 15 ± 1°C until they reach 1 to 3 months of age before being used. Only livers were subjected to subcellular fractionation for the fish samples so a starving period was not added for this organism. At the end of the breeding period, individuals were removed from the tank, euthanized with clove essential oil and their livers were collected. These breeding and euthanization methods for *O. mykiss* followed recommendations from Environment Canada (SPE 1/RM/13, 2000).

At the end of each experiment, between 60-100 mg wet weight of tissues (i.e. 80-90 daphnids, 40-45 chironomids or one portion of a trout liver) were padded dry using Kimwipes® and pooled in 1.5 mL preweighed PP microcentrifuge tube, before being

stored at -80ºC.

Subcellular fractionation protocols

Centrifugations (< 25,000 *g*) were performed using an IEC Micromax centrifuge (Thermo IEC) whereas a WX ULTRA 100 centrifuge (Sorval, Ultra Thermo Scientific) equipped with a F50L-24 X1.5 rotor (Fisher Scientific) was used for ultracentrifugations (≥ 25,000 *g*).

Daphnia magna

The efficiency of three homogenization procedures, named I, II and III hereafter, were compared (Fig. 1). All procedures were tested in four replicates, and a temperature of 4°C was maintained during all steps, including homogenization and centrifugation.

Each *D. magna* sample was suspended in Tris-HCl (25 mM; OmniPur, affiliate of MERCK) sucrose buffer (250 mM; pH 7.4; Sigma Aldrich) at a ratio of 1:8 (weight [mg]: buffer volume [µL]) for procedures I and II, and 1:4 for the procedure III.

Procedure I: *D. magna* samples were ground by a motorized Potter-Elvehjem homogenizer equipped with a 2-mL teflon pestle (Cole Parmer U-04368) at 570 rpm for 2 s twice, with 30-s intervals.

Procedure II: *D. magna* samples were disrupted with an ultrasonic probe (Branson 250, with a 4.8 mm diameter microtip probe), at a power of 22 W, with pulses at 0.2 s s^{-1} (20%) for 1 min.

Procedure III: This procedure is a combination of the two others. *D. magna* samples were first ground with a Potter-Elvehjem pestle at 570 rpm 10 x 2 s, with a 30-s interval of rest between each homogenization period. The resulting homogenate was centrifuged at 800 *g* for 15 min (step 1 in figure 1). Then, the supernatant (S1) was collected and the pellet was resuspended in Tris-sucrose buffer at a ratio of 1:4 before being disrupted by following procedure II. The resulting homogenate was pooled and mixed using a vortex with the supernatant (S1).

After each homogenization procedure, an aliquot of 40 µL, corresponding to the homogenate fraction, was collected for estimating total enzyme activity and the

remaining homogenate was centrifuged at 800 *g* for 15 min to separate the debris fraction (P1) from the other fractions. Then, the resulting supernatant (S1) was collected and was subjected to a second centrifugation step at 15,000 *g* for 30 min (step 2 in figure 1). The pellet (P2) representing the mitochondrial fraction was then isolated and an ultracentrifugation step was performed on the remaining supernatant (S2) at 100,000 *g* for 60 min (step 3 in figure 1). The pellet (P3) was separated from the supernatant (S3) at this step. They stand respectively for the lysosomal/microsomal fraction and the cytosolic fraction.

Chironomus riparius

The best subcellular fractionation procedure obtained for *C. riparius* was similar to the one described for *D. magna* with a one-step homogenization involving a grinding of the sample with a Potter-Elvehjem homogenizer at 570 rpm, for 10 times 2 s, with a 30-s interval of rest between each homogenization period. This best protocol was tested either with samples stored at 80°C or with fresh samples. The description of the ten other fractionation protocols tested with their specific parameters are given in Table I in the assessment part of this article.

Oncorhynchus mykiss

For the subcellular fractionation protocol*, O. mykiss* samples were ground with a Potter-Elvehjem pestle for 2 s twice with 30-s intervals in Tris-Sucrose buffer at a ratio of 1:4. The resulting homogenate was centrifuged at 1500 *g* for 15 min. The supernatant (S1) was collected and the pellet was resuspended in Tris-Sucrose buffer at a ratio of 1:4 before being disrupted with an ultrasonic probe at 22 W, 0.2 s s^{-1} for 10 s. The homogenate was then pooled with the supernatant (S1), mixed with a vortex, and an aliquot of 40 µL, corresponding to the homogenate fraction, was collected. The remaining homogenate was centrifuged again at 1,500 *g* for 15 min (step 1 in figure 1). The resulting supernatant was then subjected to a second centrifugation step at 25,000 *g* for 30 min. The supernatant (S2) was collected and the pellet (P2) was isolated with the formed intermediate layer on top of it (step 2 in figure 1). Finally, an ultracentrifugation step was performed on (S2) at 190,000 *g* for 60 min and the pellet (P3), the lysosomal/microsomal fraction, was separated from the supernatant (S3), the cytosolic

fraction (step 3 in figure 1).

This customized protocol was also tested with the collection of the intermediate layer with the supernatant (S2). The seven other protocols tested are given in Table 2 in the assessment part of this article.

Efficiency of the subcellular fractionation procedure

The efficiency of each fractionation procedure was compared using specific enzymes expected to be present in the mitochondrial and cytosolic fractions. The lysosome separation was also investigated using an enzymatic biomarker but only during fine-tuning steps following the first enzymatic assays. This decision not to include the efficacy of lysosome separation in the enzymatic assay selection of the most promising method was motivated by the fact that lysosome separation is rarely performed in subcellular fractionation studies because, among other things, this subcellular component has a negligible mass and metal accumulation compared to other fractions in most cases, and also by the fact that the joint separation of lysosomes either with mitochondria or microsomes may differ between studies and authors (Bustamante et al., 2006; Podgurskaya and Kavun, 2006; Taylor and Maher, 2012). Finally, to confirm the separation and the nature of each subcellular fraction, supplemental analyses, including microscopic observations, or polymerase chain reaction (PCR), were carried out and described in Supplemental Information (SI; Figures S1, S2 and S3).

Enzymatic analyses

Enzyme reactions were performed in triplicate in 96-well microplates (microlon 200, Greiner Bio-one, Sigma Aldrich). The enzymatic activities were assessed by spectrophotometry with a Cary 50 MPR microplate reader (Varian) and expressed as units (IU) of enzyme activity per mg of wet weight tissue (IU or mIU mg^{-1}).

In order to solubilize membranes before initiating the enzymatic assays, 200 µL of Triton™ X-100 (1%; Molecular Grade, Fischer Scientific) in Tris buffer (25 mM, pH 7.4) was added to each pellet (debris, mitochondria/lysosome and lysosome/microsome) and was then mixed by vortex agitation.

Citrate synthase (CS; EC 2.3.3.1)

Citrate synthase (CS) is a mitochondrial biomarker located in the mitochondrial matrix. Its activity was measured according to Caron et al. (2016). In each well, 10 µL of each subcellular fraction was mixed with 170 µL of a reaction solution composed of phosphate buffer (1 mM, pH 8), Tris (100 mM; Merck), acetyl coenzyme A (0.2 mM; Sigma Aldrich) and 2-nitro-benzoic acid (0.1 mM; DTNB; Sigma Aldrich). After a 2-min period, a first measurement was taken at 412 nm over 7 min in order to set the baseline. Then, 20 µL of the oxaloacetate substrate (98%, Sigma Aldrich) was added, initiating the enzymatic reaction. The formation of DTNB-SH, assessed by measuring the increase in absorbance at 412 nm over 7 min, enabled the determination of CS activity. An extinction coefficient of 13.6 mM^{-1} cm^{-1} was used to calculate CS activity expressed as the formation of 1 µmol of DTNB-SH min^{-1} mg^{-1} at pH 8.0 and 25°C.

Cytochrome c oxidase (CCO; EC 1.9.3.1)

Cytochrome c oxidase (CCO) is a mitochondrial enzymatic biomarker located in the mitochondrial membrane. Its activity was measured according to the procedure optimized by Rosabal et al. (2014). The enzymatic reaction was started by mixing in the wells 10 µL of each subcellular fraction with 190 µL of a reaction solution composed of a phosphate buffer (0.1 M, pH 7) and the substrate cytochrome C (0.07 mM, >95%, Sigma Adrich) previously reduced by adding sodium dithionite (>85%, Sigma Aldrich) in aerated condition. For the reference sample, the 10 µL of subcellular fraction was replaced by 10 µL of $K_3Fe(CN)_6$ (>99%, Sigma Aldrich). The oxidation of 1 µmol of ferrocytochrome C by CCO, monitored by measuring the decrease in absorbance at 550 nm over 7 min, enabled the determination of CCO activity. An extinction coefficient of 18.5 mM^{-1} cm^{-1} was used to calculate CCO activity expressed as the oxidation of 1 µmol of ferrocytochrome C min^{-1} mg^{-1} at pH 7.0 and 25°C.

Lactate dehydrogenase (LDH; EC 1.1.1.27)

Lactate dehydrogenase (LDH) is a cytosolic biomarker. Its activity was measured according to Rosabal et al. (2014). In each well, 10 µL of each subcellular fraction was mixed with 170 µL of a reaction solution composed of a phosphate buffer (0.1 M, pH 7) and reduced nicotinamide adenine dinucleotide (0.16 mM, 98%, ß-NADH,

Sigma Aldrich). After a 2-min period of rest, a first measure was taken at 340 nm over 7 min in order to set the baseline. Then, 20 µL of the pyruvate substrate (5 mM, 99%, Sigma Aldrich) was added, initiating the enzymatic reaction. The oxidation of NADH to NAD^+ accompanying the reduction of pyruvate to lactate was monitored by measuring the decrease in absorbance at 340 nm for 7 min, and enabled the determination of LDH activity. An extinction coefficient of 6.22 mM^{-1} cm^{-1} was used to calculate LDH activity expressed as the oxidation of 1 µmol of NADH min^{-1} mg^{-1} at pH 7.0 and 25°C.

Acid phosphatase (E.C. 3.1.3.2)

Acid phosphatase is an enzyme located in the lysosome. The concentration of acid phosphatase of each subcellular fraction was measured using commercial colorimetric assays (CS0740, Sigma-Aldrich). In each well, 50 µL of each subcellular fraction or for the blank, 50 µL of a citrate buffer solution (0.09 M, pH 4.8), was mixed with 50 µL of a substrate solution composed of a citrate buffer solution (0.09 M, pH 4.8) and 4-nitrophenyl phosphate (5.39 mM) previously equilibrated to 37°C. In parallel, three wells were filled with 300 µL of a standard solution made by mixing 5 µL of a 4-nitrophenol solution (10 mM), diluted in 995 µL of NaOH (0.5 N). After a 10-min incubation period at 37°C, except for the wells containing a standard solution, the reaction was stopped by adding 0.2 mL of a NaOH (0.5 N) stock solution. The amount of 4-nitrophenol formed was assessed by measuring the absorption at 405 nm and enabled the determination of acid phosphatase activity. An extinction coefficient of 18.3 mM^{-1} cm^{-1} was used to calculate acid phosphatase activity reported as the hydrolyzation of 1 µmol of 4-nitrophenol phosphate per min^{-1} mg^{-1} at pH 4.8 and 37°C.

Calculations and statistical analyses

All enzymatic activities are presented as mean ± standard deviation (SD). For a given enzyme, enzyme total activity was measured as the sum of its enzyme activity in each fraction. The proportion of enzymatic activity for a given enzyme in a fraction was calculated by dividing the activity in the specific fraction multiplied by 100 by the sum of the activity in all fractions.

In order to assess the recovery of enzyme activity in the four subcellular fractions,

a 40-µL aliquot of homogenate was collected in each sample of all tested species after the homogenization step. Range values (min-max) of average enzyme activity recoveries for each species, considered as the ratio of the sum of enzyme activity in the four fractions (fraction enzyme activity divided by its mass) divided by the enzyme activity estimated on the 40-µL homogenate and multiplied by 100 were as follows (n = 13): CCO, 77.4-123%, CS, 87.7-93.6%, LDH, 78.2-131%.

An arcsine transformation was applied on every percentage data prior to statistical analysis. Data involving two treatments were compared using Student's t-test; if more treatments were compared a one-way ANOVA followed by a Tukey pairwise comparison test was performed. Homogeneity of variance and normality were always confirmed respectively by Levene's test and Shapiro-Wilk's test before any of this statistical test. When $p < 0.05$, results were considered as significantly different. Past statistics software (version 3.15) was used to perform statistical analyses.

Assessment

Subcellular fractions theoretically isolated from our procedures are: cytosol, lysosomes/microsomes, mitochondria and debris (Fig. 1). However, some fractions can be further divided. Hence, heat-sensitive proteins (enzymes) and heat-stable proteins (metallothioneins) can be isolated from the cytosolic fraction by heating followed by centrifugation. Also, debris can be divided into two subfractions (cellular debris and metal-rich granules) by using a treatment with NaOH followed by centrifugation (Wallace and Luoma, 2003). We cannot isolate these subfractions in this enzymatic validation study since heating or NaOH treatments would severely disrupt enzymatic activity.

In the following assessment, we compare the enzymatic results of all protocols tested for each species and we select the one considered as the most promising, i.e. the protocol that allows us to reach the highest yield of cells disruption efficiency while limiting the overlap between fractions. We then examine if our enzymatic results support the clear separation of fractions as predicted from the literature (henceforth called "predicted fractions": cytosol, lysosomes/microsomes, mitochondria and debris). When our results indicate that one of these predicted fractions is mislabelled, we propose a new

fraction (referred to as a "validated fraction") that will enhance the accuracy of interpretation of metal handling strategies in future studies.

Subcellular fractionation in the crustacean *Daphnia magna*

Three homogenization methods were tested for *D. magna*. For these three methods, total enzyme activities were measured (Fig. 2) and the proportion of enzyme activity in each fraction was assessed (Fig. 3).

With respect to cell disruption, the combined procedure using the Potter-Elvehjem pestle and the sonicator (protocol III) yielded significantly higher total enzymatic activities for LDH, a cytosolic enzyme, than the two one-step protocols (protocols I and II) (Fig. 2). Furthermore, the proportions of CCO, CS and LDH activities in the debris fraction were lower with protocol III (Fig. 3). Based on these results, protocol III was the most efficient to disrupt sample cells. The protocol using only the Potter-Elevhjem pestle was the least efficient, yielding less than a third of total LDH activity (Fig. 2) compared to protocol III, and leading to high proportions of enzymes in the debris fraction (between 29.0 ± 4.2 and 42.0 ± 1.8%, Fig. 3). The protocol using the sonicator only was therefore the second best option for cell disruption.

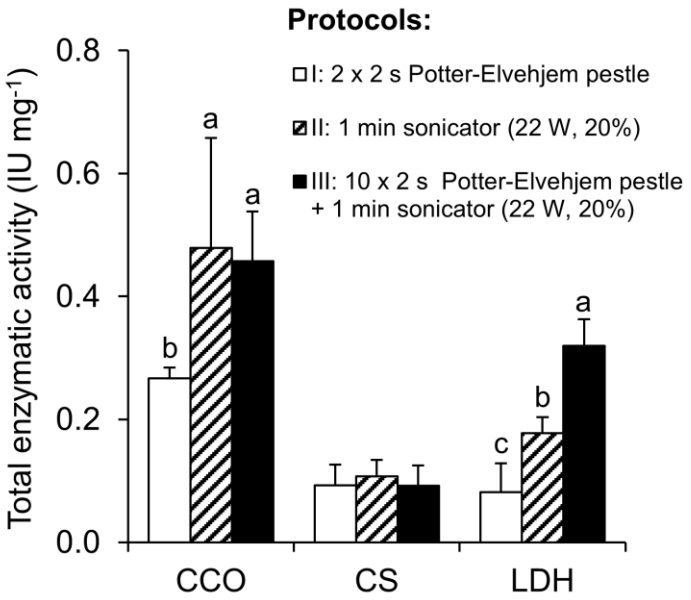

Figure 2. Total (mean ± SD; in IU mg^{-1} of biomass wet weight; $n = 4$) CCO (mitochondrial membrane biomarker), CS (mitochondrial matrix biomarker) and LDH (cytosolic biomarker) enzymatic activities in *D. magna* homogenates for each subcellular partitioning protocol tested. Error bars represent standard deviation. Different letters indicate a significant difference among the protocols for a given fraction (ANOVA, followed by Tukey pairwise comparison test, $p < 0.05$)

For the separation of fractions, protocol III was again the most efficient. Indeed, the proportion of cytosolic LDH found in the cytosol reached 92.0 ± 0.6% for protocol III, which was 43 and 11% higher than for protocols 1 and 2, respectively (Fig. 3c). Moreover, the highest proportions of mitochondrial enzymes (CCO and CS) isolated in the mitochondria fraction were obtained with protocol III (Fig. 3a,b). Protocol III was therefore identified as the most efficient one for *Daphnia* in this study.

Regardless of the protocol, 61.9 – 74.4% of the CS (an enzyme related to the mitochondrial matrix) activity was recovered in the cytosol whereas CCO (an enzyme bound to mitochondrial membrane) was mostly isolated in the mitochondrial fraction (Fig. 3a,b). These results suggest that all protocols lead to the leaking of the mitochondrial matrix into the cytosol fraction. We therefore identify new validated

fractions for this organism: the mitochondria fraction should be referred to as the "mitochondrial membrane" fraction, and the cytosol fraction should be identified as the "cytosol and mitochondrial matrix" fraction. These data represent a first attempt to adapt and validate subcellular metal partitioning protocols for a crustacean species and therefore provides a benchmark for future methodological studies on similar taxa.

It is likely that the use of sonicator is particularly useful for organisms with a reinforced chitinous exoskeleton. Lavoie et al. (2009) who optimized their protocol for two algae, *Chlamydomonas reinhardtii* and *Raphidocelis subcapitata*, also recommended, after comparing different homogenization methods, the use of a sonicator which enabled reaching the highest cell disruption efficiencies. In addition, our results with the two-step homogenization are comparable with those of Rosabal et al. (2014) who customized their protocol for *Chaoborus*, a zooplanktonic insect. On the basis of total enzyme activities measured in homogenates, these authors similarly recommended the use of a two-step homogenization.

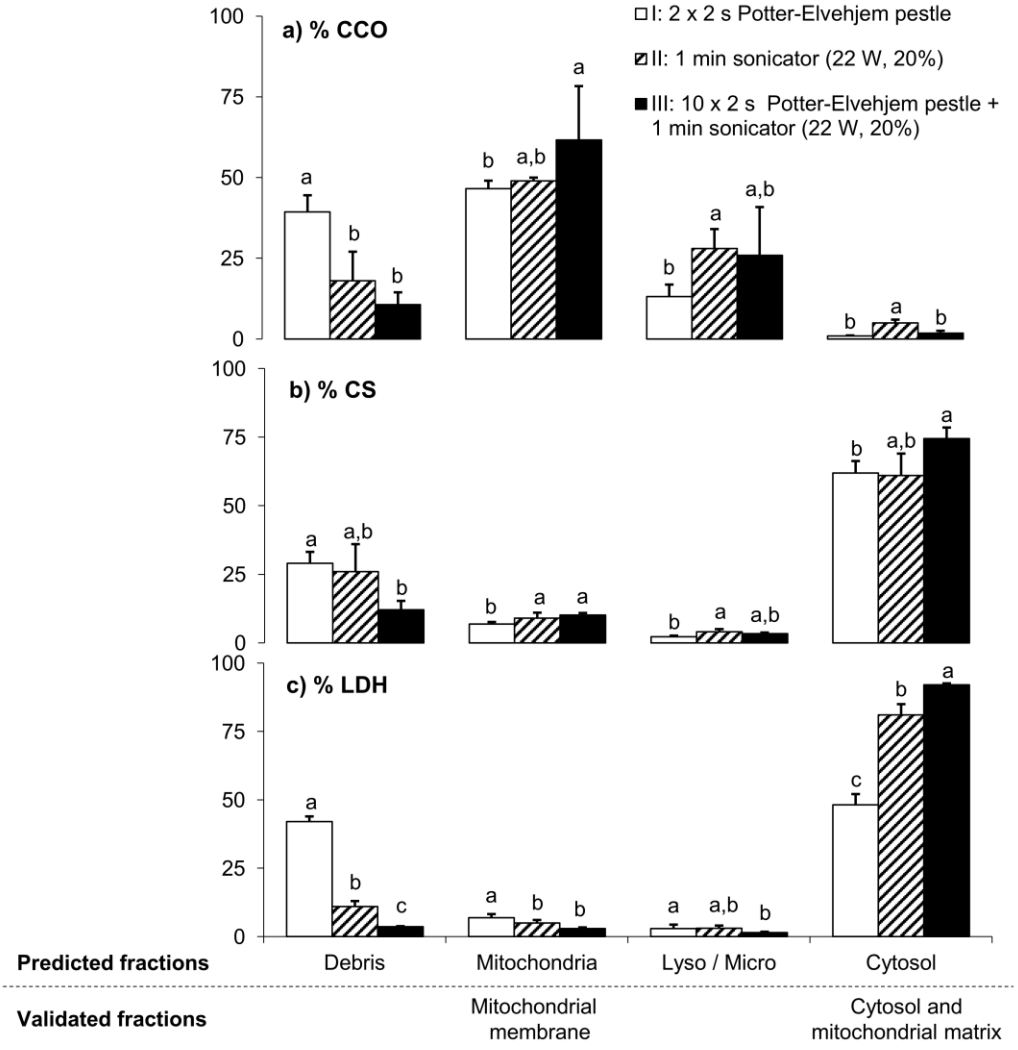

Figure 3. Percentages (mean ± SD; in %; $n = 4$) of a) CCO (mitochondrial membrane biomarker), b) CS (mitochondrial matrix biomarker) and c) LDH (cytosolic biomarker) enzymatic activities in each subcellular fraction of *D. magna*, for each subcellular partitioning protocol tested. Error bars represent standard deviations. Lyso / Micro: Lysosomes/Microsomes. Different letters indicate a significant difference among the protocols for a given fraction (ANOVA, followed by Tukey pairwise comparison test, $p < 0.05$).

Subcellular fractionation in the insect larvae *Chironomus riparius*

Homogenization procedure

For *C. riparius*, a total of 11 fractionation protocols involving different homogenization methods were tested. Unlike *D. magna* results, total enzyme activities

showed no trend (SI, Table SII), so these were not used to identify the best homogenization protocol for *C. riparius*.

Based on the results of the distribution of enzymes activites among fractions following each protocol (Table I), we used selection criteria to compare these 11 protocols, namely: (1) cell disruption was deemed successful if we measured less than 25% of the CCO and CS activity in the debris fraction and more than 90% of the LDH activity in the cytosol; (2) separation of fractions was considered acceptable if more than 50% of the CCO was recovered in the mitochondrial membrane fraction. The only protocol meeting all criteria was the one using the Potter-Elvehjem pestle 10 x 2 s, with a 30-s interval of rest between each homogenization period (Protocol 11, Table I). It was therefore selected as the best option tested for this species. This procedure was replicated four times and yielded standard deviations ranging from 0.1 to 6.2% for the different enzymatic tests, indicating that the method was highly replicable. Note that even with the most gentle homogenization method (e.g. cut in three pieces, one simple compression; Protocol 1), the proportion of CS activity recovered in the cytosol fraction exceeded 50% (Table I). This suggests that most of the mitochondrial matrix is fractionated along with the cytosol. As a result, similarly to *D. magna,* validated fractions with our best protocol for *C. riparius* differs from predicted fractions. Thus, the fraction previously called mitochondria should be referred to as mitochondrial membrane while the cytosol fraction contains the mitochondrial matrix.

Protocols including a homogenization procedure with the Dounce glass micro-pestle, until ten turns by hand, showed the poorest results for our two selection criteria (protocols 2-3). With this tool and method, on average, only 26 ± 1% of CCO activity was recovered on the mitochondrial fraction and more than 40% of the mitochondrial enzyme activities were recovered in the debris. Protocol 4, consisting in 25 turns of the Dounce glass micro-pestle by hand, enhanced the recovery of CCO in mitochondria to 56% and reduced the percentage of CS in debris below 25%. Nevertheless, the percentages of LDH in cytosol and CCO in debris did not meet our selection criteria with this protocol. Dounce Glass micro-pestles seem therefore inadequate tools for the homogenization of these organisms.

Even though protocols with the sonicator recovered less than 90% of LDH activity in cytosol (Protocols 6-7), the percentages of mitochondrial enzyme activities recovered in debris were close to the threshold of 25% set in our first criterium. Nonetheless with this tool, CCO activities in mitochondria did not exceed 50% as specified in our second selection criterium. Besides, 30 s of sonicator (protocol 6) in comparison with 15 s (protocol 7) decreased the proportion of CCO activity measured in mitochondria in favor of lysosomes/microsomes which reached a maximal value of 38%. Therefore, it seems that sonication can damage mitochondrial membranes.

This study is the second to customize and validate subcellular partitioning protocols for Diptera larvae. Indeed, Rosabal et al. (2014) performed the same enzymatic analysis to tailor the fractionation protocol for *Chaoborus albatus* larvae. Clear separation of fractions was obtained with a two-step homogenization protocol using mechanical disruption with Kontes pellet pestle followed by vortexing. However, their study was partly biased by the fact that enzymatic activities in debris were measured after NaOH addition, which likely led to losses of activity in this fraction. As a result, the proportion of enzyme activities attributed to non-debris fractions was overestimated. In particular, this bias led to apparent high CS activities in the mitochondria fraction (>80%), which seems unlikely considering our results.

Table I. Subcellular fractionation protocols tested for *C. riparius* and the proportion of enzymatic activities recovered in each fraction. Selection criteria are presented at the bottom of the table and protocols passing these criteria are highlighted in green. D, Debris; M, Mitochondria; L, Lysosomes/Microsomes; C, cytosol**.**

				Percentage of CCO (%)				Percentage of CS (%)				Percentage of LDH (%)			
#	**Homogenization tool**	**Procedure**	**n**	D	M	L	C	D	M	L	C	D	M	L	C
1	Surgical razor blade	Cut in 3 pieces	2	33 ± 12	33 ± 4	27 ± 9	6 ± 7	22 ± 7	4.2 ± 0.4	1.6 ± 0.5	72 ± 7	13 ± 12	1 ± 2	1.8 ± 0.4	84 ± 14
2	Dounce glass micro-pestle	1 simple compression in micro-tube by hand	3	72 ± 10	26 ± 9	2 ± 2	0.2 ± 0.1	39 ± 8	5 ± 2	1.1 ± 0.3	55 ± 8	9 ± 2	0.9 ± 0.3	0.9 ± 0.3	90 ± 2
3		10 turns by hand	1	46	25	29	0.2	42	4	2	53	15	0.3	2	84
4		25 turns by hand	1	29	56	15	0.3	24	8	2	66	7	1	2	90
5	Kontes pellet pestle	5 x 2 s	1	61	29	10	0.1	41	5	1.0	53	20	0.4	1	79
6	Sonicator (22 W, 20%)	15 s	1	26	44	26	3	29	3	2	67	15	2	2	82
7		30 s	1	20	36	38	6	23	7	2	68	29	4	4	64
8	Potter-Elvehjem pestle (570 rpm)	1 x 2 s	1	39	46	15	0.3	22	5	3	70	4	1	3	92
9		3 x 2 s + 2 x 2 s	1	50	34	16	0.2	34	5	2	59	9	0.8	2	89
10		5 x 2 s	3	40 ± 7	50 ± 7	10 ± 6	0.2 ± 0.0	24 ± 6	7 ± 2	3 ± 1	66 ± 7	4 ± 1	1 ± 1	2.4 ± 0.3	93 ± 2
11		10 x 2 s	4	23 ± 2	59 ± 2	17 ± 3	0.4 ± 0.1	16 ± 6	13 ± 3	4 ± 1	68 ± 6	5 ± 2	2 ± 1	3 ± 1	91 ± 3
		Selection criteria		CCO in D < 25%	CCO in M > 50%			CS in D < 25%							LDH in C > 90%

Effects of the conservation step

Since in all our protocols CS activities exceeded 50% in the cytosol (Table I), we investigated if modifying the conservation step could decrease mitochondrial leakage. The use of fresh samples rather than frozen ones led to a statistically significant change in the enzymatic activities in many fractions (Fig. 4), when using our selected protocol. In frozen samples, homogenization seemed successful, since, we found high LDH activities in the cytosol, and low CS and CCO activities in the debris. However, freezing led to a disruption of mitochondrial membranes, since most of the CS was found in the cytosol, (on average 68 ± 6%). When using fresh samples, most of the mitochondrial enzymes (CCO and CS) were found in the debris, indicating that homogenization was not as efficient as with frozen samples (Fig. 4). Indeed, CCO and CS activities measured in debris of fresh samples represented on average, both enzymes together, 63 ± 2% of their total activity, a yield three to four times higher than for the sample stored at -80°C. However, the use of fresh samples lessened the leakage of mitochondria, since less CS activity was detected in the cytosol. Overall, these results indicate that freezing *Chironomus* samples may lead to better homogenization but higher leakage of organelles.

Our results are consistent with other studies on the effects of a freezing period at -80°C on mitochondria (Fuller et al., 1989, Gwo and Arnold, 1992; Gnaiger et al., 2000). Freezing will remain an unavoidable step for most laboratory and field studies in limnological and ecotoxicological applications. For such studies where cryopreservation is used, we recommend the use of the validated fraction “Cytosol and mitochondrial matrix”. In some targeted experiments, cryopreservation could be avoided; in these cases, additional testing is recommended to increase homogenization efficiency.

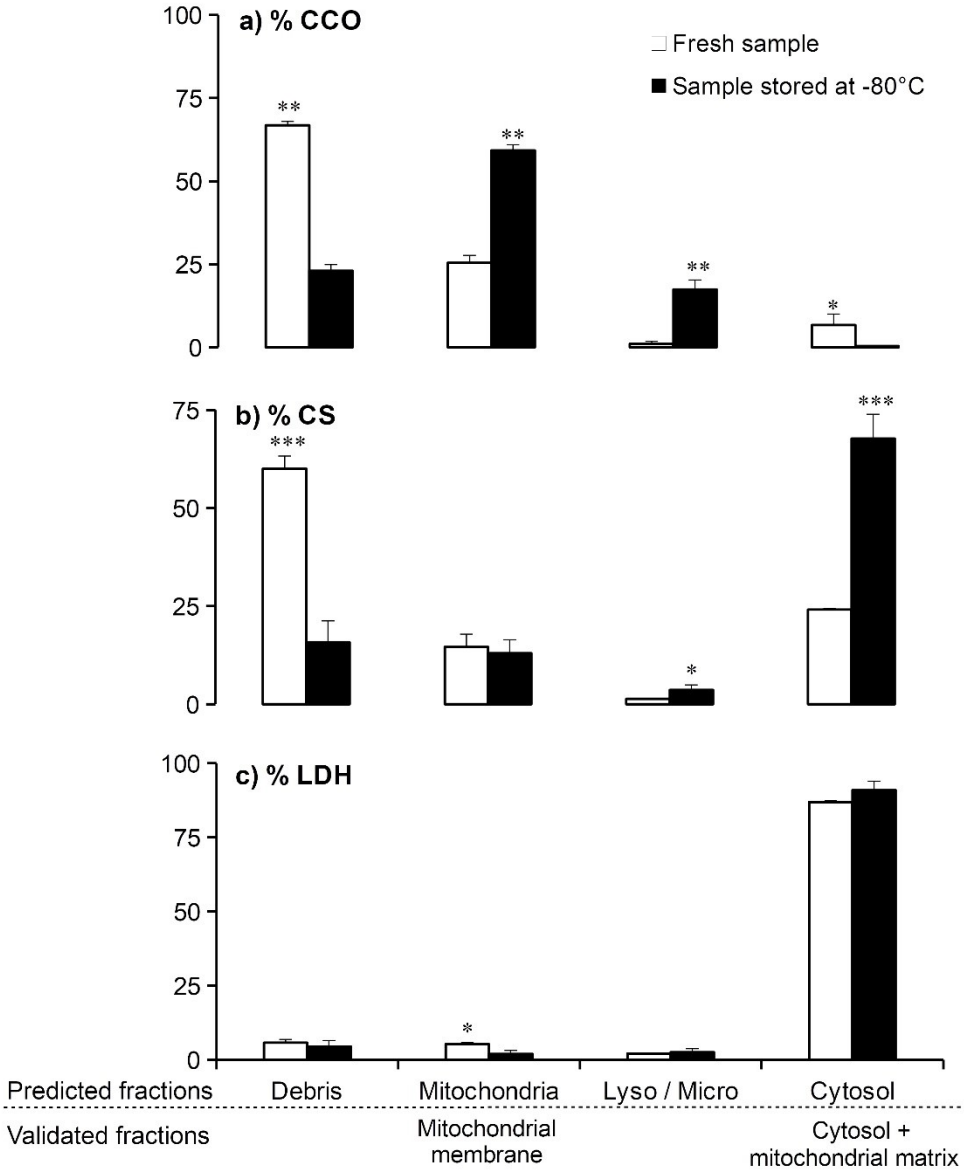

Figure 4. Percentages (mean ± SD; in %; $n = 4$) of a) CCO (mitochondrial membrane biomarker), b) CS (mitochondrial matrix biomarker) and c) LDH (cytosolic biomarker) enzymatic activities in each subcellular fraction of *C. riparius* with the most promising protocol performed either on fresh samples (white) or samples stored at -80°C (black). Error bars represent standard deviations. Lyso / Micro: Lysosomes / Microsomes. Asterisks denote a significant difference among treatments for a given fraction *$p < 0.05$, **$p < 0.01$, ***$p < 0.001$ (Student's t-test).

Subcellular fractionation in liver of the trout *Oncorhynchus mykiss*

Procedure adaptation

For *O. mykiss*, eight fractionation protocols involving different homogenization methods and centrifugation speeds for the recovery of the mitochondrial pellet (15,000 - 25,000 *g*) were tested (Table II). In these protocols, we encountered a lipid rich intermediate layer on top of the mitochondrial pellet for *O. mykiss* liver samples. This layer was left on the mitochondrial pellet for all protocols described in Table II. For *O. mykiss*, as for *C. riparius* and unlike *D. magna*, the measured total enzyme activities did not show any trend in all tested protocols (SI, Table SIII), so this parameter was not used to identify the best protocol.

Unlike the results obtained for *D. magna* and *C. riparius*, some of our tested protocols with *O. mykiss* yielded relatively high CS activities in mitochondrial fractions (Table II). Furthermore, none of these protocols with *O. mykiss* yielded more than 90% of LDH activity in the cytosol, one of the criteria we set for our selection of the best protocol for *C. riparius*. Therefore, based on the results of the distribution of enzymes activities among fraction following each protocol (Table II), our selection criteria for *O. mykiss* were: (1) cell disruption was deemed successful if we measured less than 10% of the CCO and CS activities in the debris fraction and more than 70% of the LDH activity in the cytosol; (2) separation of fractions was considered acceptable if more than 50% of the CCO and more than 40% of the CS activities were detected in the mitochondrial fraction.

The only protocols meeting all criteria were the ones involving the combined use of a Potter-Elvehjem pestle and a sonicator (Protocols 5 and 8; Table II). Among the methods meeting all criteria, the one that yielded the less CCO and CS in debris while yielding the most CS in the mitochondrial fraction and the most LDH activity in the cytosol, was protocol 8, which was identified as the best one. This protocol consisted in a first homogenization with the Potter-Elvehjem pestle used 2 s twice with a 30 s interval resting period and a second homogenization with the ultrasonic probe (10 s). This procedure was replicated four times and yielded standard deviations ranging from 0.4 to 6.5% for the different enzymatic tests, indicating that the method was highly replicable.

In comparison, protocols involving a single-step or a two-step homogenization with only the Potter-Elvehjem pestle (Table II; Protocols 1-3) led to a relatively high proportion of mitochondrial enzymes activities in the debris (*ca.* 19-33%), and a low percentage of CS activity in the mitochondrial fraction (< 30%). Thus, sonication as a second homogenization method helped improve both homogenization and fraction separation. However, the protocol including the sonicator for more than 10 s (Protocol 4) led to high CCO activity in lysosomes/microsomes (51%) and CS activity in cytosol (56%). We conclude that the use of the sonicator (22 W, 20%), while necessary, should be for less than 30 s in order to prevent important damages to mitochondria.

For the protocols using the Potter-Elvehjem pestle and the sonicator (for 10 s or less) (Protocols 6-8), we tested different centrifugation speeds to isolate mitochondria. The protocol with a 25,000 *g* centrifugation step was the only one to meet all criteria and also led to a better separation between the lipid layer on the mitochondrial pellet.

Our study is the first attempt to customize the subcellular fractionation protocol for a fish. In their study, Kamunde and MacPhail (2008) also performed CS enzymatic assays to validate their subcellular fractions of *O. mykiss* liver. They observed that CS activity was about ten times higher in the mitochondrial fraction than in the cytosolic fraction. However, they did not measure CS activity in their debris fraction. According to our results (Table II), with their single step homogenization procedure consisting in 6 turns of a 2-mL Potter-Elvehjem pestle, an important part of CS activity should be retained with the non-homogenized sample in the debris. Even with this assumption, it does not explain the difference between their CS activity results and ours and why their mitochondria appeared totally undamaged with their protocol. The osmolarity of the homogenization buffer might explain this difference, since they used a higher salinity buffer (phosphate buffer saline used by Kamunde and MacPhail (2008) as opposed to the Tris/Sucrose buffer used here). Indeed, the hypotonicity of the tris/sucrose buffer could have led to swelling and bursting of the mitochondria by osmose in our experiment. Therefore, additional tests with buffers of different osmolarities are recommended.

Table II. Subcellular fractionation protocols tested for *O. mykiss* and the proportions of enzymatic activities recovered in each subcellular fraction. Selection criteria are presented at the bottom of the table and protocols passing these criteria are highlighted in green. D, Debris; M, Mitochondria; L, Lysosomes/Microsomes; C, Cytosol

				Percentage of CCO (%)				*Percentage of CS (%)*				*Percentage of LDH (%)*			
#	**Homogenization**	**Centrifugation speed for Mitochondria**	**n**	*D*	*M*	*L*	*C*	*D*	*M*	*L*	*C*	*D*	*M*	*L*	*C*
1	Potter-Elvehjem pestle 5 x 2 s	15,000 *g*	1	33	39	22	6	34	17	6	43	11	10	0.0	79
2	Potter-Elvehjem pestle 10 x 2 s	15,000 *g*	1	23	42	30	5	21	22	8	49	5	11	0.0	84
3	Potter-Elvehjem pestle 2 x 2 s + Potter-Elvehjem pestle 2 x 2 s	15,000 *g*	1	19	53	24	4	22	29	8	41	6	17	0.0	77
4	Potter-Elvehjem pestle 5 x 2 s + Sonicator 30 s	15,000 *g*	1	16	29	51	5	17	14	13	56	5	8	0.0	88
5	Potter-Elvehjem pestle 2 x 2 s + Sonicator 5 s	20,000 *g*	1	10	72	16	3	8	40	6	46	9	21	7	70
6		15,000 *g*	1	9	66	23	2	10	44	5	42	4	22	0.0	74
7	Potter-Elvehjem pestle 2 x 2 s + Sonicator 10 s	20,000 *g*	1	6	58	35	1	5	35	17	43	2	21	0.0	77
8		25,000 *g*	4	6 ± 3	67 ± 7	26 ± 6	0.9 ± 0.7	7 ± 4	47 ± 5	14 ± 3	33 ± 6	1.8 ± 0.4	26 ± 3	0.0 ± 0.0	72 ± 3
	Selection criteria			CCO in D < 10 %	CCO in M > 50 %			CS in D < 10 %	CS in M > 40 %						LDH in C > 70 %

.

Characterisation and management of the lipid layer

In all protocols described in Table II, a dense whitish layer, presumably of a lipidic nature (SI, Fig. S4), formed over the mitochondrial pellet.

The presence of this potentially lipid-rich layer which did not occur with the two other organisms could explain why we collected a significantly higher proportion of CS and LDH activities in mitochondria with *O. mykiss* liver samples in comparison to *D. magna* and *C. riparius*. Indeed, a significant part of the mitochondrial matrix and the cytosol might be present in this layer, which has been included with the mitochondrial fraction in all procedures described in Table II. We investigated further this question by comparing enzymatic activity results of our best fractionation protocol performed with or without the layer on top of the mitochondrial pellet (Fig. 5).

Firstly, CCO activities among our fractions did not differ significantly depending on our management of the lipid-rich layer (Fig. 5a). Secondly, for CS and LDH, a significant part of the activities was transferred from the mitochondria to the cytosol when this layer was collected with the supernatant. The CS and LDH activities in mitochondria dropped respectively from $47 \pm 5\%$ to $23 \pm 4\%$ and from $26 \pm 3\%$ to $16 \pm 4\%$ and the cytosol fraction accumulated $60 \pm 3\%$ of the CS activity when the lipid layer was collected with supernatant (Fig. 5b,c).

Our results indicate that the layer contains both a part of the mitochondrial matrix and to a lesser extent of the cytosol. This suggests that, as for *D. magna* and *C. riparius,* mitochondria integrity are not completely preserved during the subcellular fractionation of *O. mykiss* liver and a significant part of its matrix accumulate in the layer observable on the top of the mitochondrial pellet. It is up to the operator to leave or not this layer with the mitochondrial pellet during fractionation. In the first case, it should be assumed that the mitochondrial matrix fraction contains both the mitochondrial membrane and cytosolic fractions whereas in the second case, as for *D. magna* and *C. riparius*, the mitochondrial fraction should be referred to as mitochondrial membrane and the cytosolic fraction as cytosol and mitochondrial matrix fraction.

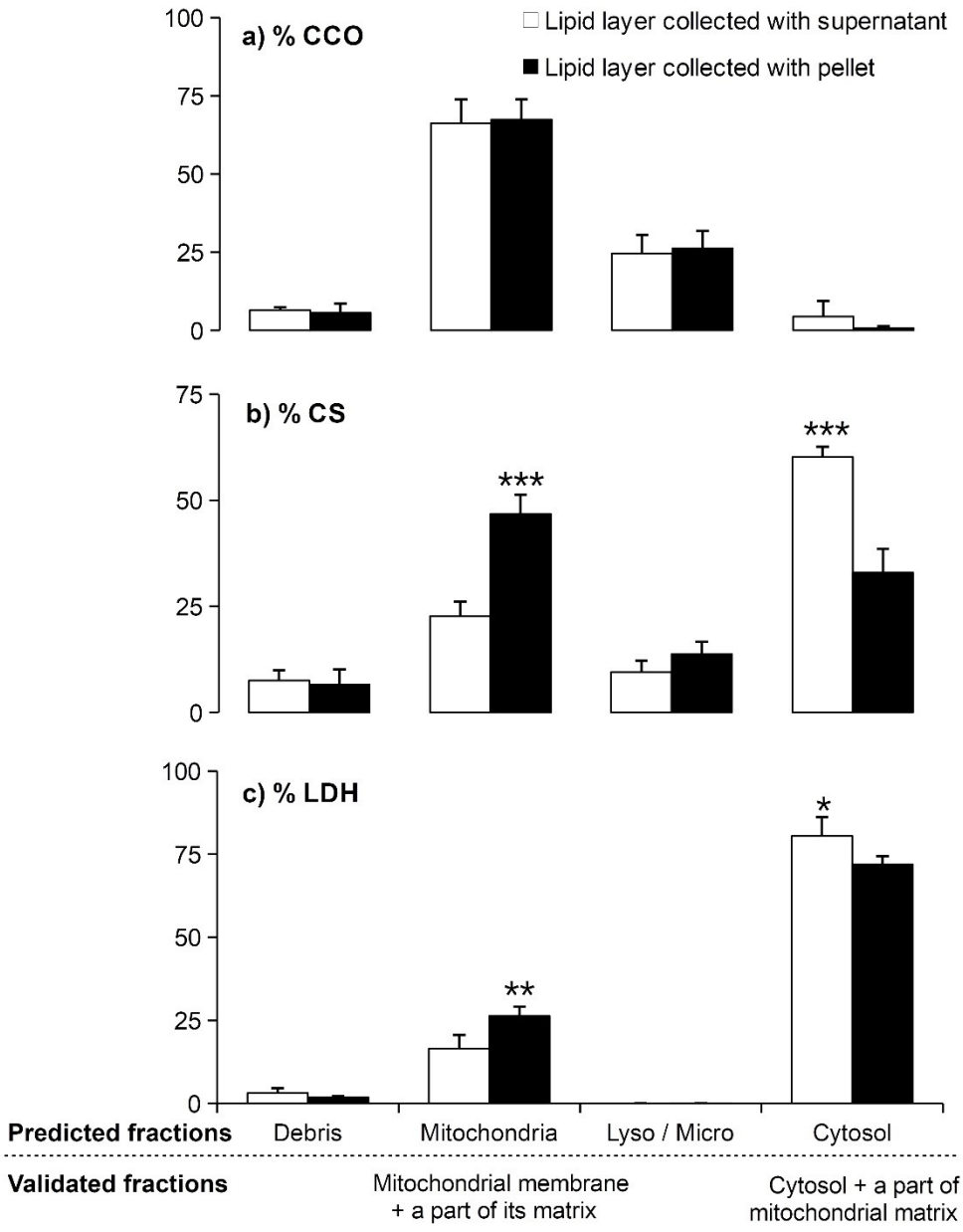

Figure 5. Percentage (mean ± SD; in %; $n = 4$) of a) CCO (mitochondrial membrane biomarker), b) CS (mitochondrial matrix biomarker) and c) LDH (cytosolic biomarker) enzymatic activities in each subcellular fraction of *O. mykiss* liver with the most promising protocol performed when the lipid-rich layer is collected with the mitochondrial pellet (black) or with the supernatant (white). Error bars represent standard deviations. Lyso / Micro: Lysosomes / Microsomes. Asterisks denote significance difference among treatments for a given fraction $*p < 0.05$, $**p < 0.01$, $***p < 0.001$ (Student's t-test).

Validation of lysosomes separation

The lysosome separation with the best fractionation protocols selected for each organism was also validated by performing an acid phosphatase (APHO) assay, an enzyme specific of lysosomes (Fig. 6). The decision not to include the efficacy of lysosome separation in the selection criteria for the most promising fractionation method was motivated by several reasons, the most important of which being that the joint separation of lysosomes either with mitochondria or microsomes may differ between studies and authors (Bustamante et al., 2006; Podgurskaya and Kavun, 2006; Taylor and Maher, 2012).

For all organisms, fewer than 20% of the APHO activity was recovered in the lysosome/microsome fraction (Fig. 6). For *D. magna,* mitochondrial fractions represented 50 ± 4% of the APHO activity. For *O. mykiss* the main part of APHO activity, around 80%, was split equally between the mitochondrial and the cytosolic fraction. Finally, for *C. riparius*, debris, mitochondria and cytosol accounted each for 35 ± 2%, 22 ± 2% and 30 ± 4% of the APHO activity, respectively.

According to our results, the fraction predicted as lysosomes/microsomes should be referred to as microsomes for our three organisms (Fig. 6). This isolated microsome fraction, as far as it has not been verified, remains a predicted fraction, however. For *O. mykiss* and *D. magna,* lysosomes and mitochondria were isolated together, and the fraction previously called mitochondria should be therefore referred to as mitochondria/lysosomes, particularly for *D. magna*.

Other authors working on *O. mykiss* liver and gills subcellular fractionation (Kamunde and MacPhail, 2008; Sappal et al., 2009) also performed APHO enzymatic activity assays to control the separation of lysosomes after subcellular fractionation. They concluded, by measuring almost ten times more APHO activity in lysosomes/microsomes fraction than in cytosol, that lysosomes were separated with microsomes. Taylor and Maher (2012) also reached this conclusion by comparing the APHO activities measured between mitochondria and lysosomes/microsomes fractions following the subcellular fractionation of a bivalve. In the first case (Kamunde and MacPhail, 2008; Sappal et al., 2009), the authors did not include the mitochondrial fraction in their APHO activity assay, and in the second case (Taylor and Maher, 2012) it is the cytosol that was missing.

Our results (Fig. 6) demonstrate that both of these two fractions can collect an important part of lysosomes and hence have to be included in any APHO activity assays on subcellular fractionation to validate lysosome separation.

Moreover, some studies already considered that the subcellular components recovered after a 10,000 – 15,000 *g* centrifugation step were a combination of mitochondria and lysosomes (Simon et al., 2005; Bustamante et al., 2006; Podgurskaya and Kavun, 2006). Therefore, in subcellular studies, lysosomes should definitely not be included with the microsomes without prior validation.

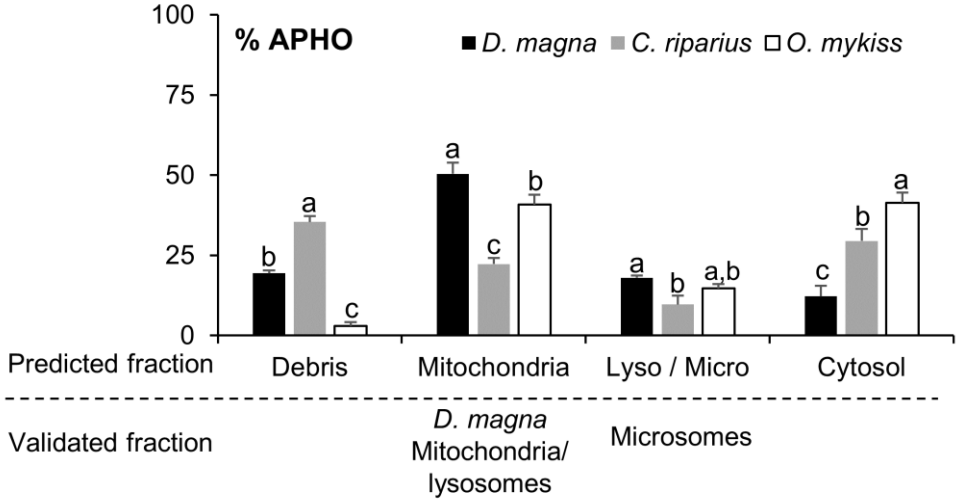

Figure 6. Percentage (mean ± SD; in %; $n = 3$) of acid phosphatase (lysosomal biomarker) activity in each subcellular fraction of *D. magna*, *C. riparius* and *O. mykiss* with their respective best fractionation protocol. Error bars represent standard deviation. Lyso / Micro: Lysosomes / Microsomes. Different letters indicate a significant difference among the organism for a given fraction (ANOVA, followed by Tukey pairwise comparison test, $p < 0.05$)

Discussion

Our results clearly indicate that subcellular fractionation protocols must be customized and validated for the fractionated organism. In the following paragraphs, the need to adapt the strength of the homogenization step to the hardness of the tissues of the organism or fractionated organ is discussed. Next, we examine the significant differences

revealed in our study between the predicted separated fractions and the validated ones and discuss their potential consequences on metal subcellular fractionation studies. Finally, the limitations of the approaches to optimizing fractionation protocols carried out and described in this study is discussed.

Homogenization step and debris fraction

In order to maximize cell disruption efficiency, customized protocols for each of our organisms involved a different homogenization step. Unlike *C. riparius*, for *O. mykiss* and *D. magna* a second homogenization step with ultrasounds was essential. Without it, other homogenization protocols for these two organisms led on average to 26.7 ± 7.3% of mitochondrial enzyme activities in debris fractions, suggesting that a significant part of non-homogenized samples remained in the debris. Lavoie et al. (2009) reached the same conclusion working on an alga, *Chlamydomonas reinhardtii*: without ultrasounds, other homogenization methods led to a significant part of non-homogenized sample in the debris. This can be an important source of bias when interpreting metal subcellular distribution data.

Simon et al. (2005) studied the uranium subcellular fractionation in gills and visceral mass of a freshwater bivalve following two different homogenization protocols. They observed that the homogenization step used did not impact U distribution in gills, but for visceral mass the proportion of U in the debris fraction was doubled when the homogenization step disruption efficiency increased by a factor of two. Therefore, an inadequate homogenization step could lead to a bias in the relative metal distribution among the different fractions. Consequently, data of all previous studies on metal subcellular distribution which did not include a homogenization step optimized for their fractionated organism should be considered with caution.

According to our results, it is imperative to adapt the strength of the homogenization step to the hardness of the tissues of the organism or fractionated organ. Some species such as *D. magna* and Crustacea in general, which have already been the subject of subcellular fractionation studies, e. g. *D. magna* (Lapointe et al., 2009; Wang and Guan, 2010), *Gammarus sp*. (Seebaugh and Wallace, 2009; Geffard et al., 2010),

Palaemontes sp. (Goto and Wallace, 2009; Seebaugh and Wallace, 2009), have a reinforced chitinous exoskeleton compared to other invertebrates. Thus, homogenization must be significantly more aggressive to avoid a bias in metal content in the debris fraction. The use of a sonicator appears, to some extent, to be the most appropriate approach for the homogenization step of these organisms. Conversely, our results on *C. riparius* tend to indicate that for some organisms with fragile tissues such as Diptera larvae and most likely many other insect larvae, homogenizations that could be considered relatively weak (e. g., trimmed with a surgical razor blade, two seconds of grinding with an Elvehjem-Potter pestle) lead to enzymatic results very close to our selection criteria in terms of homogenization efficiency (Table I). Hence, a bias in metal content in the debris fraction for Diptera larvae studies (Béchard et al., 2008; Rosabal et al., 2012; Gimbert et al., 2016) seems highly unlikely even though most of these studies have not optimized their homogenization methods to their fractionated species. Our results suggest as well that this tissue's fragility can be linked with the sample storage at -80°C prior to fractionation and that the fractionation of fresh Diptera larvae may call for a stronger homogenization; to our knowledge no studies have examined this point as they all used frozen samples. Finally, in addition to taking into account the general hardness of the tissue of the fractionated organism, the customization of the homogenization step for *O. mykiss* livers as well as for *D. magna* demonstrated the advantages of using a two-step homogenization method. For *O. mykiss* in particular, our results show that an increase in strength or time of homogenization does not enable to reach the threshold enzymatic selection criteria values for homogenization efficiency (Table II). Selection criteria values could only be met with a two-step homogenization method which had already been recommended in others studies on *D. magna* (Lapointe et al. 2009), *Lymnea stagnalis* (Ng et al., 2011), *O. mykiss* (Leonard et al., 2014), and *Chaoborus* larvae (Rosabal et al., 2014).

Separation steps

Mitochondria

Our study is the first to introduce the concept of validated subcellular fractions, differents from the predicted ones, and to demonstrate that, during fractionation, the

mitochondrial matrix is more likely recovered in the cytosolic than in mitochondrial fraction, especially for invertebrates.

Effects of this overlap between mitochondrial matrix and cytosol on the conclusions of metal subcellular distribution studies greatly depend on the research objectives. Thus, studies aiming to identify the so-called trophically-available metal (TAM) fractions will only be slightly affected by this overlap since most of them consider the TAM to be formed of the combination of the mitochondrial, lysosomes/microsomes, and cytosolic fractions at least (Wallace and Luoma, 2003; Rainbow et al., 2011). On the other hand, results from studies on metal subcellular detoxification, especially in invertebrates (Buchwalter et al., 2008; Dumas and Hare, 2008; Bednarska and Świątek, 2016), must be considered with caution if their mitochondrial fraction has not been previously validated for their working organism. Indeed, mitochondria is regarded as an important metal sensitive fraction. However, based on our results, the amount of metal accumulated in this fraction may be underestimated due to leakage of the mitochondrial matrix into cytosol; which seems almost inevitable with invertebrates such as *C. riparius* or *D. magna*.

Nonetheless, this predicted metal leakage from mitochondria to cytosol assumes that a significant part of metal measured in mitochondria was internalized in its matrix. In our case, regardless of the species, our best protocols recovered more than 60% of CCO activity in the mitochondrial fraction suggesting the accumulation of the mitochondrial membrane in the right fraction. Essential elements such as zinc, copper or iron have known functions in mitochondria and can form a pool in its matrix (Cobine et al., 2004; Pierrel et al., 2007). However, few studies worked on nonessential metal localization inside mitochondria, hence metal release from the mitochondrial matrix to the cytosol due to the subcellular fractionation protocol should be confirmed with new tests to assess the importance of this transfer. Indeed, the spillover of metals from the mitochondria to the cytosol fraction could be limited if most of the nonessential metals are located on the mitochondrial membrane instead of being located within the mitochondrial matrix.

Fractions can be pooled to infer on metal subcellular toxicity. For example, the Metal Sensitive Fractions (MSF) (Wallace et al., 2003; Campana et al., 2015) or the

Biologically Active Metals (BAM) (Taylor and Maher, 2012; Leonard et al., 2014) typically include both Heat-Denaturated Proteins (HDP) and mitochondria. As a result, if the mitochondrial matrix is pooled with HDP and not with Heat Stable Protein (HSP) after the heat treatment, metals in the mitochondrial matrix will likely still be measured in MSF and the overlap between this fraction and the cytosol will not affect the interpretation of subcellular toxicity.

Finally, in our study, we did not systematically test the effect of using different homogenization buffers, even though we performed some tests with mannitol, ethylenediaminetetraacetic acid or 4-(2-hydroxyethyl)-1-piperazineethanesulfonic acid (P-Y. Cardon unpubl.). Lavoie et al. (2009) demonstrated that the use of a growth medium (Modified High Salt Medium) instead of a sucrose buffer for the subcellular fractionation of an alga, *Chlamydomonas reihnardtii*, greatly reduced the proportion of CS activity recovered in cytosol. Furthermore, Kamunde and MacPhail (2008) recovered around ten times more CS activity in the mitochondria fraction from *O. mykiss* livers than in the cytosol fraction with their protocols using phosphate buffer saline as homogenization buffer . This result is very different from ours (for which less than half of CS activity was recovered in the mitochondria fraction) obtained with protocols involving Tris/Sucrose as homogenization buffer. Therefore, in some cases, an optimization of homogenization buffer could maybe be a potential solution to maintain mitochondria integrity during subcellular fractionation.

Lysosomes/microsomes

The separation of lysosomes was also validated in our study using our acid phosphatase assays results. These indicated that lysosomes should not be included with the microsomal fractions without prior validation. With our protocols customized for *O. mykiss* and *D. magna*, lysosomes and mitochondria are more likely recovered in the same fraction, as observed by others (Berthet and De Duve, 1951; Simon et al., 2005; Podgurskaya and Kavun, 2006). Furthermore, for *O. mykiss* and *C. riparius,* an important part of lysosomes was also recovered in the cytosol fraction. Therefore, interpretation of results of metal subcellular distribution from studies that considered the separation of lysosomes without prior validation must consider the potentially important overlap

between this fraction and the mitochondrial and cytosolic fractions (Giguère et al., 2006; Kamunde, 2009; Cooper et al., 2013). However, many studies did not make the separation between mitochondrial and microsomal fractions, labelling the fraction containing these two components as “organelles” (Wallace and Luoma, 2003; Rainbow et al., 2007; Geffard et al., 2010). This solution seems all the more relevant since the fraction named microsomes includes subcellular components, such as peroxisomes and other cellular vesicles that are very likely to end up with lysosomes. Also, the classification of lysosomes between metal sensitive and detoxified fraction differs according to the authors: some of them consider that lysosomal breakdown-products of metallothionein can form metal-rich granules (Nassiri et al., 2000) and that lysosomes should be included with the metal detoxified fraction (Bustamante et al., 2006; Frelon et al., 2013) while others indicate that metal can lead to a destabilization of lysosomes and therefore a leakage of their digestive enzymes into the cytosol (Eaton and Quian, 2002; Wadige et al., 2014) with a subsequent toxicity.

Limits of optimization approaches

The use of enzymatic biomarkers in our study enabled us to develop fractionation protocols that maximized the cell disruption yield by the homogenization step, and to validate the separation of mitochondrial membrane and matrix, lysosomes and cytosol. Thereby, enzymatic assays must be considered as relevant methods for assessing fractionation protocol efficiency and could be systematically performed as a quality control step in future subcellular fractionation studies. Nonetheless, these assays present certain limits.

Indeed, an important assumption of our enzymatic tests is that each enzyme is located in one and only one subcellular compartment. Nonetheless, some studies have demonstrated that, for instance, a CS isoform can also be found in cytosol in some species, notably yeast and fungus (Rosenkrantz et al., 1986; Hossain et al., 2016). Even if to our knowledge no isoforms of CCO, CS or LDH have been observed in invertebrate or fish cells, this potential source of uncertainty should be considered. As mentioned previously, LDH is often used to assess cell disruption efficiency of the homogenization step (Seib et al., 2006; Manunta et al., 2007; Rosabal et al., 2014). Our results show that

caution must be taken in interpreting LDH total activity for this purpose. Indeed, for *O. mykiss* and even more for *C. riparius,* we did not measure any correlation between the homogenization strength and the total LDH activity. For *C. riparius* samples stored at -80°C for instance, we measured as much total LDH activity with a simple compression as with our best homogenization procedure, that is to say 10 x 2 s of Potter-Elevhjem pestle (SI, Fig. S4). Therefore, to assess the homogenization cell disruption efficiency, total LDH activity should be systematically measured with other approaches, such as the assessment of the presence of mitochondrial enzymes in the debris fraction. Different methods can also be used to evaluate this efficiency like the measurement of the percentage of disrupted cells with an electronic particle counter (Lavoie et al. 2009) or through observation with a microscope (Simon et al., 2005; Bustamante et al., 2006; Penen et al., 2017).

Furthermore, the proportion of debris (i.e. membranes, granules and nuclei) recovered in the other fractions was not assessed in our work even though this fraction is a significant one with respect to mass and represents more than half of the metal accumulated in many studies (Wallace and Luoma, 2003; Rainbow et al., 2007; Leonard et al., 2014). Moreover, Andersson (1992) has already observed that DNA could accumulate in the cytosol following subcellular fractionation and our own PCR analysis (SI. Fig. S1) suggested the presence of DNA in every fraction following the fractionation of *D. magna*. However, we did not find a relevant enzymatic biomarker for the debris or at least the DNA in the literature. We explored the use of other methods such as PCR analysis (SI, Fig. S1), observation by scanning electron microscopy (SI, Fig. S2) or by fluorescence microscopy (SI, Fig. S3), but these lead only to presence-absence results.

Finally, the separation of the debris fraction between metal-rich-granules and cellular debris, and the separation of the cytosolic fraction between HSP and HDP were not examined in our study as the required treatment (addition of NaOH or heating) would degrade enzymes. Also, the possible transfer of metals from HDP to HSP during the heat treatment of the cytosol was pointed out by some authors (Bragigand and Berthet, 2003; Geffard et al., 2010). To verify this possible transfer, metal distribution results between HDP and HSP following the usual heat treatment can be compared with metal

distribution results between cytosolic compounds with a size exclusion chromatography method (Gimbert et al., 2016).

To conclude, other aspects than the ones treated in our study could be optimized in fractionation protocols. Even if enzymatic biomarker assays are a relatively fast and easy method to assess the subcellular fractionation protocol efficiency, it has several limits and could be complemented by other methods like microscopy to evaluate the efficiency of the whole fractionation protocol.

Comments and recommendations

The most promising subcellular fractionation protocols achieved for our organisms with their validated fractions are summarized in Fig. 7.

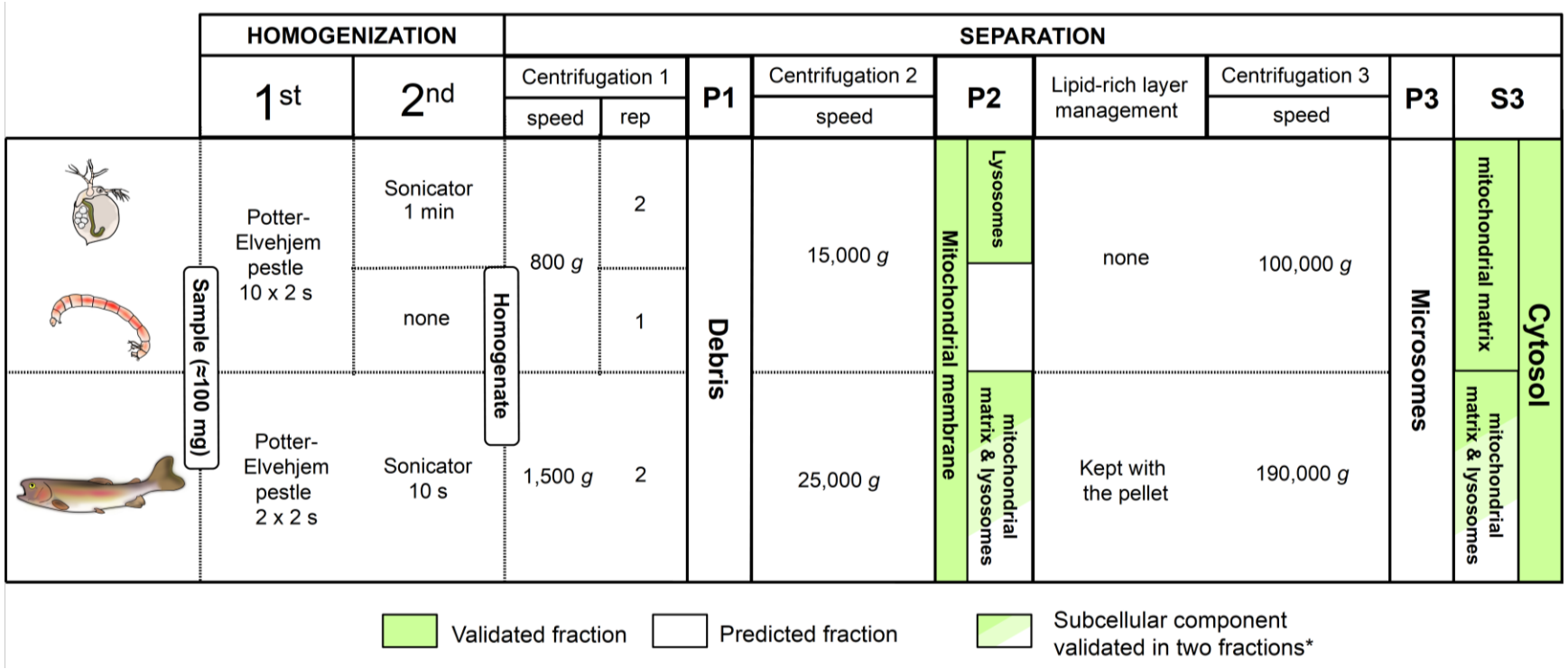

Figure 7. Most promising fractionation protocols achieved for each organism. *More than 30% of enzymatic activities was recovered in both fractions. P: Pellet; S: Supernatant; Rep: Number of repetition of this step.

Fractionation protocols set up for our three species (Fig. 7) reflect compromises between homogenization efficiency and adequate separation of subcellular components. As a result, it should be considered as a framework for future studies working on similar taxa. Also, according to our data, several recommendations can be suggested to improve future metal subcellular fractionation studies, both in terms of data quality and the relevance of their interpretations:

1. The homogenization method should be adapted to the target species to avoid a potential overestimation of metal accumulation in debris. For organisms with rigid external structure, such as *Daphnia sp.*, Crustacea, many zooplankters and potentially some aquatic and terrestrial insects, sonication seems the best tool to achieve a high cell disruption efficiency, although the use of a two-step homogenization approach appears particularly useful to reach this objective as well. For organisms with soft tissues sensitive to freezing/thawing such as *C. riparius* larvae and most likely many other insect larvae, a grinding with a Potter-Elvehjem pestle seems sufficient. For organs like liver, a two-step homogenization should be preferred while sonication appears as an effective tool but only when used for a second homogenization step. Measurement of the proportions of LDH, CCO and CS activities recovered in the debris fraction is a relevant method to assess these homogenization efficiencies.

2. Fractions separated with a subcellular fractionation protocol must be validated for the fractionated species prior to any analysis of metal subcellular distribution. Fraction-specific enzymes like CCO, CS, LDH and APHO can be used for validation. In any case, without prior validation, it should be assumed that an important part of mitochondrial matrix is recovered with the cytosol and that lysosomes are separated from microsomes.

3. The formation of intermediate layers on top of any subfraction pellet during fractionation, like the lipid-rich one observed for *O. mykiss* liver sample (Fig. 7), must be indicated, with description of its management, in any subcellular fractionation protocol. The management of this layer must be considered as an important parameter of the protocol.

Acknowledgments

This research was funded through the Natural Sciences and Engineering Research Council (NSERC) Discovery grant and an NSERC strategic grant (TRIVALENCE) to M. Amyot. We would like to thank the technical assistance provided by the *Ministère du Développement Durable, de l'Environnement et de la Lutte contre les Changements Climatiques* (MDDELCC, *division biologie et microbiologie*). This work was supported by the NSERC CREATE Mine of Knowledge network through a scholarship to P-Y. Cardon held a scholarship from NSERC. M. Amyot and C. Fortin are supported by the Canada Research Chair Program.

Supporting Information (SI)

Subcellular fractionation protocol tested

A summary of all fractionation protocols tested on *Daphnia magna, Chironomus riparius* and *Oncorhynchus mykiss* is given in Table SI. The homogenization step, in particular the tool used and the number of repetitions of that step, received the most attention regardless of the species.

Table SI. Summary of all fractionation protocol tested with each organism. Protocols involving a second homogenization step involve a second 1st centrifugation. Potter-Elvehjem pestle was used at 570 rpm and sonicator at a power of 22 W, with pulses at 0.2 s s^{-1} (20%)

	Conservation	Homogenization					Separation			
		1st		2nd		Buffer	Centrifugation 1 (15 min)	Centrifugation 2 (30 min)	Lipid-rich layer management	Centrifugation 3 (60 min)
		Tool	Procedure	Tool	Procedure		Speed	Speed		Speed
D. magna	-80°C	Potter-Elvehjem pestle	2 x 2 s	none		Tris 25 mM, Sucrose 250 mM	800 *g*	15,000 *g*	none	100,000 *g*
			10 x 2 s	Sonicator	1 min					
		Sonicator	1 min	none						
C. riparius	-80°C	Surgical razor blade	Cut in 3 pieces	none			800 *g*	15,000 *g*	none	100,000 *g*
		Dounce glass micro-pestle	1 simple compression in micro-tube by hand	none						
			10 turns by hand	none						
			25 turns by hand	none						
		Kontes pellet pestle	5 x 2 s	none						
		Sonicator	15 s	none						
			30 s	none						
		Potter-Elvehjem pestle	1 x 2 s	none						
			3 x 2 s	Potter-Elvehjem pestle	2 x 2 s					
			5 x 2 s	none						
			10 x 2 s	none						
	Alive		10 x 2 s	none						
O. mykiss	-80°C	Potter-Elvehjem pestle	10 x 2 s	none			1,500 *g*	15,000 *g*	Collected with the pellet	190,000 *g*
			5 x 2 s	none						
				Sonicator	30 s					
			2 x 2 s	Potter-Elvehjem pestle	2 x 2 s					
				Sonicator	5 s			20,000 *g*		
					10 s			15,000 *g*		
								20,000 *g*		
								25,000 *g*		
								25,000 *g*	Collected with the supernatant	

PCR

Following fractionation, DNA was extracted in each fraction by using DNeasy Blood & Tissue kit (Qiagen, Toronto, Canada). PCR were performed using iTaq^{TM} DNA Polymerase (Bio-Rad, Mississauga, Ontario), and by using a Bio-Rad CFX96 Touch Real-Time PCR Detection System (Bio-Rad, Mississauga, Ontario) with the following program: 95ºC for 3 min, 40 cycles of 95ºC for 30 s and 72ºC for 30 s (Fig. S1). PCR primer sequences for the nuclear genes coding for Monooxygenase and Glutathione-S-transferase were chosen from Poynton et al. (2008) works on *D. magna*, and were ordered from the Custom DNA Oligos services of Sigma-Aldrich Canada (Oakville, Ontario).

Both nuclear genes were observable in every fraction (Fig. S1). Therefore, we should assume the presence of DNA in every fraction following *D. magna* fractionation with our protocol. This can be a potential source of bias when interpreting metal subcellular distribution data.

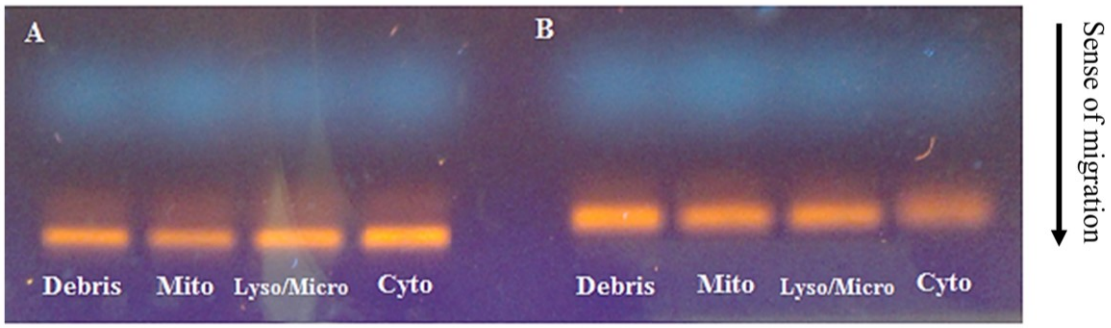

Figure S1. PCR result on *D. magna* for A, monooxygenase and B, glutathione-S-transferase.

Scanning electron microscopy (SEM)

Fresh samples of debris pellets were prepared for SEM following the method of Hayat 1978, an exception was made for the drying step, which was done with Hexamethyldisilazane (HMDS), as in Bray et al. (1993).

On each picture (Fig. S2), nuclei were observed among cellular debris. Therefore, the presence of this subcellular component in this fraction following fractionation is confirmed for *C. riparius* and *D. magna* with our most promising protocol.

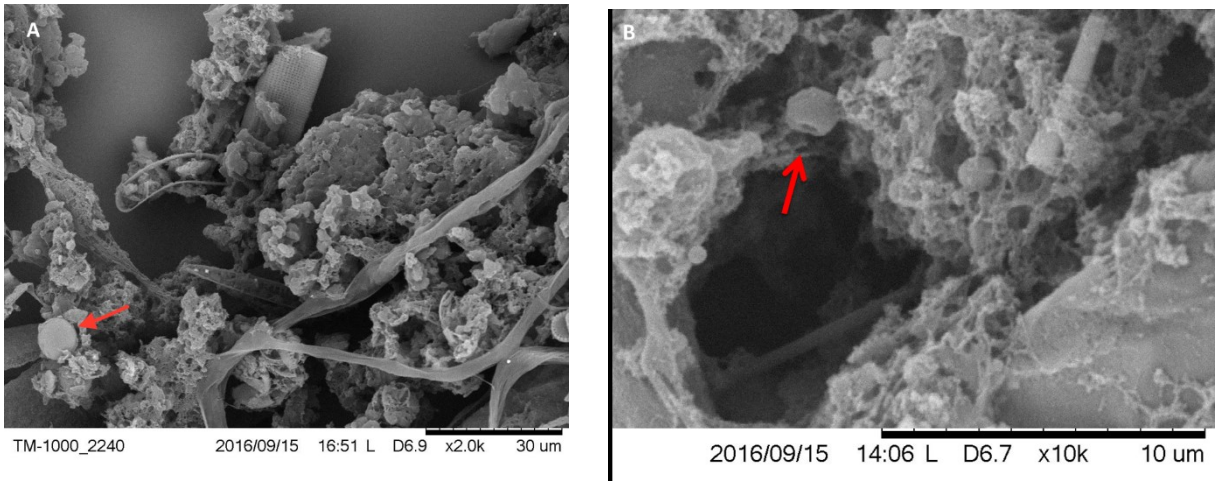

Figure S2. Pictures of fresh samples of *C. riparius (A)* and *D. magna* (B) debris pellet observed by Scanning electron microscopy (SEM). Red arrows indicate the presence of nuclei.

Fluorescence microscopy

Fresh samples of debris pellets were incubated in an Acridine Orange solution at 10 mg mL^{-1} in nanopure water (ThermoFisher Scientific, Ontario, Canada), and were observed after decantation by epifluorescence (Fig. S3) under a Leica DMR microscope using a Leica I3 Filter Cube (Leica Microsystems, Ontario, Canada).

The observation of fresh samples of *C. riparius* debris pellet by fluorescence microscopy confirmed our conclusion from the Fig. S2. Indeed, in Fig. S3 we also observed nuclei in debris pellet and confirmed the presence of this subcellular component in this fraction.

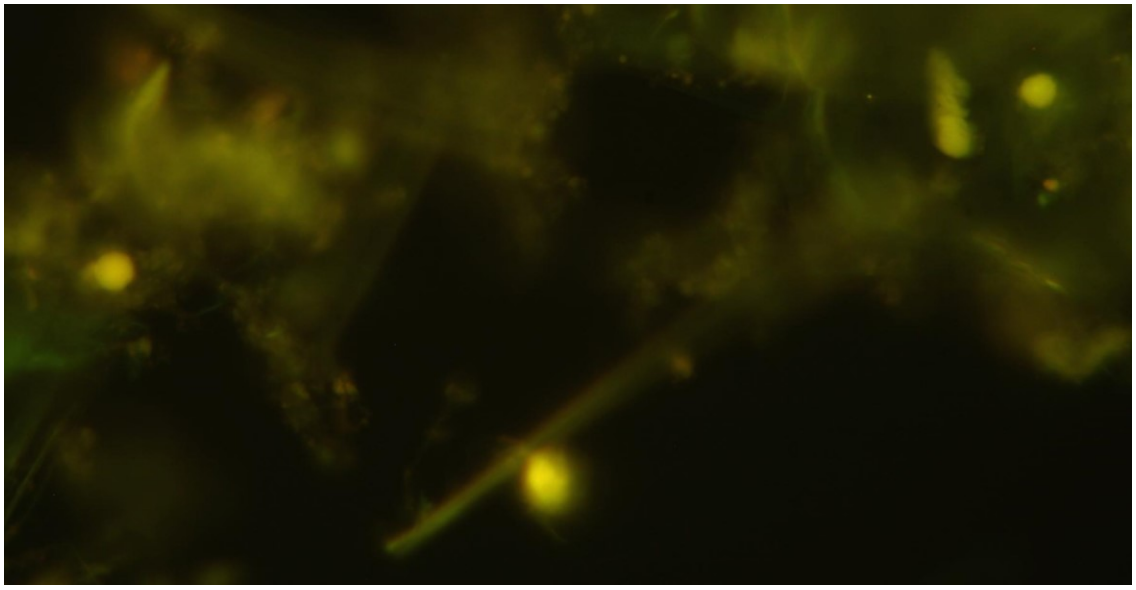

Figure S3. Picture of a fresh sample of *C. riparius* debris pellet observed by fluorescence microscopy

Total enzymatic activities in *C. riparius* and *O. mykiss*

Total CCO, CS and LDH activities recovered in *C. riparius* and *O. mykiss* homogenates with all tested protocols are given respectively in Tables SII and SIII.

Total CCO, CS and LDH enzymatic activities in *C. riparius* homogenates did not appear to be linked with the presumed strength of the homogenization step.Thus, for *C. riparius* the procedure consisting in cutting the sample into three pieces with a surgical razor blade (protocol 1, Table SII) leads, on average, to more total CCO activity, 1.29 ± 0.26 IU mg^{-1}, than using the Potter-Elvehjem pestle 10 x 2 s (protocol 11, Table SII), 1.06 ± 0.09 IU/mg, the latter being the most promising for *C. riparius*. In addition, with the latter protocol, we measured as much total LDH activity as with a simple compression by hand in a micro-tube (protocol 2, Table SII), 0.23 IU mg^{-1}. Similarly, for *O. mykiss* homogenization procedure 4 (Table SIII) leads to measure less total enzymatic activity, regardless of the enzyme, than the homogenization procedure 5 which consists of the same two-step homogenization but with shorter homogenization periods.

Our results with *C. riparius* and *O. mykiss* do not allow us to use total LDH activity to evaluate the cell disturbance efficiency of the homogenization step as performed with

D. magna in our study and also in other studies (Seib et al., 2006; Manunta et al., 2007; Rosabal et al., 2014).

Table SII. Total (mean ± SD if n>1; in IU mg^{-1}) CCO, CS and LDH enzymatic activities in *C. riparius* homogenates for each subcellular partitioning protocol tested

				Total enzymatic activity (IU mg^{-1})		
#	**Homogenization tool**	**Procedure**	**n**	**CCO**	**CS**	**LDH**
1	Surgical razor blade	Cut in 3 pieces	2	1.29 ± 0.26	0.21 ± 0.02	0.16 ± 0.09
2	Dounce glass micro-pestle	1 simple compression in micro-tube by hand	3	0.70 ± 0.26	0.25 ± 0.09	0.23 ± 0.07
3		10 turns by hand	1	0.72	0.24	0.18
4		25 turns by hand	1	1.56	0.27	0.24
5	Kontes pellet pestle	5 x 2 s	1	0.95	0.19	0.19
6	Sonicator (22 W, 20%)	15 s	1	1.16	0.34	0.20
7		30 s	1	1.81	0.24	0.11
8	Potter-Elvehjem pestle (570 rpm)	1 x 2 s	1	1.52	0.38	0.29
9		3 x 2 s + 2 x 2 s	1	0.86	0.27	0.21
10		5 x 2 s	3	1.42 ± 0.12	0.35 ± 0.12	0.23 ± 0.05
11		10 x 2 s	4	1.06 ± 0.09	0.55 ± 0.07	0.23 ± 0.03

Table SIII. Total (mean ± SD if n>1; in IU mg^{-1}) CCO, CS and LDH enzymatic activities in *O. mykiss* homogenates for each subcellular partitioning protocol tested

				Total enzymatic activity (IU mg^{-1})		
#	**Homogenization**	**Centrifugation speed for Mitochondria**	**n**	**CCO**	**CS**	**LDH**
1	Potter-Elvehjem pestle 5 x 2 s	15,000 *g*	1	1.9	0.24	10
2	Potter-Elvehjem pestle 10 x 2 s	15,000 *g*	1	2.1	0.23	14
3	Potter-Elvehjem pestle 2 x 2 s + Potter-Elvehjem pestle 2 x 2 s	15,000 *g*	1	3.6	0.23	14
4	Potter-Elvehjem pestle 5 x 2 s + Sonicator 30 s (22 W, 20%)	15,000 *g*	1	2.2	0.20	13
5	Potter-Elvehjem pestle 2 x 2 s + Sonicator 5 s (22 W, 20%)	20,000 *g*	1	3.8	0.33	23
6	Potter-Elvehjem pestles 2 x 2 s + Sonicator 10 s (22 W, 20%)	15,000 *g*	1	4.2	0.34	20
7		20,000 *g*	1	2.6	0.22	14
8		25,000 *g*	4	3.3 ± 0.68	0.21 ± 0.02	14 ± 4.0

Lipid extraction

The single-step procedure of lipid extraction developed by Axelsson and Gentili (2014) was performed on the supernatant and intermediate layer obtained after centrifugation of mitochondria for both *O. mykiss* and *D. magna* (Fig S4).

The intermediate layer observable on the top of the mitochondrial pellet of *O. mykiss* liver sample showed a systematic greasy appearance. In order to investigate this, lipid analyses were performed on the clear supernatant (Fig. 1, S2) and the mitochondrial pellet (Fig. 1, P2) intermediate layer of *O. mykiss* and *D. magna* (Fig. S4). Percentage lipid content of the clear supernatant did not show any difference between the two species and represented on average 1.3 ± 0.3 % of the clear supernatant mass. For *O. mykiss* however, the percentage lipid content of the intermediate layer reached from 2.6 to 7.5 % of the mass of this layer. These results tend to indicate that the intermediate layer appearing on top of the mitochondrial pellet of *O. mykiss* liver samples, which had already been reported on other species and organs (unpublished data), is lipid-rich and could be the result of the species/organ lipid content.

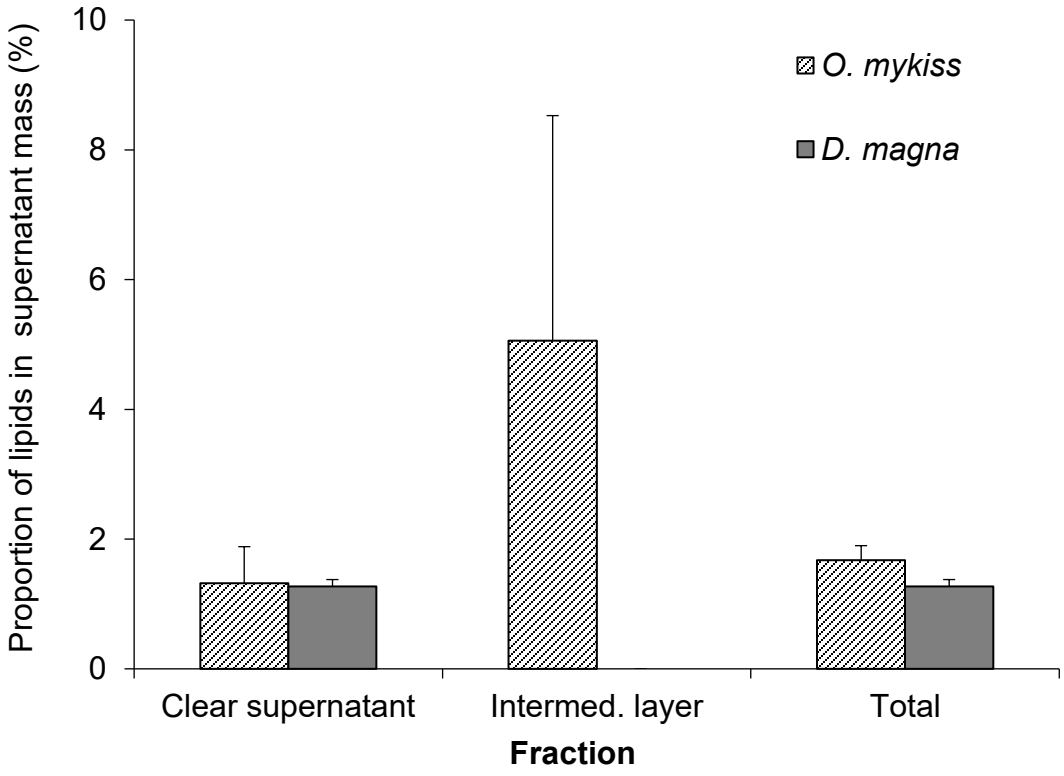

Figure S4. Proportions of lipids (mean ± SD; in %, n=3) in the total supernatant mass, in the clear supernatant and the intermediate layer of *O. mykiss* and *D. magna* obtained after centrifugation of the mitochondria fraction. Total stand for the two layers measured together.

CHAPITRE 2. Toxicité et gestion intracellulaire de l'Y chez trois organismes dulcicoles : *Daphnia magna*, *Chironomus riparius* et *Oncorhynchus mykiss*

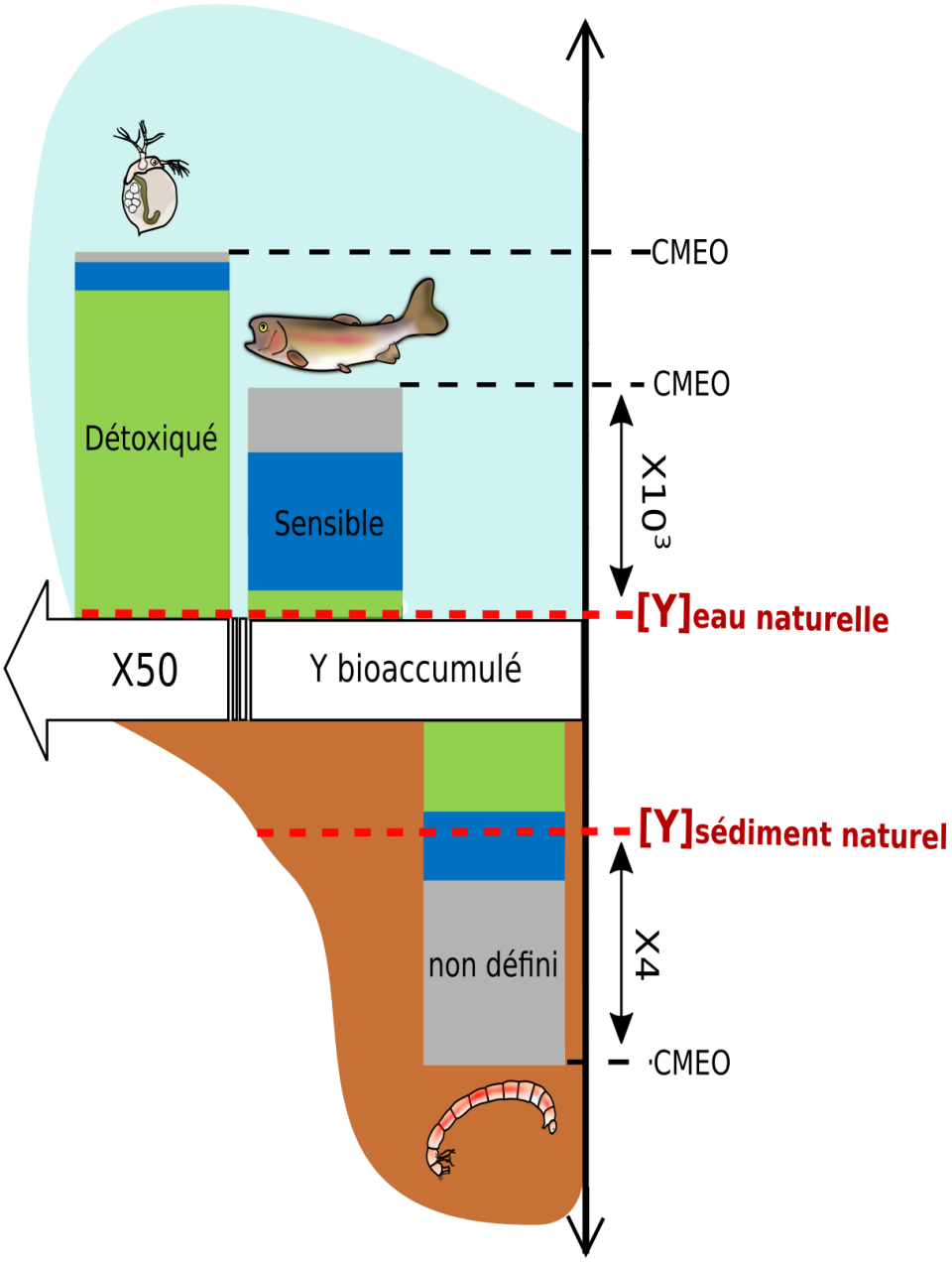

Toxicity and subcellular fractionation of yttrium in three freshwater organisms: *Daphnia magna, Chironomus riparius* and *Oncorhynchus mykiss*.

Authors: Pierre-Yves Cardon[1], Gaëlle Triffault-Bouchet[2], Antoine Caron[1], Maikel Rosabal[3], Claude Fortin[4], and Marc Amyot[1*]

[1] GRIL, Université de Montréal (UdeM), Département de sciences biologiques, Pavillon Marie-Victorin, 90 avenue Vincent-d'Indy, Montréal (Québec), Canada, H3C 3J7

[2] Centre d'expertise en analyse environnementale du Québec (CEAEQ), Division de l'écotoxicologie et de l'évaluation du risque, 2700 rue Einstein, Québec (Québec), Canada, G1P 3W8

[3] GRIL, Université du Québec à Montréal (UQAM), Département des sciences biologiques, 141 avenue du président-Kennedy, Montréal (Québec), Canada, H2X 1Y4

[4] Institut National de la Recherche Scientifique, Centre Eau Terre Environnement (INRS-ETE), 490 rue de la Couronne, Québec (Québec), Canada, G1K 9A9

In prep

Abstract

Demand for rare earth elements (REE) has exploded since the 1990s leading to the development of many mining projects worldwide. However, little is known on how organisms can handle these metals in natural aquatic systems. Through laboratory experiments, we assessed the chronic toxicity and subcellular fractionation of yttrium (Y), one of the four most abundant REE, in three freshwater organisms commonly used in aquatic toxicology: *Daphnia magna*, *Chironomus riparius* and *Oncorhynchus mykiss*. In bioassays using growth as an endpoint, *C. riparius* was the only organism showing toxicity at Y exposure concentrations close to environmental ones. Lowest observable effect concentrations (LOEC) of Y assessed for *D. magna* and *O. mykiss* were at least 100 times higher than Y concentration in natural freshwater. A negative correlation between Y toxicity and water hardness was observed for *D. magna*. When exposed to their respective estimated LOEC, *D. magna* bioaccumulated 15 to 45 times more Y than the other two organisms exposed to their own LOEC. This former species sequestered up to 75% of Y in the NaOH-resistant fraction, a putative metal detoxified subcellular fraction. To a lesser extent, *C. riparius* bioaccumulated 20 to 30% of Y in this detoxified fraction. In contrast, Y subcellular distribution in *O. mykiss* liver did not highlight any notable detoxification strategy; Y was accumulated primarily in mitochondria (ca. 32%), a putative metal sensitive fraction. This fraction was also the main sensitive fraction where Y accumulated in *C. riparius* and *D. magna*. Hence, Y interaction with mitochondria could be involved in its toxicity. In conclusion, there is a wide range of cellular handling strategies for Y, with *D. magna* accumulating high quantities but sequestering most of it in detoxified fractions, whereas *O. mykiss* tends to accumulate less Y but in highly sensitive fractions.

Introduction

Rare earth elements (REE) global demand is increasing since the 1990s (Alonso et al., 2012; Massari and Ruberti, 2013) as a result of REE use in almost all activity sectors, from high technology and electrification of transport, to medicine and agriculture (Gwenzi et al., 2018). Therefore, the contamination of water ecosystems by these metals from mining activity, agriculture, and the disposal of urban and electronic wastes, is of growing concern for environment protection agencies. Contamination of freshwater ecosystems contaminated by REE have already been reported (Atibu et al., 2016; Kulaksız and Bau, 2011).

Some studies on REE toxicity on freshwater organisms concluded that even if REE is a group of metals with similar chemical properties, toxicity differences have been observed between heavy REE (HREE) and light REE (LREE) (Borgmann et al., 2005; Cui et al., 2012). Among the four most abundant REE, yttrium (Y) is the only one classified as a HREE. Nevertheless, to our knowledge, in comparison with lanthanum (La), cerium (Ce), and neodymium (Nd), Y toxicity has received little attention.

Animal sensitivity toward metals and their handling strategies depend, among others, on the considered metal and species. Some animals have developed strategies based on the regulation of metal assimilation, excretion, and depuration rates (Pan and Wang, 2009). Others handle metal contamination at a subcellular level. Indeed, metal assimilated by an organism is partitioned between subcellular components that can be operationally isolated through procedures involving centrifugation, heating, and chemical reagents (Cardon et al., 2018; Wallace et al., 2003). Some of these components such as mitochondria and heat-denatured proteins (HDP) appear sensitive to metals, and the accumulation of metal in these metal-sensitive fractions (MSF) may be related to their malfunction. On the contrary, metals accumulated in other subcellular components such as heat-stable proteins (HSP), also called metallothionein-like proteins, and metal-rich granules (MRG), also called NaOH-resistant fraction, are considered as metal detoxified fractions (MDF) (Campana et al., 2015). The proportion of bioaccumulated metals recovered between MDF and MSF may explain the differences in sensitivity to metal

accumulation between organisms for a given metal (Campana et al., 2015; Wang and Wang, 2009).

Hypotheses and concepts related to metal thresholds for these two kinds of fractions have been investigated in ecotoxicology since 2003 (Wallace et al., 2003). For example, the concept of "spillover" assumes that a given metal only begins to accumulate in MSF when its concentration in MDF exceeds a threshold (Cooper et al., 2013). Similarly, the tissue residue approach considers that adverse toxicological effects occur in organisms when a metal reaches a concentration threshold on MSF (Rainbow et al., 2015).

This study aims 1) to evaluate Y chronic toxicity to three species commonly used in aquatic toxicology – the water flea (*Daphnia magna),* the harlequin fly *(Chironomus riparius)*, and the rainbow trout (*Oncorhynchus mykiss)* – and to define lowest observable effect concentrations (LOEC); 2) to determine Y subcellular distribution in each organism along exposure gradients including these LOEC. LOEC are compared with existing data on Y and REE concentrations in freshwater ecosystems to better understand the actual ecotoxicological risk induced by this metal on the environment. Also, the Y subcellular detoxication strategy of each organism are discussed in light of their strategies for other metals.

Material and method

Toxicity Bioassays

D. magna and *C. riparius* were cultured in house at the *Centre d'expertise en analyse environnementale du Québec* (CEAEQ, Quebec City, QC, Canada). *O. mykiss* individuals were purchased from the *Pisciculture des Arpents Verts* (Sainte-Edwidge, QC, Canada) and were acclimated to laboratory conditions for at least 3 weeks prior to use. A solution prepared with a Y standard (10,000 µg mL^{-1} Y in 3 wt % HNO_3, TraceCERT®, FLUKA) was used to spike the water and the sediment. Unless otherwise mentioned, all exposure concentrations were determined as described in section "Yttrium measurements and quality control". Detailed descriptions of each bioassay are given in supporting information (SI). Moreover, monitoring of Y dissolved in the exposure

mediums are presented in Tables S2, S3 and S4 respectively for *D. magna*, *C. riparius* and *O. mykiss* and Y speciation at the beginning of each test is presented in SI, table S5. Briefly, the initial exposure solution pH and hardness were comprised between 7.4 – 7.9 and 45 – 130 mg L^{-1} of $CaCO_3$. No organic ligands were added and, in these conditions, Y was mainly present in the form of YCO_3 (61-80%).

Daphnia magna

A 7-day *D. magna* growth test was performed in semi-static conditions (water renewed daily) at a hardness of 130 mg L^{-1} of $CaCO_3$. The reconstituted water and the adjustment of its hardness were made according to USEPA protocols (United States Environmental Protection Agency, 2002) (SI, Table SI). *D. magna* neonates (<24 h) were exposed individually in reconstituted water at five nominal Y concentrations: 0, 200, 400, 800, 1200 µg L^{-1}. Additional experiments at 66 and 90 mg $CaCO_3$ L^{-1} were also performed.

Every day, each *D. magna* was transferred, with a polypropylene (PP) pipette, in a new PP beaker containing 24 mL of the contaminated water. Since the presence of algae can affect the Y bioavailability via complexation with cellular exudates, the addition of algae as food source (5.10^5 cells of *Raphidocelis subcapitata* mL^{-1}) was delayed for 6 hours after the daily transfer of *D. magna*. To assess Y exposure over the testing period, the concentration of dissolved Y was measured before the transfer of the organisms (t = 0 h), at 6 hours (before the addition of algae) and at 24 h every two days. Moreover, hardness, pH, temperature, and conductivity were measured daily. The size of each *D. magna*, from the top of the head to the end of the tail spine, was measured under a binocular scope (magnification factor X4) at the end of the assay.

Chironomus riparius

A 10-day sediment growth test with a sediment collected from Lac Croche at the Station de biologie des Laurentides (QC, Canada), spiked with Y (52, 144 and 450 mg kg^{-1} dried weight, dw), was carried out with *C. riparius* as described elsewhere (Environnement Canada, 1997). Details of the preparation of the Y spiked sediment and of the characteristics of the natural sediment are given in the section “exposure medium”.

The test was conducted in static conditions. Experimental chambers consisted of glass jars filled with 170 g of the sediment previously spiked with Y and 900 mL of reconstituted water (SI, Table SI). A one-month aging period for this experimental medium was set with a renewal of 80% of the water at the end. After this period, thirty organisms (<48 h old after hatching) were introduced in each jar. Organisms were fed all along the test with 1.5 mL of a fish flake suspension of Tetramin® (10 g L^{-1}). Over the test temperature was set at 21.7 °C and water was aerated continuously.

The concentration of dissolved Y in the water was measured at days 1, 5, and 10. The total concentration of Y in the sediment was measured before the beginning of the test.

At the end of the assay, *C. riparius* were transferred in PP jars filled with 500 mL of reconstituted water free of Y for 24 hours to clean their gut content. Then, they were counted, measured, rinsed in 1 mM EDTA solution to remove Y adsorbed to their body surface, dried with Kimwipe sheets and pooled in 1.5 mL preweighed and acid washed PP microcentrifuge tube, weighed, and stored at -80°C.

Oncorhynchus mykiss

A 28-day growth test with five Y concentrations (0, 250, 500, 1000 and 2000 µg L^{-1}) was conducted with *O. mykiss* according to the international standard ISO 10229 (ISO 10229, 1994) with some modifications. For each concentration tested, ten individuals of *O. mykiss* were exposed in 20 L of Y spiked reconstituted water (SI, Table SI), in semi-static conditions, 80% of the test water being renewed every 48 hours. The water hardness was set at 45 mg L^{-1} of $CaCO_3$.

The experimental chambers consisted of a PP bag set in a glass aquarium. Trout were fed twice daily at a rate of 2% of body weight per day with a commercial feed (Skretting Nutra XP). To minimize the dissolved Y lost because of Y complexation to food and faeces, remaining food and faeces were removed with a 50-mL glass pipette one hour after the feeding period. Total organic carbon, as well as total and dissolved Y concentrations were measured at t = 0 h (after the renewal of the water), at t = 24 h and at t = 48 h (before the renewal of the water); these measurements were repeated four times during the experiment. pH, temperatures and conductivity were measured daily.

At the beginning of the assay, fish were anesthetized with clove extract (Lotus Aroma), sized and weighed. All fish weighed more than 2.0 g and less than 3.1 g. The weight difference between each batch of ten fish was lower than 10% of the average weight of the five batches. After 14 days, fish were anesthetized, sized, and weighed for a second time. This operation was repeated a last time at the end of the experiment. An average growth rate for the fish as a function of Y exposure was assessed with the size measured at day 0, 14, and 28. Finally, for each exposure level, fish livers were extracted with a surgical steel razor blade and pooled by three in 1.5 mL preweighed and acid-washed PP microcentrifuge tubes, weighed, and stored at -80 °C.

Subcellular fractionation protocol

Samples of each organism were partitioned into six subcellular fractions with the fractionation protocol developed by Wallace et al. (2003) customized for our three species (Cardon et al., 2018). Figure S1 in SI presents the fractionation protocol with the customization applied for each species. In a previous publication, we validated the location of mitochondria (membrane and matrix), lysosomes and cytosol between fractions (SI, Fig. S1) by performing enzymatic biomarker assays on the separated fractions (Cardon et al., 2018). Thus, a distinction is made between these validated fractions and those predicted from the literature for which, to our knowledge, no relevant method of validation has been developed so far. These predicted fractions are the cellular debris (e.g. nuclei and membranes), the NaOH-resistant fraction, microsomes, the heat-denatured proteins (HDP) and the heat stable proteins (HSP).

Briefly, for each organism, 60-100 mg of tissue (whole organism: *D. magna, C. riparius;* liver: *O. mykiss)* was sampled and suspended in Tris-HCl (25 mM; OmniPur) sucrose buffer (250 mM; pH 7.4; Sigma Aldrich) at a final ratio of 1:8 (weight [mg]: buffer volume [µL]). Samples were homogenized on a motorized Potter-Elvehjem homogenizer equipped with a teflon pestle at 570 rpm (Fisher Scientific) and, except for *C. riparius*, were sonicated (22 W, 20%) (Branson 250, with a 4.8 mm diameter microtip probe) over a second homogenization step. After each homogenization, an aliquot of 40 µL was collected for estimating the total Y burden of the sample and the remainder was centrifuged at 800-1500 *g* for 15 min at 4°C to separate the debris fraction from the

other fractions (SI, Fig. S1). The resulting supernatant was collected and was subjected to a second centrifugation step at 15,000-25,000 *g* for 30 min at 4°C (SI, Fig. 1). The mitochondrial pellet was then isolated and an ultracentrifugation step was performed on the remaining supernatant at 100,000-190,000 *g* for 60 min at 4 °C. The pellet was separated from the supernatant at this step (SI, Fig. S1). This supernatant was heated at 80 °C for 10 min, cooled one hour at 4°C and finally centrifuged at 50,000 *g* for 10 min to separate the HSP from the HDP. To separate cellular debris from NaOH-resistant fraction, the debris fraction was filled with 500 µL of MilliQ water and vortexed. The mixture was heated at 95 °C for 2 min, then 500 µL of NaOH 1 N (99.998%, Sigma–Aldrich) was added, and the temperature was set at 80 °C for one hour. Finally, the suspension was centrifuged at 10,000 *g* for 10 min at 20°C (SI, Fig. S1).

Yttrium measurements and quality control

To minimize Y accidental contamination, all labware was soaked in HNO_3 (15%, v/v, Optima grade, Fisher Scientific) and rinsed seven times in MilliQ water before use.

Centrifuged pellet fractions resulting from the subcellular partitioning (NaOH-resistant fraction, mitochondrial membranes, microsomes and HDP), aliquots sampled as homogenate and *O. mykiss* remaining parts were freeze-dried for 24 h, weighed and stored at -80 °C. The freeze-dried fractions and the two other ones (Debris and HSP) were digested at 65 °C in 500 µL of HNO_3 (70%, v/v) whereas *O. mykiss* body remaining parts, representing heavier mass, were subjected to the same procedure but in 4 mL of HNO_3. Then, 9.5 mL and 45 mL of MilliQ water were added in the digestates of subcellular fractions and body remaining parts, respectively.

Concentrations of Y in subcellular fractions, homogenates, water and sediments were measured with an inductively coupled plasma-mass spectrometer (ICP–MS; Thermo Elemental X Series). To ensure quality of these measurements, samples of similar weight of a certified standard reference material, BCR 668 (mussel tissue, Institute for Reference Materials and Measurements) underwent the same digestion procedure and analysis. Mean (± SD) recoveries of BCR 668 reference sample (n = 9) were within the certified range for Y (103 ± 10%). The 40 µL of homogenate sampled

over the fractionation procedure were analyzed to confirm metal recovery following subcellular fractionation. Recoveries were expressed as the ratio of the sum of the Y burden in the six fractions divided by the total sample Y burden assessed from the 40 µL of homogenate, multiplied by 100. Mean (± SD) recovery values of Y were 90 ± 11% (n = 12) for *D. magna*, 70.0 ± 0.1% (n = 12) for *C. riparius* and 87 ± 22% (n = 9) for *O. mykiss*. Note that it was assumed in Cardon et al. (2018) that around 25% of *C. riparius* samples were probably not efficiently homogenized with the subcellular fractionation procedure performed on this species. It could explain why we obtained lower recovery values for *C. riparius*.

Calculation and statistical analysis

To assess the effect of Y on growth, the relative size of animals was calculated as the size of the organism for a given Y exposure level divided by the mean size of the controls .

Yttrium concentrations in every subcellular fraction were expressed as the Y burden in the fraction divided by the total sample wet weight (ww) (mg kg^{-1} ww). Yttrium burden in a given fraction was divided by the sum of Y burden in all fractions and multiplied by 100 to assess the relative contribution of each subcellular fraction to the total Y burden in terms of percentages (%).

Data are expressed as means ± coefficient of variation (CV) for Y total bioaccumulation and relative organism size, and as mean ± standard deviation (SD) for Y exposure measurements and Y bioaccumulation in fractions. Significant differences of organism size at the end of the bioassays or of Y burden in a given fraction/organism between Y exposure levels were tested with an analysis of variance (ANOVA), followed by Tukey pairwise comparison test ($p < 0.05$). The assumptions of normality and homoscedasticity were verified by Shapiro-Wilk's and Levene's tests, respectively. Statistical analyses were performed using R software version 3.4.4.

Results and discussion

Toxicity and bioaccumulation in the three aquatic animals studied

The exposure conditions, including Y concentrations, in the *D. magna*, *C. riparius* and *O. mykiss* bioassays are presented in SI, in Tables S2, S3 and S4 respectively.

Table I. Sublethal toxicity (in % of relative size, mean ± CV), lethal toxicity (in survival rate) and bioaccumulation (mg kg^{-1} ww, mean ± CV) of Y for each organism in whole at the end of the bioassays. [#]Y nominal concentration (Y dissolved measurement were not performed at this exposure level). [&]The relative body size is the ratio of the average body size for a given exposure concentration divided by that measured for the controls (lowest exposure concentration). Different letters indicate a significant difference of relative body size or Y bioaccumulation for a given organism among Y exposure level (ANOVA, followed by Tukey pairwise comparison test; $p < 0.05$). *The Y dissolved concentration over the 28-day exposure of *O. mykiss* to Y are given in SI, Table S4. Since these values showed strong variations, we also indicate the nominal values here and use these nominal values for the discussion.

			YTTRIUM EXPOSURE			TOXICITY		BIOACCUMULATION
	n	Medium	Hardness (mg L^{-1} of $CaCO_3$)	[Y]	Units	Relative animal size(%)[&]	Survival rate(%)	mg Y kg^{-1} ww
D. magna	10	Artificial water	130	0.2	µg dissolved Y L^{-1}	100 ± 13[a]	100	0.022 ± 29%[a]
				202		98 ± 22[a]	100	45 ± 41%[a,b]
				400[#]		94 ± 13[a]	90	33 ± 21%[a,b]
				798		74 ± 9[b]	80	55 ± 66%[b]
				1187		-	0	-
C. riparius	30	Y-spiked natural sediment	45	15	mg total Y $kg^{-1}$of dw	100 ± 2[a]	92	0.12 ± 28%[a]
				53		90 ± 5[b]	83	0.39 ± 20%[a]
				99		91 ± 0.2[b]	99	0.78 ± 13%[b]
				465		82 ± 2[c]	72	2.1 ± 10%[c]
O. mykiss	9	Artificial water	45	0.1[(0)]	µg dissolved Y L^{-1} * (Nominal Y*)	100 ± 0[a]	100	0.001 ± 56%[a]
				36[(250)]		96 ± 0.1[a,b]	100	2.0 ± 21%[b]
				79[(500)]		91 ± 0.04[b]	100	3.1 ± 16%[c]
				454[(1000)]		-	0	-
				1110[(2000)]		-	0	-

Daphnia magna

Yttrium Toxicity to D. magna

After seven days of exposure to Y, a decrease of *D. magna* relative size as a function of exposure was observed at a hardness of 130 mg L^{-1} of $CaCO_3$ (Table 1). Indeed, a significant loss of 26% of *D. magna* relative size was measured at 798 µg L^{-1}, corresponding to the LOEC of this test. With respect to mortality, no daphnids survived an exposure to 1187 µg L^{-1} Y (Table 1). Both mortality and LOEC were reached at lower exposure levels for the tests conducted in water with lower hardness (SI. Fig. S3). For example, 100% of mortality was reached for an Y exposure level of 706 µg L^{-1} at 90 mg L^{-1} of $CaCO_3$. In addition, a significant decrease of *D. magna* size was observed from 191 µg L^{-1} of Y at 66 mg $L^{-1}$of $CaCO_3$ (SI, Fig. S3). The negative correlation between water hardness and Y toxicity observed has also been reported for other REE from bioassay performed on *H. azteca* (Borgmann et al., 2005; Vukov et al., 2016), *Daphnia carinata* (Barry and Meehan, 2000) and *Daphnia pulex* (Vukov et al., 2016). Depending on hardness conditions, LOEC for *D. magna* ranged from 191 to 798 µg L^{-1} of dissolved Y (Table 1 and SI, Fig. S3). For comparison, Ma et al. (2016) reported a LOEC close to 400 µg L^{-1} of dissolved Ce for *D. magna* growth at a hardness of 252 mg $L^{-1}$of $CaCO_3$. Also, a significant mortality of *D. carinata* was observed by Barry and Meehan over a 6-day exposure to 39 µg La L^{-1} (Barry and Meehan, 2000). Both studies were performed in water with higher hardness than our maximal one, 130 mg L^{-1} of $CaCO_3$. This could suggest that HREE, like Y, are less toxic than LREE. This trend had already been reported for *H. Azteca* (Borgmann et al., 2005). Nonetheless other authors measured a positive correlation between REE toxicity and their atomic number (González et al., 2015); lutecium being the most toxic. Thus, further investigations would be required to compare HREE and LREE toxicity.

The LOEC measured in our study and others mentioned before are far higher than the REE concentrations which have been measured in aquatic ecosystems. For instance, Amyot et al. (2017) reported an average concentration for the sum of REE of 0.9 µg L^{-1} and of 0.1 µg L^{-1} of Y in 14 lakes of southern Quebec (Canada). Weltje et al. (2002) measured for the sum of REE, dissolved concentrations ranging from 0.003 (Lu) to 0.7

(Ce) µg L^{-1} in several freshwater ecosystems. Finally, in the Rhine, a river contaminated by anthropogenic La and Gd (Kulaksız and Bau, 2011), a dissolved total REE level of 0.21 µg L^{-1} was recorded, which is 1000 times lower than our LOEC.

Yttrium bioaccumulation in D. magna

With respect to bioaccumulation, the control Y exposure level (0.2 µg L^{-1}) excluded, *D. magna* Y content ranged from 33 ± 7 to 55 ± 36 mg Y kg^{-1} ww but no trend was observed with exposure concentration (Table 1). This bioaccumulation is 11 to 141 times higher than the ones measured for the two other organisms. Such high bioaccumulation values for an REE in zooplankton have already been observed before in the laboratory (Yang et al., 1999) but they are more than two orders of magnitude higher than those reported on average in the field. For instance, mean Y concentrations in temperate (Amyot et al., 2017) and arctic (MacMillan et al., 2017) freshwater zooplankton reached 0.2 ± 0.1 and 9.2 mg kg^{-1} dw, respectively.

Chironomus riparius

Yttrium toxicity to C. riparius

A significant decrease of 10 to 18% of *C. riparius* body relative size was measured as a function of Y concentration in the sediments (Table 1). At the maximal level of Y exposure, 465 mg kg^{-1}, the survival rate only reached 72 ± 1%, our lowest value for this bioassay (Table 1). Few studies have tested the REE toxicity as a function of sediment concentrations, and none on chironomids. A LOEC of 50 mg La kg^{-1} sediment for *Caenorhabditis elegans*, a value close to our LOEC for *C. riparius* (53 mg kg^{-1}dw) was reported (Herrmann et al., 2016). In addition, a MicroTox® test performed with sediments from Northern Quebec (Romero-Freire et al., 2018), determined IC_{10} for total REE (inhibition concentrations causing a 10% reduction in the endpoint) ranging from 0.45 to 48 mg kg^{-1}.

In natural environment, the concentrations of REE in sediments that have already been measured can be very close to these ecotoxicological values. Concentrations ranging from 63 to 253 of mg kg^{-1} dw for Ce, the most abundant REE, and up to 39 mg kg^{-1} dw for Y in sediment from 26 freshwater ecosystems sampled around the world were

reported (Schaller, 2013). Also, an average of 154 ± 69 and 18 ± 6 mg kg^{-1} dw, of total REE and Y respectively, was measured in sediments from temperate lakes (Amyot et al., 2017).

Yttrium bioaccumulation in C. riparius

Unlike *D. magna*, a significant increase in Y accumulation by *C. riparius* was measured as a function of exposure concentrations. Yttrium accumulated after 10 days ranged from 120 ± 34 µg kg^{-1}ww at the lowest exposure level to 2088 ± 209 µg kg^{-1} ww at the highest one (Table 1).

Bioaccumulation values close to ours have been observed in natural freshwater ecosystems. Ranges of total REE levels in benthic invertebrates from arctic lakes (MacMillan et al., 2017) and temperate lakes (Amyot et al., 2017) of 0.22 – 42 (mean: 4.6 ± 12) and 0.47 – 37 (mean: 4.6 ± 5.7) mg kg^{-1} dw respectively were reported. Furthermore, Y reached on average 0.61 ± 0.54mg kg^{-1} dw in chironomids from temperate lakes (Amyot et al., 2017). These bioaccumulation values are expressed by dw^{-1} whereas ours are in ww^{-1}. To be converted in dw, our bioaccumulation values should be at least multiplied by four (Ricciardi and Bourget, 1998). However, even with this factor, they remain close to the ones measured in natural environment.

Oncorhynchus mykiss

Yttrium toxicity to O. mykiss

When exposed to a nominal exposure level of 1000 µg L^{-1}, no trout survived more than ten days (Table 1). Moreover, a significant decrease in relative body size at the end of the bioassay was observed at 500 µg L^{-1} (Table 1). At this exposure level, a loss of 9 ± 4% of *O. mykiss* body size was determined (Table 1).

Watson-Leung (2009) observed no toxic effect of La on *O. mykiss* exposed 96 hours up to a dissolved concentration of 63.3 mg L^{-1}. This threshold concentration reached 0.13 mg L^{-1} in a 96-hour bioassay for the crimson-spotted rainbowfish, *Melanotaenia duboulayi* (Stauber, 2000). This last threshold is not far from our LOEC, which is about 0.08 mg L^{-1} of dissolved Y (SI, Table S.4).

Yttrium bioaccumulation in O. mykiss

Similarly to *C. riparius* and unlike *D. magna*, *O. mykiss* bioaccumulated more Y with increasing Y exposure. The Yttrium levels in this organism at the end of the bioassay ranged from 0.001 ± 56 to 3.1 ± 16 mg kg^{-1} ww (Table 1). The exposure concentration for this maximal value corresponds to our LOEC: 500 µg L^{-1}.

To our knowledge, the high bioaccumulation value of REE measured in our whole fish has never been observed in natural freshwater ecosystems and is at least five times higher than those reported on the field. For instance, among tissues from ten freshwater fish species from a reservoir in Washington State, a maximum REE level in *Catostomus catostomus* of 0.69 mg kg^{-1} ww including 0.057 mg kg^{-1} ww of Y was reported (Mayfield and Fairbrother, 2015). Furthermore, ranges of bioaccumulation values of REE ten times lower were assessed in four freshwater fish species sold in 17 cities of China (Yang et al., 2016) (from 0.034 to 0.038 mg kg^{-1} ww) and in six from Canadian temperate lakes (Amyot et al., 2017), (from 0.70 to 59 µg REE kg^{-1} dw including 0.041 to 7.4 µg Y kg^{-1} dw).

Yttrium subcellular fractionation by species

In this section, comparisons are made between Y subcellular fractionation in our species and metal fractionation in other studies working on the same species but also on other organisms. Cautions should be taken however in the interpretation of these comparisons. Indeed, most of the studies did not include an optimization of their fractionation protocol prior to their analysis as we did.

Daphnia magna

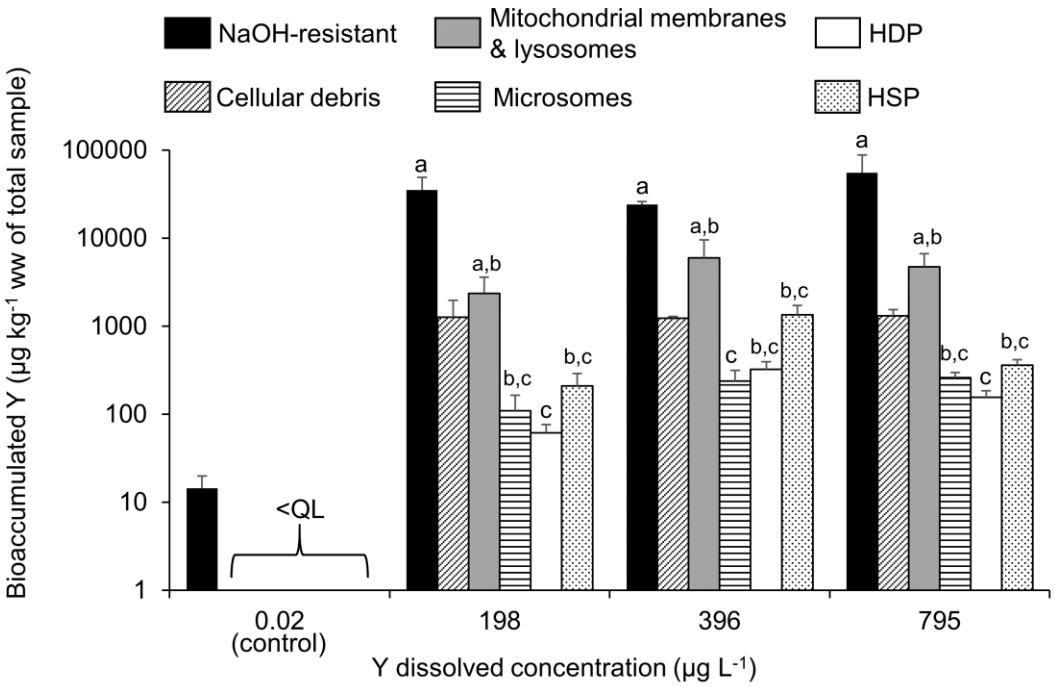

Figure 1. Bioaccumulation of Y in each validated fraction of *D. magna* (mean ± SD; in µg kg^{-1} ww of the total sample; n = 3) following the exposure level. Different letters indicate a significant difference of Y accumulation among fractions for a given Y exposure level (ANOVA, followed by Tukey pairwise comparison test, $p < 0.05$). The absence of a letter indicates that there is no significant difference. Quantification Limit (QL): 8 ng L^{-1}.

For all Y exposure levels, more than 70% of Y was recovered in the NaOH-resistant fraction of *D. magna* with an average Y content of 38 ± 14 mg kg^{-1}ww in this fraction (Fig. 1). In addition, this fraction was the only one above our quantification limit (0.022 ± 0.006 mg Y kg^{-1}ww) for our control. The fraction containing mitochondrial membranes and lysosomes contained 6 to 18 % of the total amount of Y (Fig. 1). Overall, Y subcellular distribution in *D. magna* appears constant over our exposure range. Note that, in a complementary experiment for a short exposure period of 24 hours (SI, Fig. S6), a significant decline of the proportion of Y in organelles (mitochondrial membranes, lysosomes and microsomes), from 21 ± 6% to 7 ± 1%, concomitantly with an increase in the NaOH-resistant fraction, from 62 ± 13% to 88.1 ± 0.1%, was observed over the exposure range.

The accumulation of Y mainly in NaOH-resistant fraction, a putative MDF, may explain why *D. magna* was able to bioaccumulate Y at concentrations far higher than the two other organisms (Campana et al., 2015). Only two other studies have reported metal fractionation in daphnids, and Y is the first metal found to be mainly sequestered in daphnid NaOH-resistant fraction. In contrast, around 28% of Ni (Lapointe et al., 2009) and less than 1% of Zn (Wang and Guan, 2010) were found in this fraction in previous studies. Nevertheless, an accumulation of more than 70% of a metal in the NaOH-resistant fraction has been previously reported in other crustaceans - U in *Procambarus clarkia* (Frelon et al., 2013) and Pb in *Gammarus fosarum* (Geffard et al., 2010) - but also in bivalves: Cd and Ag in *Saccostrea cucullate* (Rainbow et al., 2007), Cr and Fe in *Scrobicularia plana* (Dang et al., 2012), Zn and Cu in *Pyganodon grandis* (Cooper et al., 2013) and Pb in *Dosinia exolete* (Sánchez-Marín and Beiras, 2017).

The NaOH-resistant fraction is presumed to contain subcellular components such as metal-rich granules that are defined as detoxified. Nevertheless, we have strong suspicions that it also contains debris from the chitinous exoskeleton of *D. magna*. Indeed, several authors have used a similar NaOH treatment to isolate *Daphnia* exoskeletons from its soft tissues (Yu and Wang, 2002). Also, it is well known that REE present a strong antagonism with Ca, which accumulates in crustacean exoskeleton in the form of calcium carbonate (Greenaway, 1985; Pillai et al., 2009). REE can be absorbed at Ca uptake sites and can inhibit calcium ion channels, with stronger inhibition being reported for REE with shorter ion radius, such as Y (Beedle et al., 2002). Moreover, analysis of the distribution of REEs in crabs (*Ucides cordatus*) revealed a higher accumulation in the shells (Bosco-Santos et al., 2017) and has already led authors to assume a replacement of Ca during moulting. The same assumption could be made for *D. magna*.

Several authors have reported that the proportion of a given metal accumulated in MDF increased with the level of exposure to that metal (Rosabal et al., 2012). This would suggest a progressive subcellular detoxification of the metal in response to its level of exposure. Although this mechanism was not observed during the 7-days exposure to Y (Fig. 1), it was present in the 24 h exposure of *D. magna* to Y (SI. Fig. S6).

Even if the classification of lysosomes in either MDF or MSF can be debated, it is well established that mitochondria belong to the sensitive group. Like Y, the mitochondrial and organelles fraction was the MSF in which a higher relative metal proportion was found in *D. magna* with 40% for Zn (Wang and Guan, 2010), 5% and 8% for Ni and Tl respectively (Lapointe et al., 2009). It could suggest that the metal toxicity mechanism for this crustacean, in general, is related to an interference in its mitochondrial functions.

Chironomus riparius

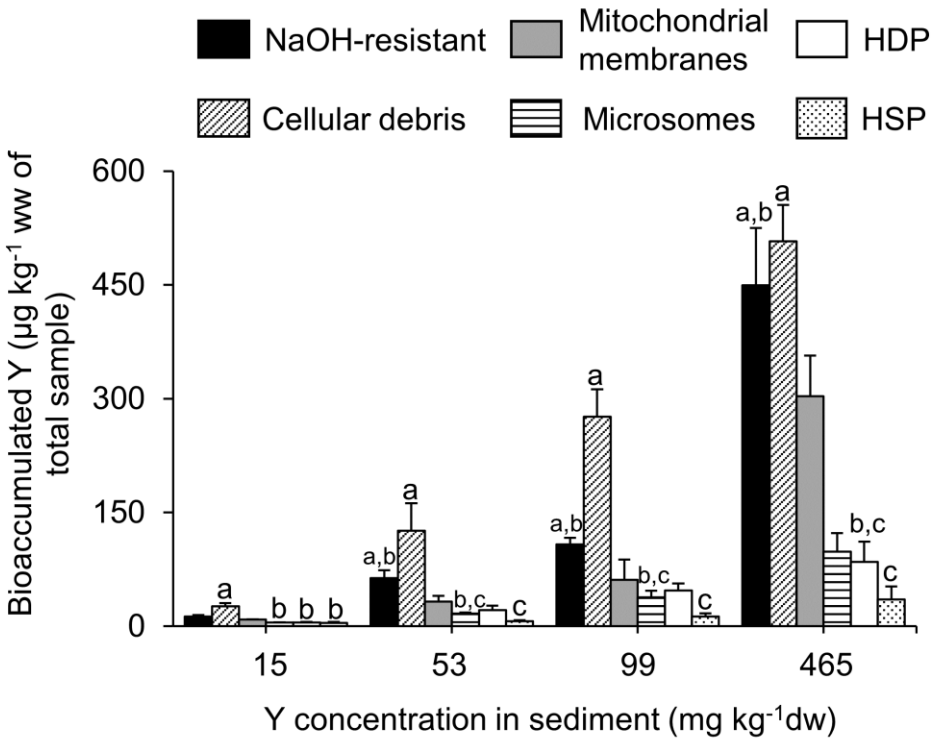

Figure 2. Bioaccumulation of Y in each validated fraction of *C. riparius* (mean ± SD; in µg of Y in the fraction per kg of the total wet weight of the sample; n = 3) as a function of exposure concentration. Different letters indicate a significant difference of Y accumulation among fractions for a given Y level exposure (ANOVA, followed by Tukey pairwise comparison test, $p < 0.05$). The absence of a letter indicates that there is no significant difference.

Cellular debris fraction was the main one that bioaccumulated the Y in *C. riparius* (Fig. 2). From 34 to 51% of Y was recovered in this fraction through our exposure range. Like *D. magna*, NaOH-resistant and mitochondrial membrane fractions are respectively the first putative MDF and MSF that bioaccumulated the Y in *C. riparius* cells (Fig. 2). The first fraction contained from 20 to 30% of Y and the second from 11 to 20%. Along our exposure range, Y distribution between fractions appeared stable, except for our maximal exposure level (465 mg kg^{-1} dw). Indeed, between this exposure level and the previous one (93 mg kg^{-1} dw), less Y was found in the cellular debris fraction while more was found in both NaOH-resistant and the mitochondrial membrane fractions. Y levels increased respectively four and five folds in these latter fractions between these two exposure levels versus only twice for cellular debris (Fig. 2).

Strategies of Y subcellular detoxification in *C. riparius* seem to differ from that of other metals already assessed for this species. If less than 15% of the Y was found in the HDP and the HSP fractions over our exposure range, these two fractions appeared respectively as the top MSF and MDF for the accumulation of Ni (Dumas and Hare, 2008), Se (Dubois and Hare, 2009a), Cd (Dubois and Hare, 2009b) and Hg (Gimbert et al., 2016) in *Chironomus sp*. However, most of the Se and Ni were found in cellular debris, with more than a third of the relative distribution in *C. riparius*. This fraction should therefore be considered as an important one to understand metal subcellular management in this species. Toxicological significance of metal accumulation in cellular debris is not currently well defined and most authors do not include this fraction when interpreting metal subcellular distribution (Campbell et al., 2005). Nonetheless, others suggest that a metal sensitive compartment integrating the cellular debris may be more relevant (Casado-Martinez et al., 2012b). Furthermore, it was established that metal binding to nucleic acid inside the nucleus (found in the debris fraction) could modify both transcription and DNA replication and induce genotoxicity (Fusconi et al., 2006). Also, Huang et al. (2011) reported that La, Ce, and Nd accumulated in nuclei and mitochondria of mice hepatocyte and induced oxidative damages. As a result, given the large proportion of Y accumulated in cellular debris for *C. riparius* at the end of our bioassays, we must assume that Y bound to this fraction likely contributes to its toxicological effects on this organism.

The significant accumulation of Y in the mitochondrial fraction of *C. riparius* at our maximal exposure level relative to lower exposure levels (Fig. 2) is consistent with the "spillover hypothesis" observed by many authors for other metals (Cooper et al., 2013). Thus, the cell capacity to detoxify Y by accumulation in the NaOH-resistant fraction would be exceeded at our maximal exposure level, leading to a spillover of Y in mitochondrial membranes, a MSF.

Oncorhynchus mykiss

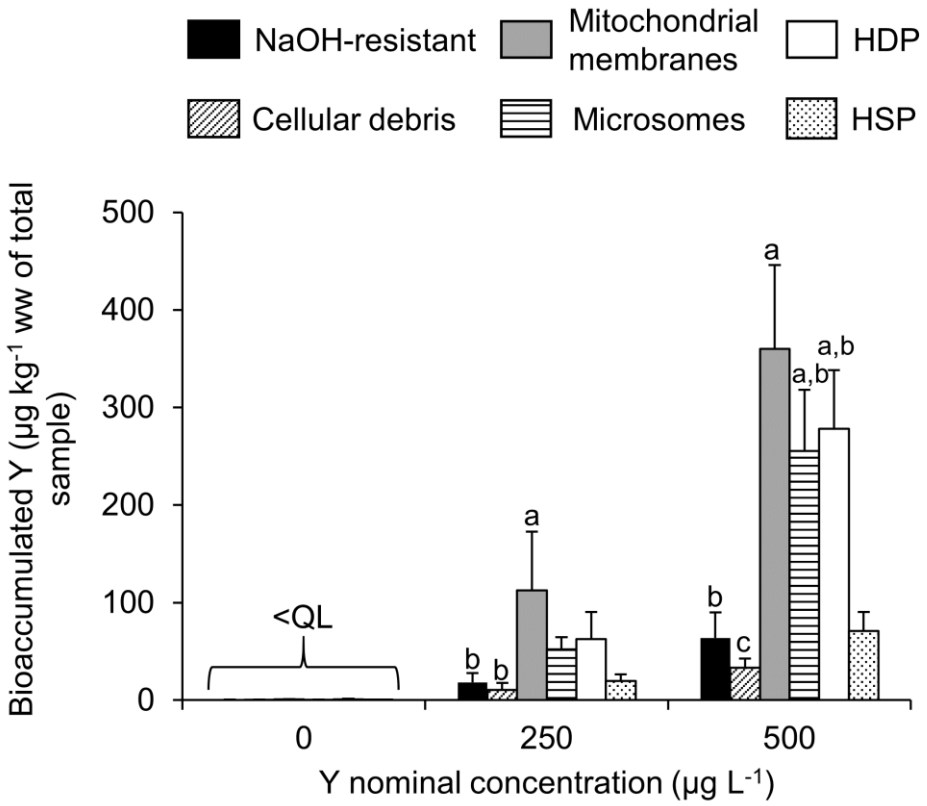

Figure 3. Bioaccumulation of Y in each validated fraction of *O. mykiss* liver (mean ± SD in µg of Y in the fraction per kg of the total wet weight of the sample, n = 3) as a function of exposure concentration. Different letters indicate a significant difference of Y accumulation among fractions for a given Y exposure level (ANOVA, followed by Tukey pairwise comparison test, $p < 0.05$). The absence of a letter indicates that there is no significant difference. Quantification Limit (QL): 8 ng L^{-1}.

Yttrium in *O. mykiss* liver cells was mainly present in mitochondrial membranes, this fraction representing between 34 and 39% of the total accumulated Y (Fig. 3) and reached a maximal concentration of 4 ± 0.4 mg Y kg dw of the fraction (SI, table S6). The remaining bioaccumulated Y was partitioned between the HDP and the microsomes fractions. They contained from 19 to 26% of Y each and accumulated statistically identical amounts of Y. Unlike *D. magna* and *C. riparius,* in *O. mykiss* liver, MDF represented less than 15% of the total amount of bioaccumulated Y. Plus, there were no significant differences between the amounts of Y bioaccumulated in the NaOH-resistant and in the HSP fractions (Fig. 3).

Several authors studied metal distribution inside fish liver cells. For instance, from 37 to 48% and from 20 to 30% of Cu was accumulated in organelles (mitochondria + Lysosomes/Microsomes) of *O. mykiss* liver cells (Kamunde and MacPhail, 2008) and *Cyprinus carpio* liver cells (Eyckmans et al., 2012) respectively, in previous studies. Thus, as well as Y, organelles appear as the first putative MSF that accumulated Cu in *O. mykiss* liver (Eyckmans et al., 2012; Kamunde and MacPhail, 2008). In addition, the low percentage of Y accumulated in MDF fraction was also observed for Hg in *S. alpinus* liver (Barst et al., 2016) less than 15% of the accumulated Hg was in the MDF. However, in *S. alpinus* liver, Hg tended to accumulate more in the HDP than in the organelles fraction (Barst et al., 2016). Moreover, at least 30% of Cd inside liver cells of *O. mykiss* (Kamunde and MacPhail, 2008) and *Perca flavescens* (Giguère et al., 2006) was found in MDF, suggesting an effective subcellular detoxication strategy for these metals in contrast to Y.

Comparison of Y subcellular detoxication between species

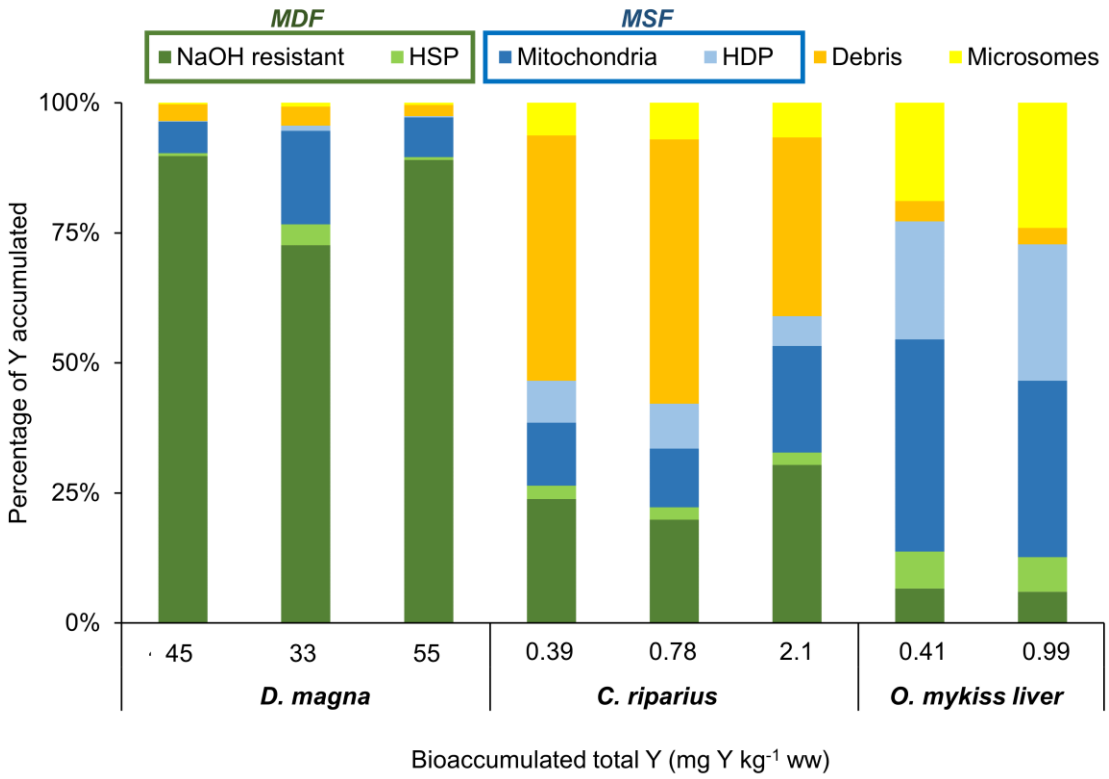

Figure 4. Percentage of Y recovered in each fraction as a function of the amount of bioaccumulated total Y in each organism: MDF, Metal Detoxified Fraction; MSF, Metal Sensitive Fraction; HSP, Heat-Stable Proteins; HDP, Heat-Denatured Proteins.

For both invertebrates, Y was mostly found in the NaOH-resistant fraction. HSP was the second fraction which is also included in the MDF and represented less than 10% of total Y in all our organisms (Fig. 4). Hence, Y bounding to granules is likely the main route of Y detoxication in cells. However, further investigations to confirm this assumption will be required. Also, it could be interesting to extent the analyses to evaluate which type of granules is involved in the Y detoxication. Indeed, Hopkin defined four types of granule depending on the ligand that compose them. Considering the Y ability to bound with calcium-binding proteins (Jakubek et al., 2009), we hypothesize that Y rich granules are most likely constituted by calcium carbonate.

Among the MSF, Y was mostly found in mitochondria in all our organisms (Fig. 4). Interaction of Y with mitochondrial functions could thus, at least partly, explain the toxic effects of Y in our organisms. Gao et al. (2003) suggested that a way for Eu^{3+} and La^{3+} to accumulate inside plant cells was to bind to membranes of mitochondria, chloroplasts and cytoplasts via Ca^{2+} channels. Besides, several authors have measured adverse effects which can be linked to accumulation in mitochondria. For instance, oxidative damages on mitochondria of mice hepatocytes following an exposure to La, Ce and Nd were observed (Huang et al., 2011). Moreover, a decrease of the Ca^{2+} dependent basal respiration rate in rat heart mitochondria following an exposure to Y was also observed (Korotkov et al., 2016).

This study represents a first attempt to compare a REE subcellular handling between different organisms at exposure levels with measured adverse effects. It emphasizes the importance of the NaOH fraction and mitochondrial membrane in understanding Y detoxication and toxicity mechanisms. It also underlines species-specific Y subcellular management like *D. magna* capacity to accumulate much higher proportion of Y in its MDF than *C. riparius* and *O. mykiss.* This study contributes to improve our knowledges about REE risk assessment and provides first insights of their subcellular handling.

Acknowledgments

We would like to thank the *Centre d'expertise en analyse environnementale du Québec* (*Ministère du Développement durable, de l'Environnement et de la Lutte contre les changements climatiques* (MDDELCC,) for their technical assistance in the breeding of organism and chemical analysis. We also thank the technicians of the Marc Amyot laboratory and INRS-ETE for the laboratory's assistance and their help in the analysis of rare earths.

Funding

This research was funded through the Natural Sciences and Engineering Research Council (NSERC) Discovery grant and an NSERC strategic grant (TRIVALENCE) to

M. Amyot. This work was supported by the NSERC CREATE Mine of Knowledge network through a scholarship to P-Y. Cardon. M. Amyot and C. Fortin are supported by the Canada Research Chair Program. All experiments were performed in the CEAEQ *de Québec* with lab ware purchased and provided by the MDDELCC.

Supporting information

Material and method

Exposure medium

Recipe of the reconstituted water used in our bioassay is given in Table SI. This reconstituted water was made according to USEPA (United States Environmental Protection Agency, 2002) and is adapted for bioassay on our three organisms. Preparation of the Y spiked sediment used for *C. riparius* bioassay is described in this section.

Water medium

Table SI. Recipe for the making of the reconstituted water

Hardness (mg L^{-1} of $CaCO_3$)	$NaHCO_3$ (mg L^{-1})	$CaSO_4$ (mg L^{-1})*	$MgSO_4$ (mg L^{-1})#	KCl (mg L^{-1})
40-45	48	30	30	2
80-90	96	60	60	4
120-140	144	90	90	6

Reconstituted water was aerated 24 h before the beginning of the assay. Then, 2 to 5 µg of selenium was added per liter. The pH was adjusted at 7.8-7.9 with HCl 10%.

* ($CaSO_4. 2H_2O$)

($MgSO_4. 7H_2O$)

Sediment exposure medium

Sediment and water were collected from Lac Croche at the *Station de biologie des Laurentides*. Several parameters including, total organic carbon, NH_3-N, N_{total}, P_{total}, S_{total}, pH, water content, trace metal concentrations, main anions and cations and REE concentrations were measured in the sediment. The sediments were than freeze-dried in PP bags. Then, 150 g dw-samples of the freeze-dried sediment, corresponding to the four tested exposure concentrations (0, 50, 100, and 450 mg Y kg^{-1} dw) were spiked with 850

mL of lake water previously mixed with an Y standard solution (10,000 µgY mL^{-1} Y in 3% by wt HNO_3, TraceCert®, FLUKA) at a given concentration. The volume of water added was measured to reach the initial humidity percentage of the sediment and the water pH was adjusted to 7.4 with NaOH 1 N or HCl 10 %. Spiked sediments were then mixed 5 minutes every day during 3 days before being stored at -20 °C. For each concentration, two sediment samples were collected before storage to measure their total yttrium concentrations. Sediments were thawed 2 days at ambient temperature before the beginning of the assays.

Subcellular fractionation

Preparation of D. magna sample

At least 50 individuals of *D. magna* were needed to get an adequate sample weight for the subcellular fractionation procedure and chemical analyses. As a result, it was impossible to use the *D. magna* survivors (<10) at the end of their bioassay for subcellular analysis, unlike *C. riparius* and *O. mykiss*. Therefore, following the *D. magna* growth test a new assay at the same range of Y exposure levels were started with 300 individuals and a PP bag filled with 15 L of Y spiked reconstituted water as experimental chamber. This new assay was conducted in the same conditions as described previously. At the end of the assay, *D. magna* were transferred, firstly for 4 hours in 15 L of reconstituted water free of Y to clean their gut content, and secondly for 5 minutes in 2 L of a 1 mM EDTA (Geffard et al., 2010) solution to remove the adsorbed Y on their bodies. After being rinsed in MilliQ water, they were dried with Kimwipe sheets, pooled by 50 in 1.5 mL preweighed and acid-washed PP microcentrifuge tubes, weighed and stored at -80 °C.

Subcellular fractionation protocol

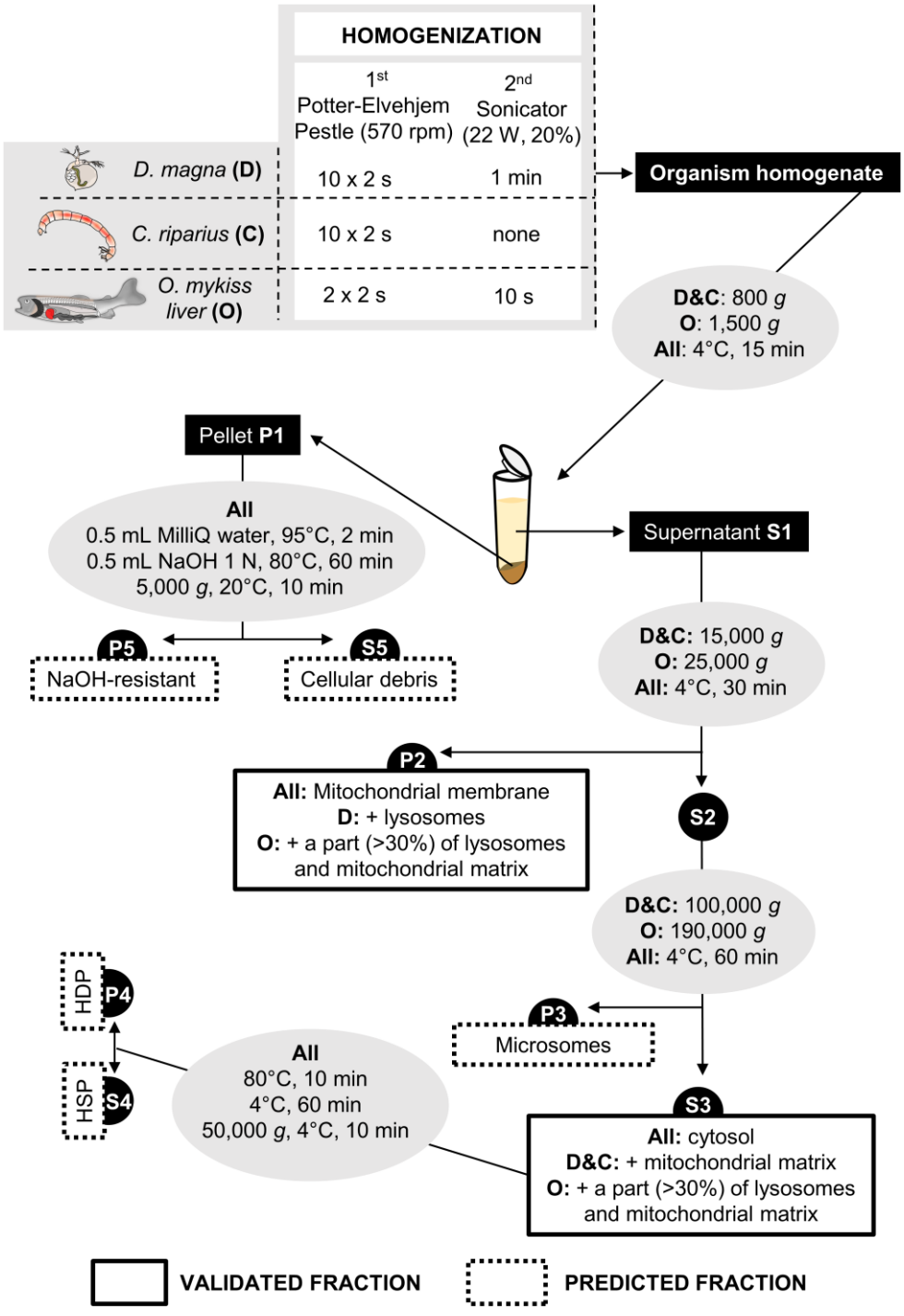

Figure S1. Subcellular fractionation protocol for each organism (D: *D. magna*; C: *C. riparius*; O: *O. mykiss* liver). P-Pellet / S-Supernatant. Centrifugations (< 25,000 *g*) were performed using an IEC Micromax centrifuge (Thermo IEC) whereas a WX ULTRA 100 centrifuge (Sorval, Ultra Thermo Scientific) equipped with a F50L-24 X1.5 rotor (Fisher Scientific) was used for ultracentrifugation (≥ 25,000 *g*).

Results

Bioassay exposure monitoring

Several physico-chemical parameters were monitored during the bioassays on our three organisms, in particular the concentration of Y dissolved in the exposure medium. Results of these monitoring are presented in Tables SII, SIII and SIV respectively for *D. magna*, *C. riparius* and *O. mykiss*. Plus, Y speciation at the beginning of each test is presented in Table SV.

For *Daphnia,* Y exposure levels remained steady between water renewals. Measured dissolved Y concentrations were close to the nominal ones, with a ratio ranging from 96 to 107% on average (Table SII).

For *C. riparius,* for the maximal exposure level, dissolved Y concentration in the water column raised from 14 ± 2 µg L^{-1} at the beginning of the bioassay to 42 ± 8 µg L^{-1} by the end (Table SIII). This increase is presumably caused by a release of Y from the sediments, which contained 465 mg Y kg^{-1} dw.

For *O. mykiss,* a sharp decline of measured dissolved Y concentration between water renewals was observed. Thus, our nominal exposure levels of 250 and 500 of µg L^{-1} yielded measured levels of only 8 ± 3 and 16 ± 9 µg L^{-1} of dissolved Y, 24 hours after the medium renewal (Table SIV). Binding of Y with the organic matter from the food and *O. mykiss* faeces likely explains this loss. Indeed, a preliminary experiment monitoring dissolved Y depletion in a Y-spiked water in the presence or absence of food (Fig. S1) showed a decrease of 61% after 24 hours in water with food and no significant Y loss in the absence of food.

For every test, Y was mainly present in the form of YCO_3 (61-80%) (Table SV).

Table SII. Observed exposure conditions for *D. magna.* Yttrium concentrations are given in μg L^{-1}

Bioassay #	Hardness (mg $L^{-1}$of $CaCO_3$)	pH	Temp (°C)	Nominal [Y]	Measured [Y] after medium renewal	Measured [Y] before medium renewal	Average measured [Y] over 24 h	Ratio $[Y]_{dissolved}/[Y]_{nominal}$
1	66 ± 1	7.7 ± 0.1	21.7 ± 0.2	0	-	0.14 ± 0.01	-	-
				50	45 ± 3	52 ± 2	49 ± 5	98%
				100	92 ± 1	105 ± 7	99 ± 9	99%
				200	178 ± 4	200 ± 17	191 ± 17	96%
				400	375 ± 9	400 ± 20	388 ± 19	97%
2	89 ± 1	7.8 ± 0.1	21.8 ± 0.1	0	-	0.3 ± 0.1	-	-
				100	98 ± 6	118 ± 5	107 ± 12	107%
				300	-	-	-	-
				500	480 ± 19	508 ± 25	492 ± 25	98%
				700	686 ± 17	730 ± 29	706 ± 32	101%
3	128 ± 3	7.9 ± 0.2	21.4 ± 0.1	0	-	0.2 ± 0.0	-	-
				200	190 ± 10	213 ± 15	202 ± 17	101%
				400	-	-	-	-
				800	790 ± 10	807 ± 6	798 ± 12	100%
				1200	1170 ± 60	1203 ± 6	1187 ± 43	99%

Table SIII. Observed exposure conditions for *C. riparius*

	Nominal sediment [Y] (mg kg^{-1} dw)	pH	Temp °C	Hardness (mg $L^{-1}$of $CaCO_3$)	Measured sediment [Y] (mg kg^{-1}dw)	Measured dissolved [Y] (µg L^{-1})
1st day	0	7.4	21.6 ± 0.2	43.8	15 ± 1	0.11 ± 0.01
	50	7.5	21.6 ± 0.1	42.5	53 ± 7	2.2 ± 0.7
	100	7.5	21.7 ±0.1	44.7	99 ± 30	2 ± 1
	450	7.6	21.6 ± 0.3	48.5	465 ± 6	14 ± 2
5th day	0	7.5	21.7 ± 0.1	-	-	0.14 ± 0.01
	52	7.5	21.7 ± 0.1	-	-	3.1 ± 0.7
	100	7.5	21.8 ± 0.1	-	-	2 ± 1
	450	7.6	21.7 ± 0.2	-	-	25 ± 6
10th day	0	7.5	21.9	46.7	-	0.3 ± 0.1
	52	7.5	21.8 ± 0.1	44.2	-	4 ± 2
	100	7.5	21.8 ± 0.1	44.5	-	1 ± 2
	450	7.6	21.9 ± 0.3	50.1	-	42 ± 8

Table SIV. Observed exposure conditions for *O. mykiss.* *all fish were dead after 2 days of exposure for this Y concentration. As a result, only one measurement could be made at this concentration.

	Nominal [Y] (µg L^{-1})	pH	Hardness (mg L^{-1} of $CaCO_3$)	TOC (mg L^{-1} of C)	Temp (°C)	Measured dissolved [Y] (µg L^{-1})	Ratio $[Y]_{dissolved}/[Y]_{nominal}$
0 h (after the medium renewal)	0	-	-	-	15.1 ± 0.1	0.12 ± 0.01	-
	250	-	-	-		123 ± 25	49%
	500	-	-	-		280 ± 1	56%
	1000	-	-	-		700 ± 57	70%
	2000	-	-	-		-*	-
24 h (between two medium renewal)	0	7.6	44 ± 1	-	15.2 ± 0.1	0.13 ± 0.01	-
	250	7.8 ± 0.1	45 ± 1	-		8 ± 3	3%
	500	7.7	45 ± 1	-		16 ± 9	3%
	1000	7.7	45 ± 1	-		433 ± 6	43%
	2000	7.7	44	-		1300*	65%
48 h (before a medium renewal)	0	7.6	45 ± 2	1.40 ± 0.15	15.1	0.1 ± 0.1	-
	250	7.8 ± 0.1	46	1.80 ± 0.15		4 ± 2	2%
	500	7.7	45 ± 1	2.00 ± 0.05		5 ± 2	1%
	1000	7.8	43	2.90 ± 0.01		250 ± 85	25%
	2000	-	-	-		920*	46%

Table SV. Yttrium speciation at the beginning of each test. Speciation analysis were performed with WHAM software version 7.0.1.

Assay	Hardness (mg $CaCO_3$ L^{-1})	pH	Temp °C	Y^{3+}	YOH^{2+}	$Y(OH)_2^+$	YSO_4^+	$Y(SO_4)_2^-$	YCO_3^+	$Y(CO_3)_2^-$	$YHCO_3^{2+}$
D. magna	66	7.7	21.7	1.7%	1.3%	0.1%	1.9%	0.1%	72.9%	21.9%	0.2%
	89	7.8	21.8	1.3%	0.9%	0.1%	1.7%	0.1%	68.5%	27.2%	0.2%
	128	7.9	21.4	0.8%	0.6%	0.0%	1.4%	0.1%	61.1%	35.8%	0.2%
C. riparius	45	7.5	21.6	5.3%	2.1%	0.1%	4.3%	0.1%	79.8%	7.9%	0.4%
O. mykiss	45	7.7	15.1	3.0%	1.4%	0.1%	2.5%	0.1%	79.1%	13.6%	0.2%

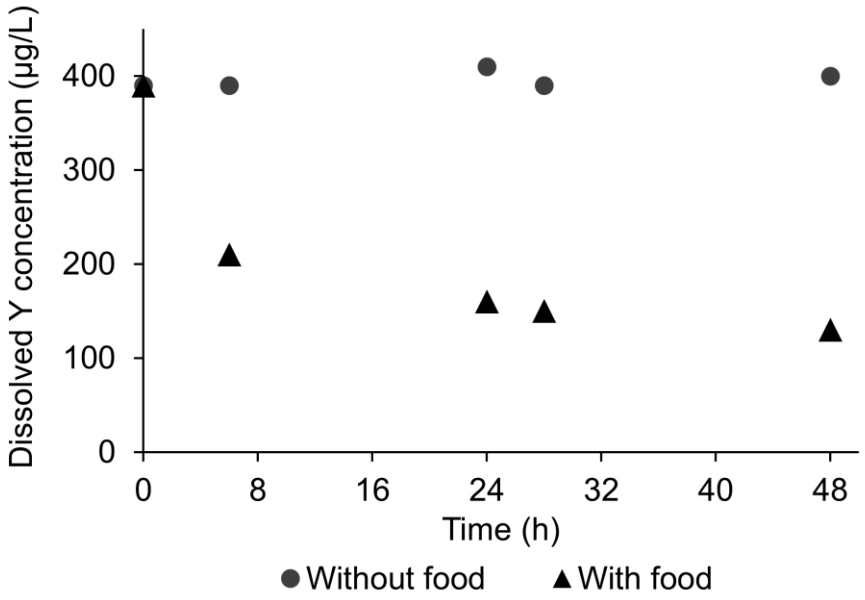

Figure S2. Dissolved Y concentration in reconstituted water supplied with or without food over a 48-hour period.

Bioassay toxicity results

Toxicity results from the bioassays performed on *D. magna, C. riparius* and *O. mykiss* are presented in this section.

Daphnia magna

D. magna size after a seven-day exposure period to a Y exposure concentration range in three water media of differing hardness is showed in Fig. S3.

Regardless of the water hardness, a decline of *D. magna* size at the end of the bioassay with increasing Y levels was assessed (Fig. S3). In addition, a covariance analysis (ANCOVA) performed on the significant linear regression ($p < 0.001$) established at each hardness between Y exposure level and *D. magna* size, showed a significant difference between the linear regression evaluated at 130 mg L^{-1} of $CaCO_3$ and those evaluated for the other two hardnesses. It suggests a significant impact of medium hardness on Y effect on *D. magna* size.

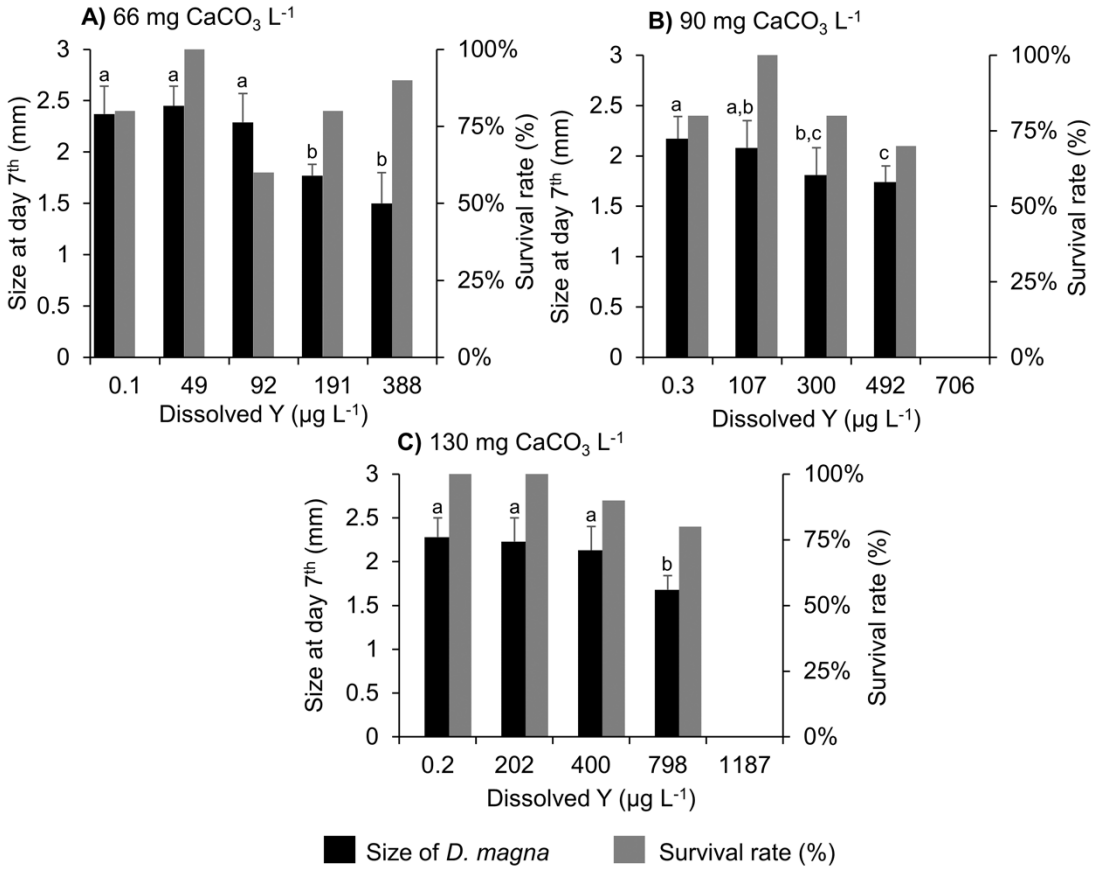

Figure S3. Effect of Y on *D. magna* size (mean ± SD; n = 6-10) and survival after a seven-day exposure period in three water mediums of differing hardness: A) 66 B) 90 C) 130 mg $CaCO_3$ L^{-1}. Error bars represent standard deviations. Different letters indicate significant difference of *D. magna* size at day 7 depending on the Y exposure level (ANOVA followed by Tukey pairwise comparison test, $p < 0.05$)

Chironomus riparius

C. riparius size and survival rate at the end of the ten-day bioassays performed on this organism is presented in Fig. S4.

A significant decline of *C. riparius* size was measured from an exposure of 53 mg kg^{-1} dw and was even more enhanced at 465 mg kg^{-1} dw (Fig. S4). Nonetheless, even if the lowest survival rate, 72 ± 1%, was measured at this latter exposure level, none significant shifting of survival rate was assessed depending on the Y exposure level.

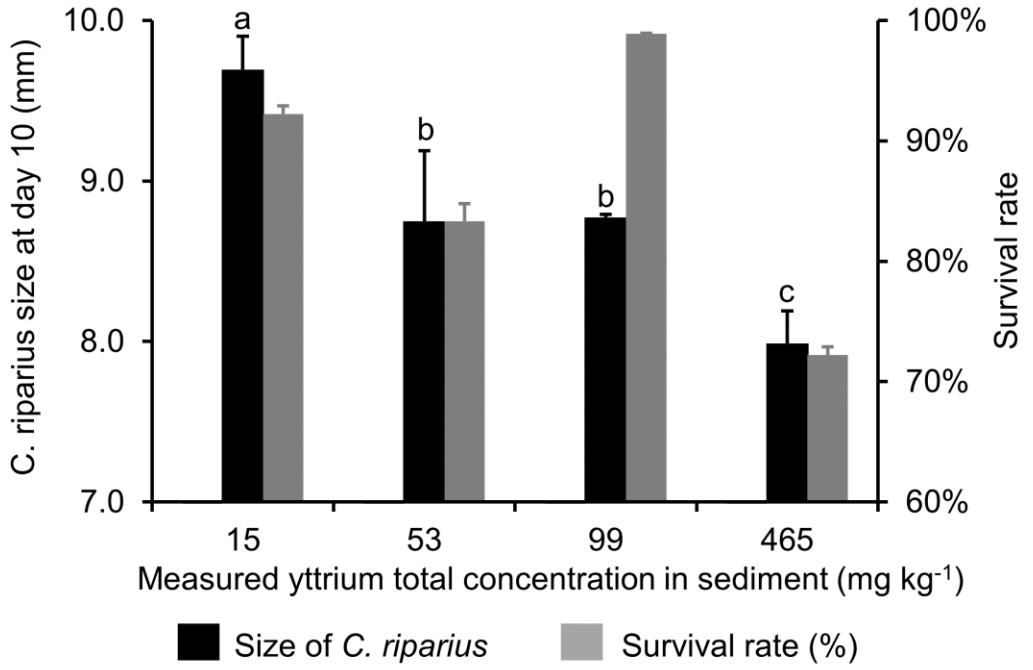

Figure S4. Effect of Y on *C. riparius* size and survival (n = 30) after a 10-day exposure period (mean ± SD). Error bars represent standard deviations. Different letters indicate significant difference of *C. riparius* size or survival rate at day 10 depending on the Y exposure level (ANOVA followed by Tukey pairwise comparison test, $p < 0.05$)

Oncorhynchus mykiss

O. mykiss size and weight at the beginning, the middle and at the end of the 28-day bioassay performed on this organism are presented in Fig. S5 (A) and (B) respectively.

A significant decrease of *O. mykiss* size and weight at 500 µg L^{-1} was observed from the 14th day on (Fig. S5). However, at the end of the bioassay this size decrease was

no longer significantly different from the *O. mykiss* size measured for a Y exposure level of 250 µg L^{-1} (Fig. S5 A). Though, *O. mykiss* weight for the Y exposure level of 500 µg L^{-1} of Y at the end of the bioassay remained significantly different from the two other levels (Fig. S5 B). Indeed, at this last day of the 28-day bioassay, at the maximal exposure level, *O. mykiss* weighed on average 3.9 ± 0.4 g against 4.8 ± 0.3 g for the two others Y exposure levels.

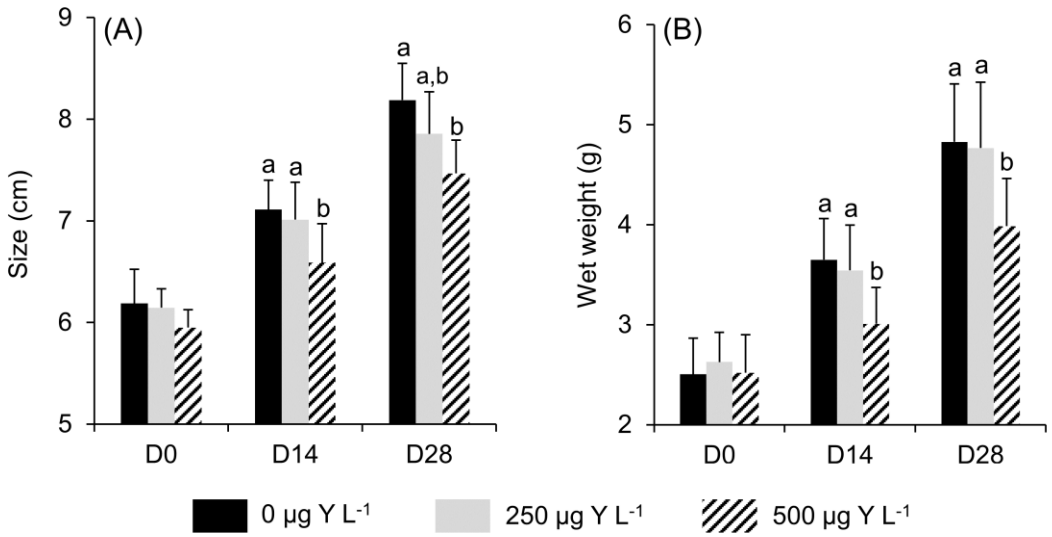

Figure S5. Effect of yttrium on *O. mykiss* size (A) and wet weight (B) over a 28-day exposure period (mean ± SD; n = 9). Yttrium exposure concentrations are presented as nominal for simplicity. Error bars represent standard deviations. Different letters indicate significant difference of *O. mykiss* size or weight at day 0, 14 and 28 depending on the yttrium exposure levels (ANOVA followed by Tukey pairwise comparison test, $p < 0.05$)

Yttrium subcellular fractionation in *D. magna* after a 24 h exposure period

A complementary experiment involving an exposure of *D. magna* to Y over 24 h was performed in addition to the 7 days exposure growth test. Percentage of Y collected in each subcellular fraction of *D. magna* after this 24 h exposure period is given in Figure S6.

A significant decline in the proportion of Y in organelles (mitochondrial membranes, lysosomes and microsomes), from 21 ± 6% to 7 ± 1%, with a concomitant increase in the NaOH-resistant fraction, from 62 ± 13% to 88.1 ± 0.1%, along the exposure range, was observed (Fig. S6).

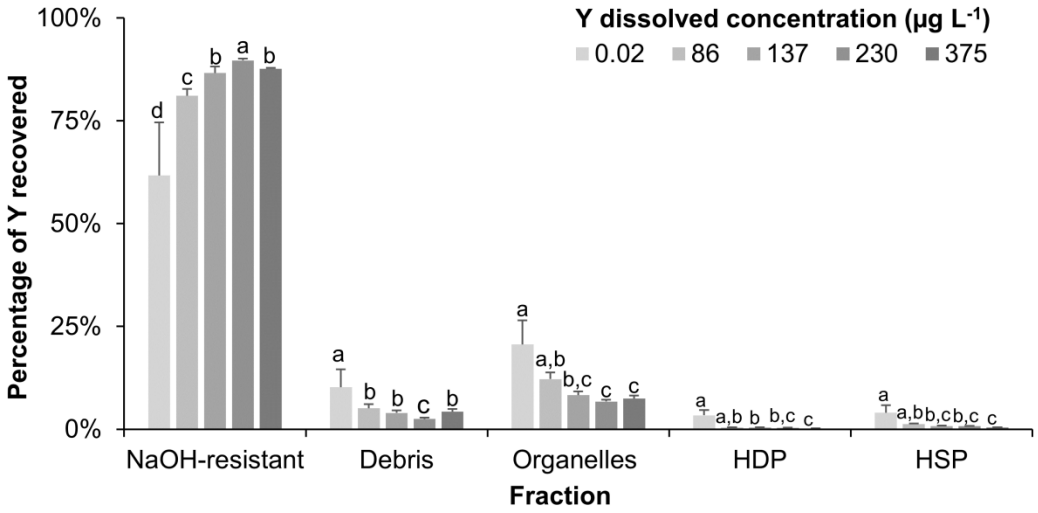

Figure S6. Percentage of Y recovered in each fraction of *D. magna* (mean ± SD; n = 5) following the exposure level after a 24-h exposure period. Different letters indicate a significant difference of percentage of Y recovered among fractions for a given Y exposure level (ANOVA, followed by Tukey pairwise comparison test, $p < 0.05$).

Yttrium concentration by subcellular fractions

Concentrations of Y in each fraction expressed as amount of Y by dried weight of fraction are presented in Table SVI. For *D. magna*, Y concentrations in NaOH-resistant fraction were at least three times higher than others. Plus, Y concentrations in *D. magna* fraction appeared constant over our exposure range (Table SVI). In contrast, Y concentrations in *C. riparius* and *O. mykiss* liver fractions increased along the exposure range. In *C. riparius,* mitochondrial membranes and NaOH-resistant fraction showed the highest Y concentrations, on average 12 mg kg^{-1} dw at the maximal exposure level. Finally, in *O. mykiss* liver Y concentrations in every fraction were very close for an

exposure of 250 µg Y L^{-1}. However, at 500 µg Y L^{-1}, Y concentration in microsome was on average 1.75 times superior than other fractions (Table SVI).

Table SVI. Concentrations of Y (mean ± SD; n = 3; mg Y kg^{-1} dw) in each fraction. Concentrations are expressed as amount of Y by dried weight of fraction. Cellular debris and HSP fractions were not freeze dried because of the NaOH and Tris/Sucrose buffer they contained respectively at the end of their fractionation. Therefore, concentrations were not measurable for these two fractions

	D. magna			***C. riparius***				***O. mykiss liver***	
Y exposure level	198	396	795	15	52	93	465	250	500
Unity	µg Y L^{-1} (dissolved)			mg Y kg^{-1} sediment dw (total)				µg Y L^{-1} (nominal)	
NaOH-resistant	2044 ± 711	512 ± 101	2062 ± 1342	0.6 ± 0.1	2 ± 0.4	4 ± 1	12 ± 4	2 ± 1	4 ± 0.4
Mitochondrial membranes	163 ± 80	165 ± 121	147 ± 11	0.4 ± 0.1	2 ± 0.4	4 ± 2	12 ± 3	1 ± 0.7	4 ± 0.6
Microsomes	8 ± 4	7 ± 3	13 ± 6	0.2 ± 0.0	0.6 ± 0.2	2 ± 0.3	5 ± 1	1 ± 0.5	7 ± 2
HDP	3 ± 2	10 ± 2	8 ± 4	0.1 ± 0.0	0.4 ± 0.1	0.9 ± 0.2	2 ± 0.6	0.9 ± 0.4	4 ± 0.4
MSF	166 ± 81	175 ± 123	155 ± 15	0.5 ± 0.1	2 ± 0.5	5 ± 2	14 ± 3	2 ± 1	8 ± 1

CHAPITRE 3 : Rôle de la distribution subcellulaire dans le transfert trophique de l'Y

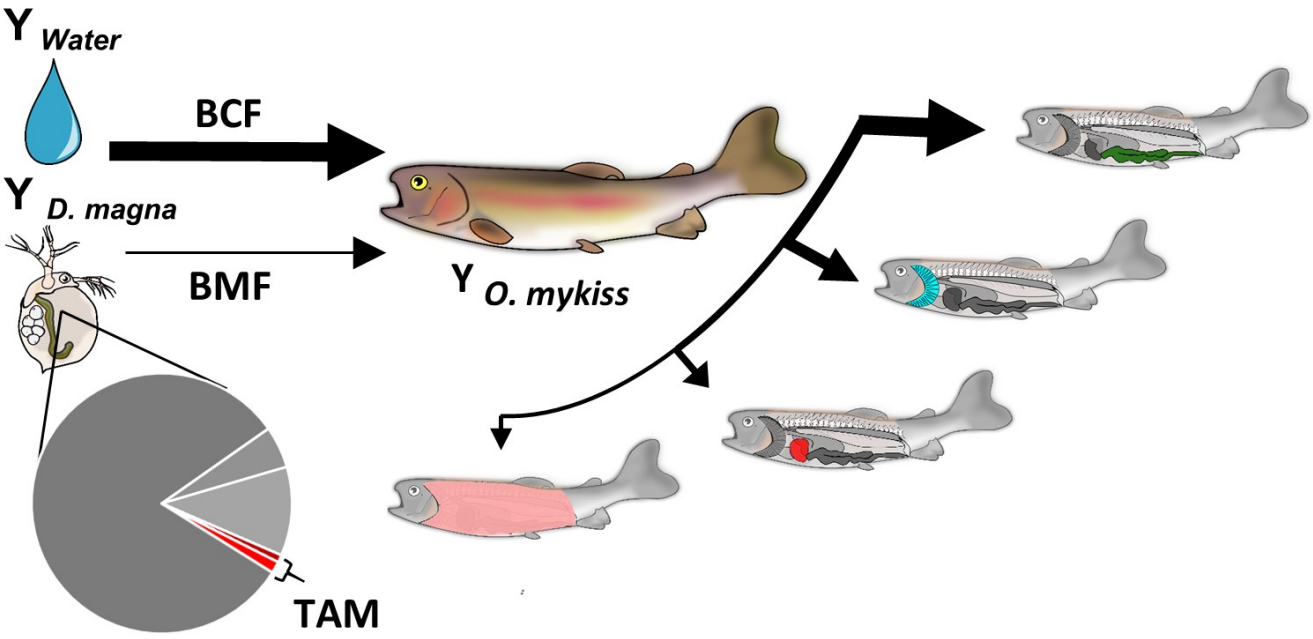

Role of prey subcellular distribution in the bioaccumulation of yttrium (Y) in the rainbow Trout.

Authors: Pierre-Yves Cardon[1], Olivier Roques[2], Nicolas Gruyer[3], Antoine Caron[1], Maikel Rosabal[4], Claude Fortin[5], and Marc Amyot[1*]

[1] GRIL, Université de Montréal (UdeM), Département de sciences biologiques, Pavillon Marie-Victorin, 90 avenue Vincent-d'Indy, Montréal (Québec), Canada, H3C 3J7

[2] Université de La Rochelle, Faculté des sciences et technologies, avenue Michel Crépeau, La Rochelle, France, 17042

[3] Centre d'expertise en analyse environnementale du Québec (CEAEQ), Division de la biologie et de la microbiologie, 2700 rue Einstein, Québec, Canada, G1P 3W8

[4] GRIL, Université du Québec à Montréal (UQAM), Département des sciences biologiques, 141 avenue du Président-Kennedy, Montréal (Québec), Canada, H2X 1Y4

[5] Institut National de la Recherche Scientifique, Centre Eau Terre Environnement (INRS-ETE), 490 rue de la Couronne, Québec (Québec), Canada, G1K 9A9

Abstract

Our knowledge of the risks associated with rare earth elements (REE) and their fate in these ecosystems is still limited. As the contamination of freshwater ecosystems by anthropogenic REE have recently been reported, it becomes increasingly urgent to understand how these metals are transferred to freshwater organisms in order to develop appropriate guidelines. We exposed rainbow trout (*Oncorhynchus mykiss)* to an REE, yttrium (Y), to either a range of Y-contaminated prey (*Daphnia magna*) or a range of Y-contaminated water. For the feeding experiment, the relationship between the Y assimilation by *O. mykiss* and the Y subcellular fractionation in *D. magna* was evaluated. This study represents a first attempt to investigate the relevance of the trophically available metal concept for an REE. Assimilation efficiency of Y by *O. mykiss* at the end of the feeding experiment was weak, ranging from 0.8 to 3%. These values were close to the proportion of Y accumulated in *D. magna* cytosol, 0.6-2%, a theoretically available fraction. Moreover, water also appeared as a weak source of Y transfer to *O. mykiss* with bioconcentration factors averaging less than 1. Regardless of the source of contamination, a similar pattern of Y bioaccumulation between *O. mykiss* tissues was revealed: muscle < liver < gills < intestine. However, at the end of a 5-day depuration period, an elimination of more than 75% of Y was measured in every tissue except liver. In contrast, an increase on average by 50% of Y concentration in the liver was observed. We conclude that the trophic transfer potential of Y seems low and that the liver is likely essential in understanding its toxicity mechanisms and biodistribution. Besides, the evaluation of Y burden in prey cytosol appears as a relevant predictor of Y assimilation by their consumers.

Introduction

Rare earth elements (REE) find applications in the electrification of transport, in wind energy, in medical imaging, in agriculture and in many new technologies (Gwenzi et al., 2018). In recent years, the environmental risks associated with REE have received increasing attention (Gonzáles et al., 2015). Indeed, as a direct consequence of our high consumption of REE (Alonso et al., 2012), cases of natural freshwater aquatic ecosystems contaminated by these metals as a result of human activity have only recently been reported (Kulaksız and Bau, 2011; Ma et al., 2018). Yttrium (Y) with scandium (Sc), are the only REE which do not belong to lanthanides series. Plus, among the four most abundant REE, Y is the only one considered as a heavy REE (HREE) and studies about Y behaviour and toxicity in freshwater ecosystems are scarce. It is therefore urgent to improve our knowledge of the risk associated with Y and HREE in general. Understanding how Y is internalised into freshwater organisms commonly consumed by humans, such as fish, is particularly important for the future assessment of the environmental and health risks of HREE.

Fish acquire metals through two uptake routes: water and food. Although water often appears to be the main source of metal assimilation, it is well established that food can also be an important source for some metals, such as selenium (Økelsrud et al., 2016) and cadmium (Croteau et al., 2005), and methylmercury (Hall et al., 1997).

Understanding the key drivers controlling metal transfer from prey to predators is challenging. If for organic contaminants, the lipophilicity of the contaminant seems to be a key parameter (Arnot and Gobas, 2006), for inorganic contaminants such as metals no consensus has yet been found. However, analysis of the subcellular fractionation of the metal considered in the prey could give an indication of its assimilative capacity by the predator. Indeed, several studies have observed a correlation between the proportion of metal accumulated in the most soluble components of prey cells (e.g. cytosolic proteins, microsomes, etc.) and the assimilation efficiency of this metal by the predator (Dubois and Hare, 2009a; Wallace and Luoma, 2003). Thus, it could be possible to predict the trophic transfer potential of a metal from the analysis of its subcellular fractionation in organisms.

In a recent study (Cardon et al., 2019), we established that more than 75% of Y is accumulated in insoluble fractions (i.e. cellular debris and NaOH-resistant fraction) in

Daphnia magna and *Chironomus riparius* which are typical trout prey. This Y accumulation in putative trophically unavailable fractions suggests a weak potential of trophic transfer for this metal. In addition, measurements of REE along trophic web of temperate (Amyot et al., 2017) and arctic (MacMillan et al., 2017) freshwater ecosystems, demonstrate a biodilution of these metals with increasing trophic levels rather than a biomagnification.

This paper aims to: 1) compare the relative importance of diet and water as uptake pathways for Y in fish; 2) study Y biodistribution and depuration in fish tissues; 3) confirm in the laboratory the weak potential of trophic transfer for Y; and 4) assess whether the analysis of Y subcellular fractionation in prey can predict this potential. For this purpose, feeding and depuration experiments on the rainbow trout, (*Oncorhynchus mykiss),* a freshwater fish commonly used in ecotoxicology and consumed by human, were performed with a range of Y-laden *D. magna* as prey. In parallel, exposures of *O. mykiss* in Y-spiked water, free of food, were set up to compare the potential of Y transfer from water and from food. Finally, Y partitioning between different tissues of *O. mykiss* (i.e., muscles, liver, intestine and gills) was assessed in each experiment to determine the main organs where this metal accumulates.

Materials and methods

D. magna was cultured at the *Centre d'expertise en analyse environnementale du Québec* (CEAEQ, Quebec City, QC, Canada). *O. mykiss* individuals were purchased from the *Pisciculture des Arpents Verts* (Sainte-Edwidge, QC, Canada) and were acclimated to laboratory conditions for at least 3 weeks prior to their use. Exposure solutions were spiked using dilutions of a standard Y solution (10,000 µg/ml Y in 3 % HNO_3 by weight, TraceCERT®, FLUKA).

Trophic transfer experiment

Exposure of prey to Y

D. magna neonates (< 24 h) were reared for 7 days in 15 L aquaria equipped with a polypropylene (PP) bag filled with dechlorinated tap water (300 individuals per aquarium). Then, they were transferred for 24 h to another aquarium filled this time with 15 L of reconstituted water (pH 7.8 ± 0.1, 89 ± 2 mg $CaCO_3$ L^{-1}, 21 ± 1 °C) spiked with Y. After this

exposure period, Y-spiked *D. magna* were transferred for 5 min in a 1 mM EDTA solution to remove Y adsorbed to their body surface, rinsed with milliQ water, before being dried on Kimwipes® and stored in a 50-mL tube at -80 °C.

To obtain a range of Y-laden *D. magna*, we prepared five batches of *D. magna* exposed to one of the five following nominal concentrations all of which were subsequently analytically determined: 0 (control), 86, 144, 240 and 400 µg Y L^{-1}.

When the mass needed of each level for the feeding experiment was reached, Y-laden daphnids were pooled into groups of 20 ± 3.5 mg of wet weight (ww), corresponding to the daily meal for one fish, and stored at -80 °C into 96-wells microplate (Greiner Bio-one) pre-soaked in HNO_3 (15%, v/v, Optima grade, Fisher Scientific), each well containing one group.

Subcellular fractionation of *D. magna*

Five samples of about 80-100 mg of *D. magna* of each Y exposure concentration were subjected to the subcellular fractionation procedure, based on Wallace et al.(Wallace et al., 2003) and customized for *D. magna* (Cardon et al., 2018). Each *D. magna* sample was suspended in Tris-HCl (25 mM; OmniPur) sucrose buffer (250 mM; pH 7.4; Sigma Aldrich) at a ratio of 1:4 (weight [mg]: buffer volume [µL]). Then, the suspended sample was ground with a Potter-Elvehjem pestle at 570 rpm 10 x 2 s, with a 30-s interval of rest between each homogenization period. The resulting homogenate was centrifuged at 800 g for 15 min. The supernatant was collected, and the pellet was resuspended in Tris-sucrose buffer at a ratio of 1:4 before disruption with an ultrasonic probe (Branson 250, with a 4.8 mm diameter microtip probe), at a power of 22 W, with pulses at 0.2 s s^{-1} (20%) for 1 min. The resulting homogenate was pooled and mixed using a vortex with the first supernatant for a final ratio between sample and buffer of 1:8. Subsequently homogenates were separated into five partially validated fractions by differential centrifugation as described in Figure 1: P2) organelles (mitochondrial membranes, lysosomes and microsomes); P3) Heat Denaturated Proteins (HDP) including enzymes; S3) Heat-Stable-Protein (HSP) including metallothioneins; S4) Debris (nuclei, cellular membrane and debris); P4) NaOH-resistant fraction (granules and potentially the daphnid chitinous exoskeleton).

Centrifugations (< 25,000 *g*) were performed using an IEC Micromax centrifuge

(Thermo IEC) whereas a WX ULTRA 100 centrifuge (Sorval, Ultra Thermo Scientific) equipped with a F50L-24 X1.5 rotor (Fisher Scientific) was used for ultracentrifugation (≥ 25,000 *g*).

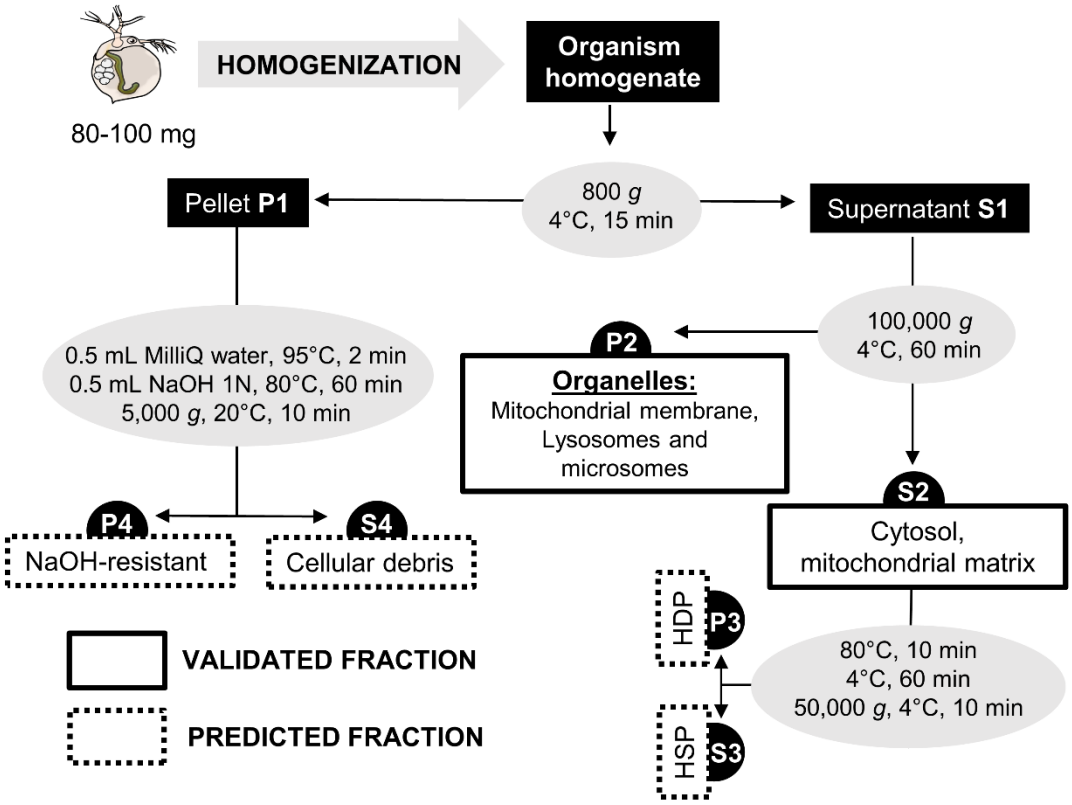

Figure 1. Subcellular fractionation protocol customized for *D. magna* (Cardon et al., 2018). P: Pellet; S: Surpernatant

Exposure of *O. mykiss* to Y-laden daphnids

Fish (0.93 ± 0.14 g) were exposed individually in a 1-L glass beaker filled with dechlorinated tap water (pH 7.8, 63 mg $CaCO_3$ L^{-1}, 15 ± 0.2 °C). Seven individuals were used for three nominal Y exposure levels of daphnids (control, 144 and 240 µg Y L^{-1}) while 25 were used for the other two levels (86 and 400 µg Y L^{-1}). For the latter exposure levels, a depuration test was set at the end of the exposure period. Prior to experiment, fish were fed with control daphnids for 10 d. Then, for 5 d, fish were fed 2% of their body weight (wet

weight of prey to wet weight of fish) daily with their corresponding Y-laden daphnids. Every day, faeces were removed with a 50-mL glass pipette 1 h after the feeding period to avoid subsequent Y release to the medium. In addition to monitoring this potential release, the water of each experimental chamber was sampled using a 20-mL PP syringe, then filtered through a 0.45 µm polyethersulfone syringe filter to measure dissolved Y concentrations daily. At the end of the exposure period, a depuration period was initiated by renewing 90% of the water in each jar with dechlorinated tap water.

Many authors determined that less than 24 h are required for fish to clear their gut content (Pouil et al., 2016; Van Campenhout et al., 2009). Hence to only measure the assimilated Y, for the control exposure level as well as 144 and 240 µg Y L^{-1}, fish were collected after a 24-h depuration period and were fed with the daphnids exposed to the control exposure level during this period. For the exposure levels 86 and 400 µg Y L^{-1}, this depuration period was raised to 5 d with five individuals collected before the depuration, as well as after 1, 2, 3 and 5 days of depuration.

Bioconcentration experiment

Fish (1.6 ± 0.2 g) were exposed for 5 d in groups of seven individuals in 20 L aquaria equipped with PP bags and Y-enriched dechlorinated tap water (pH 7.8, 63 mg $CaCO_3$ L^{-1}, 15 ± 0.2 °C). Chemical characteristics of the tap water used in the feeding and the bioconcentration experiments are given in Supporting Information (SI; Table SI). Fish were not fed 24 h before and during the exposure period. Five Y nominal exposure levels plus the control were tested: 52, 86, 144, 240 and 400 µg Y L^{-1}. In addition, dissolved Y concentrations were measured every day of the exposure. At the end of the exposure, fish were transferred to new aquaria filled with dechlorinated tap water for 24 h. After this depuration period, fish were collected. The Y speciation at these exposure levels is presented in SI, Table SIV. Yttrium was mainly present in the form of YCO_3 (41-59%) and YPO_4 (27-50%). For all exposure levels, the solubility of YPO_4, $K^0_{sp}= 10^{-25}$ M (Liu and Byrne, 1997) was exceeded. Therefore, we have to assume that a part of YPO_4 precipitated over the test.

Fish treatment and storage at the end of the experiments

For the trophic transfer and bioconcentration experiments, coefficient of variation of fish average weight between each exposure level did not exceed 5%. After being collected, fish from both experiments were euthanized with clove extract, rinsed with EDTA (1 mM), then with milliQ water, dried in Kimwipes®, and finally weighed and measured for their length. Their gills, intestine, liver, muscle tissues and remaining body parts were collected with a surgical razor blade. Tissues were put in 1.5 mL preweighed and acid washed PP microcentrifuge tube and remaining body parts were collected in 50 mL tube. They were then weighed, freeze dried, weighed again and stored at -80 °C.

Yttrium measurements and quality control

All labware was soaked in HNO_3 (15%, v/v, Optima grade, Fisher Scientific) and rinsed seven times in MilliQ water before use, to minimize Y accidental contamination. Centrifuged pellet fractions resulting from the fractionation of *D. magna* (NaOH-resistant fraction, organelles and HDP), aliquots sampled as homogenate and *O. mykiss* tissues were freeze-dried for 24 h, weighed and stored at -80 °C. Every subcellular fraction and *O. mykiss* tissues were digested at 65 °C in 500 µL of HNO_3 (70%, v/v) whereas *O. mykiss* remaining parts were subjected to the same procedure but in 4 mL of HNO_3. Then, 9.5 mL and 45 mL of MilliQ water were added in the digestates of *D. magna* fractions and *O. mykiss* tissues, respectively.

Concentrations of Y in water and in organism fractions and tissues were measured with an inductively coupled plasma-mass spectrometer (ICP–MS; Thermo Elemental X Series). To ensure quality of these measurements, samples of similar weight of a certified standard reference material, BCR 668 (mussel tissue, Institute for Reference Materials and Measurements) underwent the same digestion procedure and analysis. Mean (± SD) recoveries of BCR 668 reference sample (n = 10) were within the satisfactory range of certified values for Y (90.0 ± 0.1%). To verify metal recovery following subcellular fractionation, a 40-µL subsamples of tissue homogenate were analyzed. Recovery was expressed as the ratio of the sum of the Y burden in the five fractions divided by the total homogenate Y burden in *D. magna*, multiplied by 100. Mean (± SD) recovery values of Y was 99 ± 4% (n = 25).

Calculation and statistical analyses

Yttrium concentrations in every *O. mykiss* tissues and *D. magna* homogenates were expressed by wet weight (mg kg^{-1} ww). Yttrium burden in a given subcellular fraction of *D. magna* was divided by the sum of Y burden in all fractions and multiplied by 100 to assess the relative contribution of each subcellular fraction to the total Y burden in terms of percentages (%). Results of the depuration test were expressed as Y remaining in *O. mykiss* tissues over the depuration period. This value was calculated as the Y concentration in a tissue at a given day of depuration divided by the Y concentration in this tissue before the depuration period (day 0) and multiplied by 100 (%).

Assimilation efficiency (AE) was calculated according to Lapointe et al.(Lapointe et al., 2009) as follows:

$$\mathrm{AE} = \left[\frac{\mathrm{M}_{O.\,mykiss} - \mathrm{M}_{\mathrm{control}}}{\mathrm{M}_{D.\,magna}}\right] \times 100$$

$M_{O.\,mykiss}$ is the Y burden in fish fed Y-laden daphnids, $M_{control}$ is the average Y burden in fish fed uncontaminated daphnids and $M_{D.\,magna}$ represents the total amount of Y provided to fish from Y-laden *D. magna*.

Biomagnification factors (BMF) and bioconcentration factors were calculated as follows:

$$\mathrm{BMF} = \frac{\mathrm{C}_{O.\,mykiss}}{\mathrm{C}_{D.\,magna}}$$

$$\mathrm{BCF} = \frac{\mathrm{C}_{O.\,mykiss}}{\mathrm{C}_{water}}$$

$C_{O.\,mykiss}$, $C_{D.\,magna}$ and C_{water} represents respectively the Y concentration in *O. mykiss* whole body or tissues (µg kg^{-1} ww), in Y-laden *D. magna* (µg kg^{-1} ww) and in the water (µg dissolved Y L^{-1}).

Data are expressed as means ± standard deviation (SD). Significant differences were tested with a one-way analysis of variance (ANOVA), followed by Tukey pairwise comparison test ($p < 0.05$). Linear regression analysis was performed to study the relationship

between Y accumulation according to Y exposure level as well as Y in *O. mykiss* tissues depending on the length of the depuration period. The assumptions of normality and homoscedasticity were verified by Shapiro-Wilk's and Levene's tests, respectively. When these assumptions were not met, a natural log transformation was successfully applied on the data. For the percentage data (remaining Y over the depuration period), an arcsine transformation prior to any statistical test was applied. Statistical analyses were performed using R software version 3.4.4.

Results and Discussion

Bioaccumulation and distribution of Y among *O. mykiss* tissues depending on the exposure source

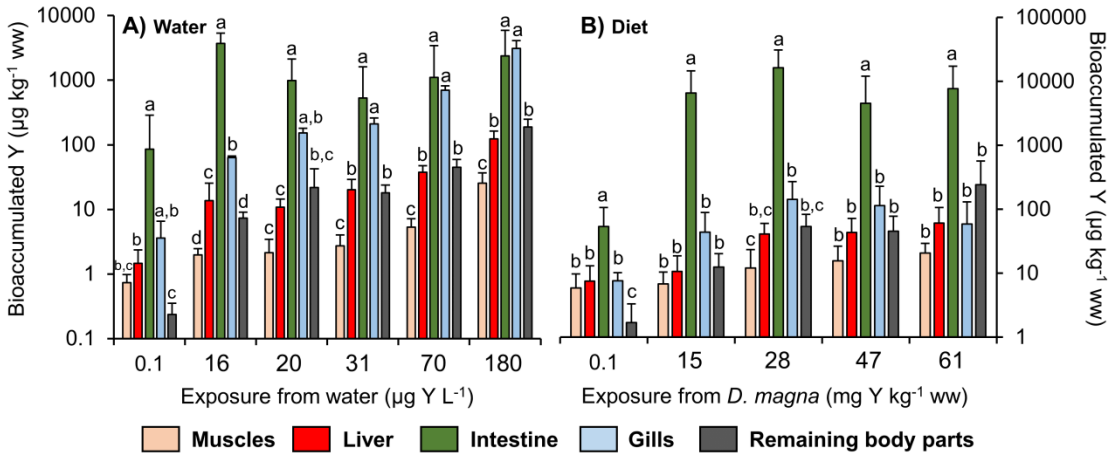

Figure 2. Bioaccumulation of Y (Mean ± SD; µg kg^{-1} ww; n=5-7) in different tissues of *O. mykiss* following two types of exposures **A)** from water (µg Y L^{-1}) or **B)** from diet (mg Y kg^{-1} ww of daphnid), and along an exposure range. Different letters indicate a significant difference of accumulation among the different tissues of *O. mykiss* for a given exposure level (ANOVA, followed by Tukey pairwise comparison test, $p < 0.05$). The lowest exposure level for both experiments represents the control. Exposure conditions over these tests, especially Y dissolved concentrations, are given in SI.

We compared the bioaccumulation of Y from water and diet in different trout organs. Regardless of the source of exposure, the Y content determined in muscle tissues appeared

significantly lower than other tissues with average values between 1 and 25 µg Y kg^{-1} ww (Fig. 2). On the other hand, along the exposure range from diet, concentrations of Y in the intestine were significantly higher than all other tissue; from 7 to 1370 times higher (Fig. 2B). Even in the water-only exposures, the maximal exposure level excluded, this tissue presented the top values of bioaccumulated Y (Fig. 2A). In addition, for both exposure trials, the amount of Y in intestine was, on average, higher than the whole fish less the intestine. However, unlike other tissues, no relationship was found between the Y concentration in intestine and the exposure range (water or food) (SI, Fig. SI). In contrast, a strong positive correlation (R^2 = 0.7) was observed between Y concentration in gills and water exposure level (SI, Fig. SIA). Thus, at the maximal exposure level of 180 µg Y L^{-1}, the highest concentration of Y, 3098 ± 1022 µg Y kg^{-1} ww, was measured in the gills (Fig. 2A). At this exposure level, concentrations of Y in the liver and in the remaining body parts were more than ten times inferior than in gills. In general, in the water exposure test, the concentrations of Y in the liver and in the remaining parts of the fish body were very close and at an intermediate level between the values measured in the muscles and gills. Nonetheless, in the diet exposure test, no significant differences were measured between Y concentrations in the liver (min-max: 11-61 µg Y kg^{-1} ww), in the remaining parts of the fish body (44-143 µg Y kg^{-1} ww) and in the gills (12-243 µg Y kg^{-1} ww) (Fig. 2B), when excluding the control. For gills, no relationship between Y exposure concentrations and the level of Y in *D. magna* was assessed over the feeding trial (SI, Fig. SIB). We presume that the source of the Y accumulated in the gills during this trial was the Y released in the water medium from the Y-laden daphnids (SI, Table SII).

The lower Y concentrations we measured in muscles compared to other tissues had already been reported in several field studies. In ten freshwater fish species from a reservoir in Washington state, muscles had lower REE concentrations (on average at least three times lower for Y) than in the whole body and carcass (Mayfield and Fairbrother, 2015). Moreover, significantly larger differences were measured in three fish from Canadian temperate lakes for which whole-body REE concentrations were on average at least 40 times higher than muscle concentrations (Amyot et al., 2017). In general, metal concentrations in fish muscles have been reported to be lower in most cases than in other organs (Subotic et al., 2014).

Besides, our results suggest that gills are among the main tissue of Y accumulation in fish. This importance of gills as REE accumulation site was already reported (Hao et al., 1996; Qiang et al., 1994). The relatively high concentrations of Y we measured in the gills may have detrimental effects on fish health. REE are known to be antagonists of Ca uptake. Lanthanum for example, is commonly used as a Ca^{2+} channel blocker in studies on metal uptake by gills (Hogstrand et al., 1996). Indeed, gills are considered as the first route of Ca uptake by freshwater fish (Marshall, 2002); Ca uptake by intestine being considered as secondary (Flik et al., 1996). Hence, the accumulation of Y in the gills of *O. mykiss* could lead to Ca deficiency by this organism. The assimilation of essential metals, such as Zn, whose internalization seems to be done through Ca^{2+} channels (Hogstrand et al., 1996) could also be limited due to the presence of Y. Therefore, we suspect that Y could have adverse effects on the ionoregulation within *O. mykiss*.

Finally, the preferential accumulation of Y in internal organs, like intestine, as well was already reported. Thus, In the laboratory, by analysing concentrations of seven REE, including Y, in several tissues of *Cyprinus carpio,* authors estimated the following concentration pattern: muscle < skeleton < gills < internal organs (Hao et al., 1996; Qiang et al., 1994). This pattern was also reported in our diet exposure trial but as well in *O. mykiss* for Cd, Cu and Se following an exposure to diet enriched with these metals (Handy, 1992; Misra et al., 2012). Unlike our Y results, for Se and Cu however, liver showed highest concentration than gills. Furthermore, in 28-d exposures to similar Y concentrations, the Y concentration in the liver of *O. mykiss* was about ten times higher than the one we measured (Cardon et al., 2019). This suggests that Y concentration in *O. mykiss* tests did not reach a steady state at the end of our tests.

Therefore, we should assume that liver could be a more important organ of Y accumulation for fish in the field than what we evaluated. Another trial involving both water and diet as exposure routes and a longer period of exposure to Y, could confirm this assumption.

Bioconcentration and biomagnification factors

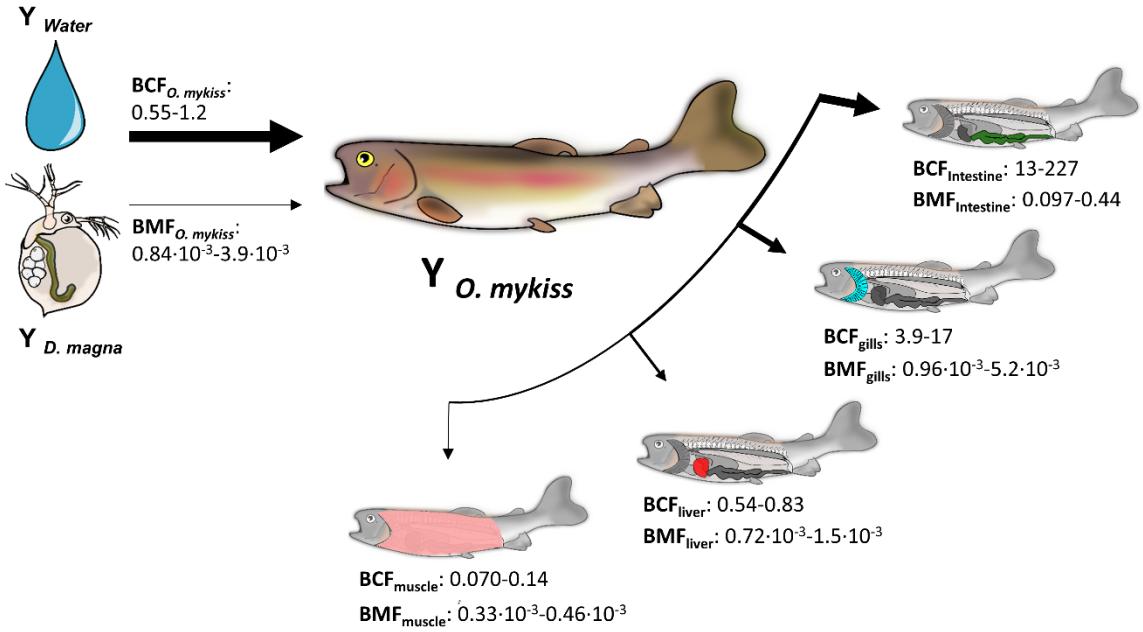

Figure 3. Range of Y bioconcentration (BCF) and biomagnification (BMF) factors (min-max) for *O. mykiss* and its organs, observed over our exposure concentration range, control excluded. Both the food and the water used to rear the fish before the beginning of the trial were not free of Y. As a result, BCF and BMF at the control exposure levels were not included in this figure.

In fish whole body, BCF value ranged from 0.55 to 1.2 L kg^{-1} and BMF from $0.84 \cdot 10^{-3}$ to $3.9 \cdot 10^{-3}$ (Fig. 3). BCF and BMF values for the muscle were the lowest and ranged from 0.070-0.14 L kg^{-1} ww and $0.33 \cdot 10^{-3}$ and $0.46 \cdot 10^{-3}$ respectively (Fig. 3). Finally, in ascending order, the values for the two factors were arranged as follows: muscles < liver < gills < intestine (Fig.3).

The BMF we assessed were three orders inferior to 1 which suggests that diet is a poor route of Y entry in *O. mykiss* (Arnot and Gobas, 2006). This would confirm what was reported in the field. For instance, for both temperate lakes (Amyot et al., 2017) and artic lakes (MacMillan et al., 2017) from Canada, REE concentrations tended to decrease with increasing trophic levels; the lowest concentrations were measured in top predators while the highest were for the primary consumers. The BCF we assessed are close to those measured in other laboratory experiments. For example, an exposure of *Cyprinus carpio* to high concentrations (60-500 µg L^{-1}) of three REE individually (Qiang et al., 1994) or a mixture of five REE (Hao

et al., 1996), for 43 and 45 days led to BCF from 8.0 to 18 L kg^{-1} for gill and from 0.22 to 3.5 L kg^{-1} for muscles. In our work, the BCF was less than 1 L kg^{-1} on average, for *O. mykiss* whole body. Thus, yttrium's ability to be accumulated by *O. mykiss* from water appears to be low and under the bioaccumulation regulatory criteria set by several environmental agencies (Arnot and Gobas, 2006). However, these low BCF values we measured for Y should be put in perspective. Indeed, the lowest Y exposure level used in our experiment (16 µg L^{-1}) was more than 1000 times higher than Y concentrations reported from natural ecosystems (Amyot et al., 2017; MacMillan et al., 2017). Besides a significant inverse relationship was observed for BCF and the Y exposure level over our trial. Note that this trend was already reported for several metals by McGeer et al. (2003). As a result, the high level of Y used in our experiment compared to natural systems may explain the low value of the BCF we evaluated.

Yttrium depuration

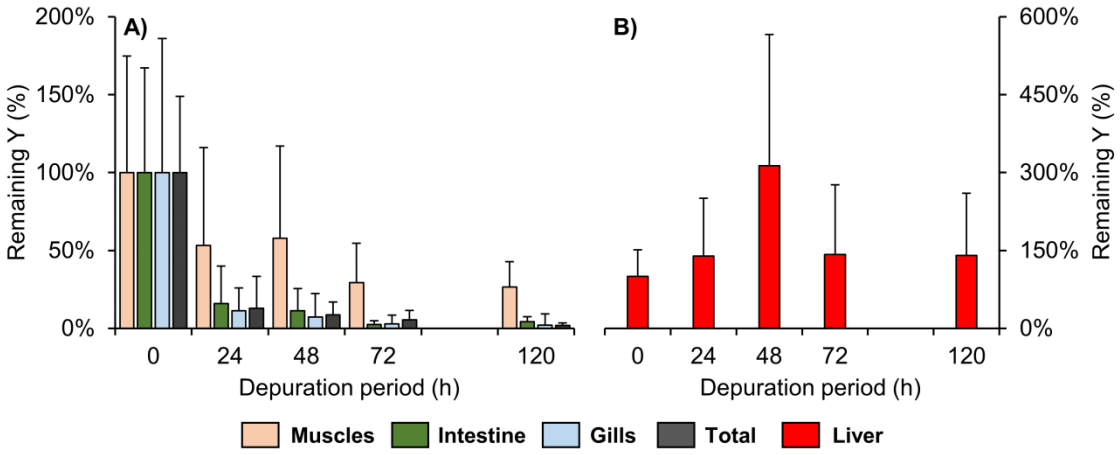

Figure 4. Percentage of remaining Y (mean ± SD, %, n=10) following the length of the depuration period in **A)** muscles, intestine, gills and whole body or **B)** liver of *O. mykiss*. Percentage of remaining Y is measured as the level of bioaccumulated Y at a given day of depuration divided by the level of bioaccumulated Y before the depuration period (day 0). The depuration test was performed at the end of the feeding experiment.

We compared Y externalization following the feeding experiment in different trout organs (Fig. 4). In intestine, gills and whole body of *O. mykiss*, on average more than 80% of the bioaccumulated Y was eliminated after 24 h of depuration, and 95% after 120 h (Fig. 4A).

In muscles the elimination rate was slower with 58 ± 59% of the bioaccumulated Y remaining in muscle tissues even after 48 h of depuration and on average only 73% was eliminated after 120 h. In contrast, Y bioaccumulated in the liver did not decrease over our 5-day depuration period (Fig. 4B) but in fact, Y levels increased by a factor of three in the following 48 h.

The rapid elimination of a significant part of the bioaccumulated Y in all tissues after 24 h represents the loss of unassimilated Y in gut contents. Many authors measured that less than 24 h are required for fish to excrete the part of their food ingested but no assimilated (Pouil et al., 2016; Van Campenhout et al., 2009). It confirms that the choice we made to add a 24-h depuration period at the end of our exposure test was sufficient to measure the concentrations of Y actually assimilated by *O. mykiss*. The increase of the Y concentration in fish liver during depuration has been reported for other metals and other organs like kidneys. Thus, even after 12 d of depuration, concentrations of Cd and Cu in the liver of *O. mykiss* were respectively multiplied by 2.0 and 1.1 (Handy, 1992). Similar results were measured for different metals in several fish and were compiled by Jezierska and Witeska (Jezierska and Witeska, 2001).

This absence of Y depuration revealed over a 5-d period for the liver in our trial reinforces the assumption made earlier. The Y concentration in *O. mykiss* tests did not reach a steady state at the end of our tests. Liver could be a more important organ of Y accumulation for fish in the field than what we evaluated in laboratory. As a result, the liver could be a key organ to study Y and REE toxicity. Initial data seem to confirm this hypothesis. Thus, Y in *O. mykiss* liver cells have been reported to be mainly accumulated in metal-sensitive components like mitochondria (Cardon et al., 2019).

Range of bioaccumulation and subcellular fractionation in daphnids

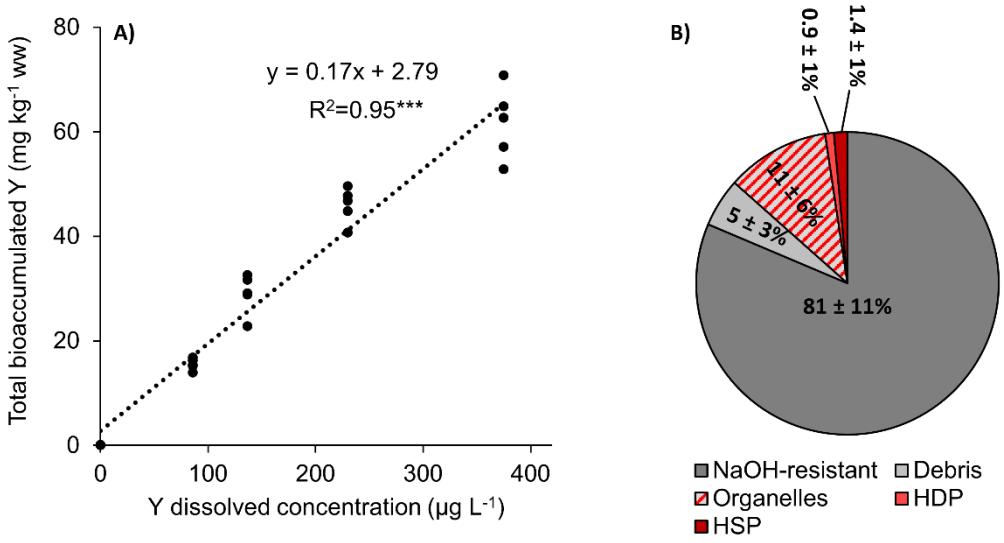

Figure 5. Characterization of Y accumulation in daphnids. **A)** Relationship between the Y exposure level and the total of Y bioaccumulated by *D. magna* (mg Y kg^{-1} ww, n = 5); **B)** Average percentage of Y (mean ± SD; %; n = 5) in each subcellular fraction of Y-exposed *D. magna.*

A strong linear relationship (R^2 = 0.95) was observed between Y bioaccumulation by *D. magna* and the Y exposure level (Fig. 5A). The amount of Y accumulation by *D. magna* ranged from 0.05 ± 0.03 to 62 ± 7.0 mg Y kg^{-1} ww. At the subcellular level, Y was mainly found in the NaOH-resistant fraction, with on average 81 ± 11 % of the total Y accumulated (Fig. 5B). Organelles contained 11 ± 6% of the total Y, while the remainder (<10%) was divided between the other fractions (debris, HDP and HSP).

Such high values of Y bioaccumulated by *D. magna* (Fig. 5A) have previously been reported in laboratory studies (Cardon et al., 2018; Xingie Yang et al., 1999), but are at least 1000 times higher than those reported in zooplankton from the field (Amyot et al., 2017; MacMillan et al., 2017). Yttrium subcellular fractionation reported here is consistent with our previous results (Cardon et al., 2018), which is to our knowledge the only other available study on REE fractionation in daphnids.

According to several authors (Wallace and Luoma, 2003) only the part of metal bound to the putative trophically available fraction, the trophically available metal (TAM), in the prey cells, will be transferred to their consumer. Therefore, the trophic transfer potential of a metal could be assessed based on its subcellular fractionation in the prey. Our results suggest a

weak potential of Y trophic transfer from *D. magna* to its predator. Indeed, by considering only Y found in the cytosol (HDP and HSP) of *D. magna* as the TAM (Wallace and Lopez, 1996), less than 5% of Y in this organism would be theoretically trophically available. Even if we include Y associated to organelles in the TAM pool, as recommended by many authors (Dubois and Hare, 2009a; Wallace and Luoma, 2003), this transfer potential remains under 15%. In contrast, the proportion of TAM (including organelles), reported for Ni, Tl and Zn in *D. magna* exceeded 40% (Lapointe et al., 2009; Wang and Guan, 2010).

Relationship between assimilation efficiency and trophically available metal

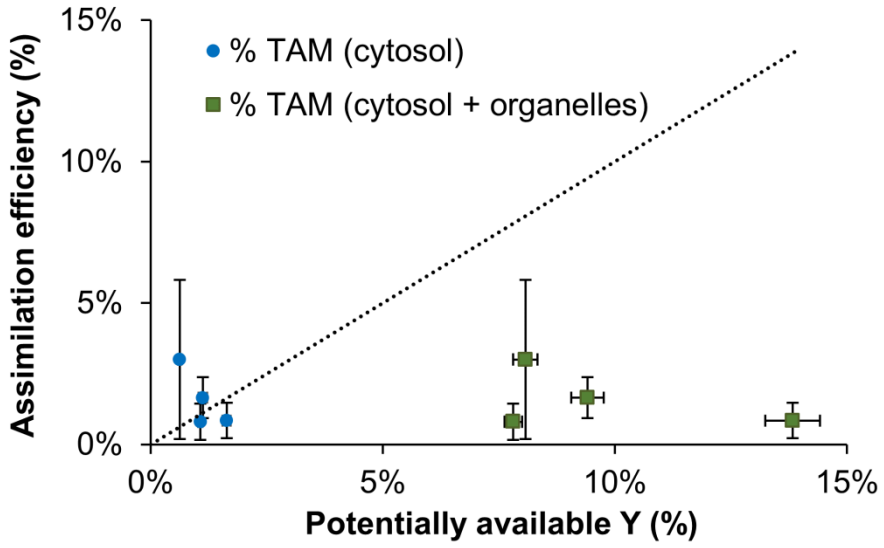

Figure 6. Relationship between assimilation efficiency of dietary Y in *O. mykiss* and the proportion of Y assumed to be trophically available (TAM) in *D. magna* with or without the inclusion of organelles in TAM (means SD, n = 5-7). The dashed line illustrates a 1:1 relationship.

Percentage of Y found in the cytosol of *D. magna* appeared to be very close to the AE in *O. mykiss*. Thus, over the trophic transfer trial, percentages of Y in *D. magna* cytosol ranged from 0.63 to 1.6% while EA ranged from 0.80 to 3.0 % (Fig. 6). When adding organelles, the TAM fraction increased significantly (range: 7.8 to 14%) and departed from the expected 1:1 line with AE (Fig. 6). Moreover, the spread of % potentially available Y increased with the addition of Y recovered in *D. magna* organelles to the pool of TAM. These results suggest that the Y bound to *D. magna* cytosol was trophically available while the Y bound to organelles was not. In contrast, many authors have concluded that a part at least of metal from organelles was available: Cd from *Potamocorbula amurensis* to *Palaemon macrodatylus* (Wallace and Luoma, 2003) and from *Gammarus lawrencianus* to *Palaemontes pugio* (Seebaugh et al., 2006), Cd, Zn, Ni, Tl and Se from *Chironomus riparius* to *Sialis velata* (Dubois and Hare, 2009b, 2009a; Dumas and Hare, 2008). Even the NaOH-resistant fraction was considered as potentially available in some studies (Cheung and Wang, 2005; Rainbow et al., 2007).

Several preys presenting similar proportion of a metal theoretically available in their cells could have significant differences of AE for their consumers (Pouil et al., 2016). In fact, it is usually accepted that subcellular components included in the TAM differ depending on the prey and the considered predator. Thus, for a given prey, the assimilation of metal containing fractions by a predator will depend on the strength of its digestive processes (Rainbow et al., 2011). To get insight on the relative strength of this digestive process for *O. mykiss*, we can compare metal AE of several fish with those of invertebrate predators fed with the same preys. Three marine fish, *Lutjanus argentimaculatus, Penophthalmus cantonensis* and *Ambassis urotaenia,* assimilated 6-33% and 5-46% of respectively Cd and Zn from copepod and clam preys (Xu and Wang, 2002) while two invertebrates, *Palaemontes varians* and *Hinia reticulata*, assimilated on average more than 60 % of the same metal from the same preys (Rainbow and Smith, 2010). Similarly, *Sialis velata*, an invertebrate predator, assimilated more than 70% of Cd, Ni and Tl from two invertebrate preys (Dubois and Hare, 2009b; Dumas and Hare, 2008), while several fish, including *O. mykiss*, fed with similar metal-laden preys, assimilated less than 10% of these metals (Béchard et al., 2008; Lapointe et al., 2009; Ng and Wood, 2008; Steen Redeker et al., 2007). Finally, the barnacle, *Balanus amphitrite*, assimilated more than 63% of Cr from zooplankton preys (Wang et al., 1999)

versus less than 12% for fish fed with similar preys (Ni et al., 2000). Regardless of the metal, AE for fish seem far lower than invertebrates. It suggests a weaker digestive process for fish than invertebrates.

Nevertheless, strength of digestive processes alone cannot explain why only cytosol appears trophically available in our study when organelles are generally included in the TAM. Like our own results, some studies comparing trophic transfer of essential metal like Zn or Se from a variety of prey to fish also reported close values between AE and metal bound to prey cytosol (Zhang and Wang, 2006). Nonetheless so far, except for Hg, most studies on the relationship between nonessential metal trophic transfer to fish and the percentage of this metal theoretically available in their prey observed AE far lower than predicted. Indeed, in the following examples, metal bound to cytosol of the prey represented more than 30% of the total bioaccumulated metal while AE of the fish fed with these preys did not exceed 10%. It was the case for the trophic transfer of Cd from *Tubifex tubifex* to *Cyprinus carpio* (Steen Redeker et al., 2007), for Cd from *Lumbriculus lumbriculus* to *O. mykiss* (Ng and Wood, 2008), for As from different preys (clam, copepod and fish) to *Terapon jarbua* (Zhang et al., 2011), for Ag from Seabream, shrimp and ragworm to *Scophthalmus maximus* (Pouil et al., 2015) and for Ni from *D. magna* or *C. riparius* to *Pimephales promelas* (Lapointe et al., 2009). Hence, beyond the strength of digestive processes, the close AE and TAM values we measured for Y could be simply the result of the weak AE of nonessential metal for fish. Predictions of trophic transfer of nonessential metals to fish based on TAM analysis in its prey should thus be made with caution.

Overall, our results confirm the value of determining subcellular fractionation of metals to predict their trophic transfer potential. We provide new evidence of this low potential for REE. Finally, our results highlight the importance of considering the liver in the assessment of rare earth-induced risk to organisms such as fish.

Acknowledgments

We would like to thank the technicians from the *Centre d'expertise en analyse environnementale du Québec* (*Ministère de l'Environnement et de la Lutte contre les changements climatiques* (MELCC) for their assistance in the breeding of organism and

chemical analyses. We also would like to thank the INRS-ETE technicians for their help in Y concentrations measurements.

Funding

This research was funded through the Natural Sciences and Engineering Research Council (NSERC) Discovery grant and an NSERC strategic grant (TRIVALENCE) to M. Amyot. This work was supported by the NSERC CREATE Mine of Knowledge network through a scholarship to P.-Y. Cardon. M. Amyot and C. Fortin are supported by the Canada Research Chair Program. The lab ware used in experiments performed at the Quebec City CEAEQ were purchased and provided by the MELCC.

Supporting Information

Monitoring of the exposure conditions

The initial chemical characteristics of the tap water used in the feeding and the bioconcentration experiments are given in Table SI. The dissolved Y concentrations over the feeding experiment depending on the level of Y-spiked daphnids provided to fish are presented in Table SII. The dissolved Y concentrations over the bioconcentration test are given in Table SIII. Finally, results of Y speciation calculations based on initial conditions of the bioconcentration experiments are given on Table SIV.

Except for the control level, we observed an increase in the Y concentration in the water over the 5 days of the feeding experiment. Compared to the initial levels on the third day, dissolved concentrations increased two to six times, and at the end of the experiment (fifth day), from four to ten times (Table SII). We hypothesize that Y-laden daphnids released Y in the water medium. In contrast, a strong depletion of dissolved Y was measured over the bioconcentration experiment. On average dissolved Y in water decreased twice after only one day of experiment (Table SII). This depletion could be due to YPO_4 precipitation. Indeed, over the bioconcentration experiment, Y was mainly present as YPO_4 (Table SIV). The YPO_4 solubility constant, Ks 10^{-25}, being exceeded for all our exposure levels we must assume that a significant part of YPO_4 precipitated over the test.

Table SI. Chemical characteristics of the water medium at the beginning of the trophic transfer and bioconcentration experiment.

	Transfer trophic test	**Bioconcentration test**
pH	7.8	7.8
DOC	1.7 mg C L^{-1}	2.0 mg C L^{-1}
Cl^-	18 mg L^{-1}	17 mg L^{-1}
Conductivity	230 µS cm^{-1}	200 µS cm^{-1}
Ca	19 mg L^{-1}	19 mg L^{-1}
K	1.1 mg L^{-1}	0.91 mg L^{-1}
Mg	3.7 mg L^{-1}	2.9 mg L^{-1}
Na	13 mg L^{-1}	11 mg L^{-1}
Suspended matter (0.45 µm)	< 1.0 mg L^{-1}	<1 mg L^{-1}
NO_3	0.95 mg L^{-1}	1.2 mg L^{-1}
NO_2	2.3 µg L^{-1}	8.0 µg L^{-1}
NH_4	<0.020 mg N L^{-1}	-
N_{total}	0.27 mg N L^{-1}	-
$P_{dissolved}$	0.074 mg L^{-1}	0.043 mg L^{-1}
P_{total}	0.083 mg L^{-1}	0.056 mg L^{-1}
SO_4	27 mg L^{-1}	24 mg L^{-1}

Table SII. Yttrium exposure condition over the trophic transfer assay

Y concentration in *D. magna* (mg kg^{-1} ww)	Dissolved Y in water over the test (mean ± CV, in µg L^{-1}, n = 5-7)		
	1st day	3rd day	5th day
0.1 (control)		0.027 ± 14%	0.022 ± 14%
15		0.065 ± 29%	0.12 ± 27%
28	0.033	0.18 ± 45%	0.34 ± 28%
47		0.18 ± 40%	0.28 ± 27%
61		0.15 ± 34%	0.27 ± 31%

Table SIII. Yttrium exposure condition over the bioconcentration assay

Y nominal exposure level (µg L^{-1})	Dissolved Y (µg L^{-1})					
	1st day	2nd day	3rd day	4th day	5th day	Average
0 (Contrlol)	0.05	0.06	0.05	0.05	0.05	0.05
52	43	18	12	10	9	16
86	73	19	11	9	7	20
144	120	27	16	14	12	31
240	190	71	52	44	32	70
400	300	190	170	150	120	180

Table SIV. Results of Y speciation calculations based on initial conditions of the bioconcentration experiments**.**

Total Y (µg L^{-1})	Y^{3+}	YOH^{2+}	$Y(OH)_2^{+}$	YSO_4^{+}	YCO_3^{+}	$Y(CO_3)_2^{-}$	$YHCO_3^{2+}$	$YHPO_4^{+}$	YPO_4
50-140	3%	1%	0.1%	1%	41%	5%	0.1%	0.4%	50%
242	3%	1%	0.1%	1%	46%	5%	0.1%	0.3%	43%
396	4%	2%	0.1%	1%	59%	7%	0.2%	0.2%	27%

Relationship between Y bioaccumulation and exposure level

Significant relationship between Y bioaccumulation in *O. mykiss* tissues and Y exposure level were observed for every tissue except for the intestine (Fig. S1). Indeed, values of bioaccumulated Y did not show any correlation following exposure level over our trials. In addition, it presented important coefficient of variation; on average 142%. Bioaccumulated Y values in gills over the trophic transfer trial as well did not show a significant linear relation with the exposure level. We assume that the source of the Y accumulated by the gill during this trial was the Y released in the water medium from the Y-laden daphnids (Table S2). All organs considered, the linear regression of Y bioaccumulation following the exposure level appeared much stronger with exposure to Y from water (Fig. S1). On average, the slope coefficient for each tissue was 1000 times higher with this exposure source than for the feeding experiment (Fig. S1).

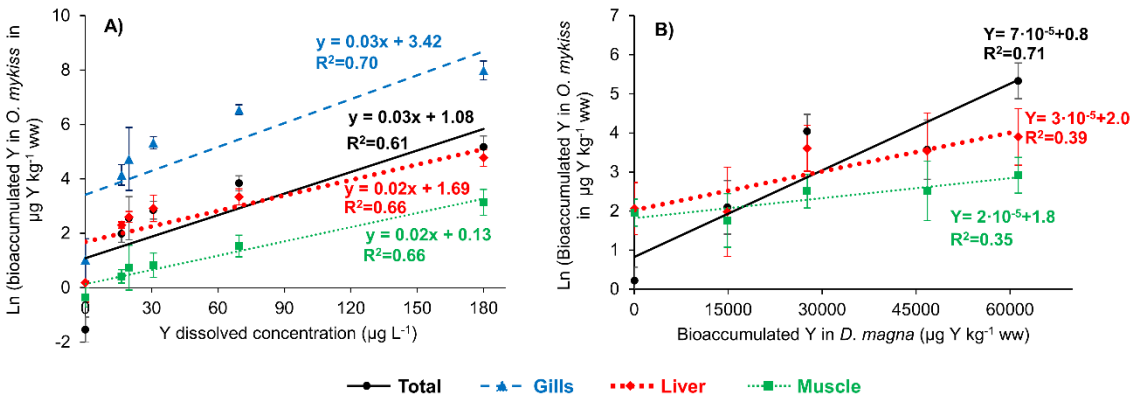

Figure SI. Relationship between Y bioaccumulated in a given tissue of *O. mykiss* (Mean ± SD, n = 5-7) and the Y exposure level following two types of exposures: A) water or B) food. Strengths of the relationships are represented with a linear least-squares R^2 coefficient and their correlation equation. Only relationships with a significant spearman correlation, $p < 0.001$ are represented in this figure. All bioaccumulation data were transformed with a Ln function to ensure the normality and homoscedasticity necessary to perform spearman's correlation test.

Conclusions et recommandations

L'engouement actuel des marchés pour les ETR devrait continuer de croître dans les prochaines années. Leur demande est en constante augmentation (Alonso et al., 2012). Leurs usages sont de plus en plus nombreux. Les projets miniers les concernant se multiplient (Paulick et Machacek, 2017), et des initiatives visant à améliorer leur recyclage commencent à se mettre en place (Binnemans et al., 2013; Schulze et Buchert, 2016).

Parallèlement, les cas de contaminations des milieux aquatiques en ETR d'origine anthropique sont de plus en plus fréquents (Ma et al., 2018). Les rejets hospitaliers par exemple, du fait de l'utilisation du Gd en imagerie médicale, constituent une importante source de contamination (Hatje et al., 2016; Kulaksiz et Bau, 2011).

Pour un usage durable de ces éléments, il est donc important d'approfondir nos connaissances sur leur toxicité et sur leur capacité à être assimilés par les organismes. Dans cette optique, l'analyse de leur fractionnement subcellulaire y contribue. En effet, la distribution intracellulaire des métaux chez les organismes renseigne sur leur assimilabilité, leurs mécanismes de toxicité ainsi que sur leur détoxication par ces organismes.

Le protocole de fractionnement subcellulaire

À travers la littérature sur le fractionnement subcellulaire, force est de constater que les protocoles de fractionnement réalisés présentent systématiquement des modifications. Dans la grande majorité des cas, la justification de ces modifications par des données sont absentes. Pourtant, il est hasardeux d'analyser le fractionnement subcellulaire des métaux chez un organisme sans avoir au préalable adapté le protocole de fractionnement à l'espèce considérée. Sans cette étape préliminaire, le protocole peut conduire à une homogénéisation incomplète, à une dégradation des organites et à des chevauchements entre les fractions récupérées (Giguère et al., 2006; Lavoie et al., 2009; Rosabal et al., 2014). Ainsi, **le chapitre 1** visait à adapter, à l'aide d'essais enzymatiques, le protocole de fractionnement aux trois organismes utilisés dans les deux autres chapitres de cette thèse.

L'homogénéisation une étape primordiale à optimiser

La méthode d'homogénéisation s'est révélée dans le chapitre 1 être une étape clef pour l'optimisation du protocole de fractionnement. Par exemple, pour des organismes avec des structures externes plus rigides, comme l'exosquelette chitineux de *D. magna*, l'utilisation de méthode d'homogénéisation plus intense apparaît essentielle.

Pour chacun des organismes, une méthode d'homogénéisation différente a été validée. Néanmoins, réaliser une double étape d'homogénéisation, comme préconisé par d'autres auteurs (Lapointe et al., 2009; Ng et al., 2011 ; Leonard et al., 2014), la première avec un pilon motorisé potter-Elvehjem et la seconde avec une sonde à ultrason conduisait aux meilleurs résultats pour *D. magna* comme pour les foies de *O. mykiss*. Cette méthode d'homogénéisation double peut donc être recommandée comme méthode initiale pour commencer tout essai d'optimisation du protocole de fractionnement pour une espèce.

Fractions validées VS fractions prédites

D'une manière générale, les résultats présentés dans le chapitre 1 confirment qu'il est indispensable de valider le protocole de fractionnement *a priori* de l'interprétation des résultats de fractionnement subcellulaire de métaux. En effet, des écarts importants entre les fractions prédites et celles véritablement séparées après validation étaient systématiquement rapportés. Ainsi, pour nos organismes la matrice mitochondriale serait récupérée avec le cytosol et les lysosomes seraient plus probablement récupérés dans la fraction supposée mitochondriale que dans celles des lysosomes/microsomes. Pour les lysosomes, nos résultats ne sont pas inhabituels puisque d'autres auteurs considéraient déjà que les lysosomes se retrouvaient avec les mitochondries (Bustamante et al., 2006; Podgurskaya et Kavun, 2006). Nos vitesses de centrifugation pour la récupération des mitochondries supérieures à celles indiquées dans le protocole établi par Wallace et al. (2003) pourraient par ailleurs expliquer ce résultat.

Pour la matrice mitochondriale cependant, le chapitre 1 représente la première étude qui semble indiquer que la dégradation des mitochondries durant leur fractionnement est inévitable. Pourtant, plusieurs auteurs ont en travaillant avec les mêmes enzymes que les nôtres concluent que leurs protocoles permettaient de séparer les mitochondries tout en

maintenant leur intégrité : pour *Chaoborus sp* (Rosabal et al., 2014), pour *O. mykiss* (Kamunde et MacPhail, 2008), et *Chlamydomonas reinhardtii* (Lavoie et al., 2009). Pour les deux dernières espèces, une différence importante entre les protocoles de fractionnement que les auteurs utilisaient et les protocoles testés dans le chapitre 1 peut être soulignée : le tampon d'homogénéisation. En effet, les auteurs de ces études utilisent tous deux un tampon d'homogénéisation très salin. Dans le cas de *C. reinhardtii,* Lavoie et al (2009) observaient véritablement une dégradation des mitochondries avec l'utilisation d'un tampon avec une osmolarité plus faible. Il serait en conséquence intéressant de travailler sur l'impact de l'osmolarité du tampon lors du fractionnement subcellulaire. Si plusieurs tampons ont été testés lors de la mise au point des protocoles de fractionnement subcellulaire présentés dans le chapitre 1, aucun ne joue véritablement sur ce paramètre de l'osmolarité. Ainsi, l'utilisation d'un tampon présentant une osmolarité élevée serait susceptible d'améliorer la préservation des mitochondries lors de leur séparation avec les protocoles définis pour nos trois organismes. Il apparaitrait judicieux de vérifier cette hypothèse lors de futurs essais.

Validation par biomarqueurs enzymatiques : avantages et limites

La réalisation d'essais enzymatiques comme présentés dans le chapitre 1 permet de valider la bonne séparation des mitochondries (membrane et matrice), des lysosomes et du cytosol et de mesurer l'efficacité d'homogénéisation du protocole. C'est une méthode simple et relativement rapide. De surcroit, contrairement aux validations par microscopie, c'est une méthode quantitative qui permet véritablement de mesurer des efficacités d'homogénéisation et de séparation des fractions. Néanmoins, que ce soit pour les débris cellulaires, la fraction résistante à la soude, les HDP et les HSP, cette méthode ne nous permet pas de valider ces fractions. Il est en effet impossible de mesurer la part de noyau, de membranes cellulaires, de métallothionéines récoltée dans chacune des fractions séparées avec les essais enzymatiques. Pourtant, il est très probable que les protocoles de fractionnement mis au point dans le chapitre 1 conduisent à des chevauchements potentiellement significatifs entre ces fractions. Certains auteurs ont par exemple observé un transfert des métaux depuis les HDP vers les HSP durant la phase de traitement à la chaleur du cytosol (Geffard et al., 2010).

Les résultats du chapitre 2 montrent qu'une faible proportion de l'Y (<15%) s'accumule dans le cytosol de nos deux invertébrés. De plus, bien que la fraction HDP est le

principal lieu d'accumulation de ce métal dans le cas du foie de *O. mykiss*, les HSP représentent pour leur part moins de 10% de la quantité en Y accumulée par cet organe. De ce fait, si un transfert d'Y s'était produit depuis les HDP vers les HSP durant l'étape de traitement à la chaleur du cytosol de nos essais, il serait faible et n'affecterait que peu les conclusions tirées de nos résultats. Pour autant, cette question du transfert des ETR comme l'Y durant l'étape de séparation des protéines demeure non élucidée. Des essais visant à comparer les résultats en ETR liés aux métallothionéines soit avec une séparation par un traitement à la chaleur soit par chromatographie d'exclusion de taille apporterait une première réponse. Pour que cette analyse ait un intérêt, il serait nécessaire cependant, dans un premier temps, d'estimer cela chez un organisme qui a une forte propension à accumuler les ETR dans ses HSP.

Au-delà de ces essais, il apparaît important que de futures études de fractionnement subcellulaire des métaux puissent trouver de nouvelles méthodes pour valider les fractions qui ne peuvent l'être par des essais enzymatiques. La méthode d'analyse par nano-SIMS permet la cartographie à un niveau subcellulaire d'élément trace et de macro-éléments (Penen et al., 2016). Ainsi, la comparaison de résultats de fractionnement subcellulaire de métaux, après mesure des concentrations en métaux dans chaque fraction par ICP, avec la distribution subcellulaire de ces métaux observée par nano-SIMS serait un exemple pertinent d'analyse à ajouter pour valider le fractionnement subcellulaire.

Toxicité de l'Y

Le **chapitre 2** s'attarde à la toxicité de l'Y sur nos trois organismes d'eau douce *D. magna*, *C. riparius* et *O. mykiss*. Cette toxicité est mise en relation à la fois avec la bioaccumulation de ce métal chez ces organismes mais aussi avec sa distribution intracellulaire chez ces derniers.

Un risque accru des ETR pour les organismes benthiques

Ce chapitre se conclut par l'établissement de seuil de toxicité de l'Y sous la forme de concentration minimale avec effet observé CMEO pour chacun de nos organismes. Ces valeurs seuils pour les organismes pélagiques sont 100 à 1000 fois supérieures aux concentrations mesurées à ce jour dans l'eau des milieux dulcicoles. Toutefois, pour

l'organisme benthique, *C. riparius*, la CMEO estimée n'est que de trois fois supérieure aux concentrations rapportées en moyenne en Y dans des sédiments naturels. De surcroit, les concentrations en ETR totaux dans les sédiments peuvent dépasser de deux fois cette CMEO. Si les ETR présentaient des effets cumulatifs, il y aurait donc potentiellement un risque de toxicité pour les organismes benthiques naturels. Une première étude concluait sur une absence d'effet synergique ou antagoniste entre les ETR (Qiang et al., 1994). Toutefois, il serait nécessaire de confirmer ce point au cours d'études supplémentaires.

Par ailleurs, les études de toxicité sur les organismes benthiques demeurent rares. Il serait en conséquence nécessaire de vérifier nos conclusions sur *C. riparius* avec d'autres ETR. La toxicité du La, du Ce et du Nd, trois des ETR les plus abondants, sur *C. riparius* devraient par exemple être testée. Le Gd ayant été mis le plus souvent en cause dans les cas de contamination en ETR d'origine anthropique (Hatje et al., 2016; Kulaksiz et Bau, 2011) devrait aussi être testé. De plus, il serait important d'inclure des milieux de différentes duretés lors de ces essais. En effet celle-ci a un impact significatif sur la toxicité des ETR comme révélé dans le chapitre 2 et dans de précédentes études (Barry et Meehan, 2000; Vukov et al., 2016). Enfin, il serait important de réaliser des bioessais d'exposition aux ETR par le sédiment sur des organismes de niveau trophique supérieur à *C. riparius*. Des études suggèrent que les espèces piscicoles benthiques accumulent plus d'ETR que leurs homologues pélagiques (Mayfield et Fairbrother, 2015). Par conséquence, il est probable que les ETR induisent un risque plus important pour des poissons benthiques que celui évalué dans le chapitre 2 pour *O. mykiss*. La tête-de-boule, *Pimephales promelas*, étant couramment utilisée en écotoxicologie pour des expositions par le sédiment serait un organisme d'essais pertinent (Environnement Canada, 2011).

Importance des mitochondries et des granules dans la gestion de l'Y

Le chapitre 2 rapporte aussi des tendances similaires pour le fractionnement subcellulaire de l'Y chez nos trois organismes.

Les membranes mitochondriales étaient la principale MSF où venait s'accumuler l'Y pour l'ensemble des organismes. Il est donc vraisemblable que la toxicité associée à cet élément, et potentiellement aux autres ETR, soit liée à des perturbations des fonctions mitochondriales. Des impacts délétères des ETR dont l'Y sur les mitochondries (ex. : stress

oxydatif, disfonctionnement de la régulation du calcium) ont déjà été observés dans les foies de souris et de rat (Huang et al., 2011; Korotkov et al., 2016). L'hypothèse de ce même type d'impact sur nos organismes d'essais peut donc être émise. De futurs essais évaluant les taux de respiration de leurs mitochondries à la suite de leur exposition à l'Y pourraient le confirmer. Il est probable que ce type d'effet se produise en amont des effets observés sur la croissance et la survie de nos organismes. Des seuils de concentrations avec effets plus faibles que ceux estimés dans le chapitre 2 pourraient ainsi être estimés.

La fraction résistante à la soude, comprenant les granules riches en métaux, apparait comme une composante subcellulaire privilégiée d'accumulation de l'Y chez les organismes de bas niveaux trophiques. Le chapitre 2 rapporte par exemple que c'est la principale fraction de métaux détoxiquée (MDF) pour l'Y chez *D. magna* et *C. riparius*. L'accumulation de plus de 80% de l'Y dans cette fraction chez *D. magna* expliquerait d'ailleurs que cette espèce puisse accumuler jusqu'à 100 fois plus d'Y que les deux autres. Quatre types de granules ont jusqu'ici été rapportés dans la littérature (Hopkin, 1989 ; Khan et al., 2010). À la vue de son analogie avec le Ca, il est fort probable que l'Y comme l'ensemble des ETR se fixe aux granules formés de carbonate de calcium. Une méthode possible pour valider cette hypothèse serait d'analyser la fraction résistante à la soude par microanalyse aux rayons X (Gibbs et al., 1998). De même, la spectroscopie d'absorption par rayon X, en permettant l'analyse de la spéciation des métaux à un niveau subcellulaire, pourrait valider la présence de l'Y dans les granules (Penen et al., 2017).

D'une manière générale, il serait intéressant de réaliser des analyses de fractionnement subcellulaire pour d'autres invertébrés et d'autres ETR. Une tendance identique à celle observée pour nos organismes pourrait être révélée. Cela confirmerait nos propres résultats, les validerait sur l'ensemble des ETR, et indiquerait des mécanismes de toxicité potentiellement identiques pour ces métaux. Il a par exemple déjà été estimé chez une algue, *C. reinhardti*, que la fraction résistante à la soude était, comme pour nos invertébrés, l'un des principaux sites d'accumulation des ETR (Racine, 2016).

L'interaction calcium-ETR

Enfin, de fortes présomptions que la fraction résistante à la soude contienne aussi l'exosquelette dans le cas des crustacés comme *D. magna* sont émises à la vue des résultats du chapitre 2.

En effet, comme lors de la séparation de la fraction résistante à la soude et des débris, plusieurs auteurs travaillant sur la distribution des métaux entre tissus mous et l'exosquelette des daphnies utilisent un traitement à la soude pour séparer ces deux composantes (Liu et al., 2002; Yu et Wang, 2002). Par ailleurs, Auffan et al. (2013) observaient que la mue était la principale voie d'élimination du Ce accumulé par *Daphnia pulex*. Enfin, l'exosquelette des daphnies diffère de celui des autres invertébrés comme les insectes par l'ajout de carbonate de calcium à sa chitine (Pillai et al., 2009; Cohen et Moussian, 2016). Or, la capacité des ETR à s'accumuler au niveau des sites de transport et d'accumulation du Ca a fait l'objet de nombreuses études. L'Y peut par exemple entrer en compétition avec le Ca pour la complexation sur certaines protéines de fixation du Ca, ou encore entrainer une inhibition des canaux ionique à calcium (Jakubek et al., 2009). D'autre part plusieurs auteurs ont déjà émis l'hypothèse de ce remplacement du Ca par les ETR que ce soit dans les carapaces des crabes à barbe, *Ucides cordatus* (Bosco-Santos et al., 2017), ou encore dans l'albumine des femelles de goéland à bec cerclé, *Larus delawerencis* (Brown et al., 2018). La réalisation d'essais visant à confirmer l'accumulation préférentielle des ETR dans l'exosquelette de *D. magna* apparaît de ce fait nécessaire.

D'une manière plus générale, l'analogie des ETR avec le Ca semble être une caractéristique fondamentale à la compréhension de leur mécanisme d'accumulation et de toxicité. Il est important de prendre en compte ce paramètre dans toutes futures études écotoxicologiques sur ces métaux.

Transfert trophique de l'Y

À l'intérieur du **chapitre 3**, le potentiel de transfert trophique de l'Y a été étudié par des essais de nourrissage de *O. mykiss* avec des individus de *D. magna* enrichis en Y. Ce potentiel a été mis en relation avec le fractionnement subcellulaire de l'Y chez ces proies et

avec le potentiel de transfert de l'Y depuis l'eau vers *O. mykiss.* Enfin, la dynamique de dépuration de l'Y par *O. mykiss* a été évaluée.

Yttrium trophiquement disponible

Dans le chapitre 3, on estime que l'efficacité d'assimilation (EA) de l'Y depuis *D. magna* vers *O. mykiss* est proche du pourcentage en Y dans le cytosol de *D. magna*; tous les deux sont inférieurs à 5%. Ces résultats confirmeraient que le concept de TAM serait pertinent dans le cas de l'Y et que seul l'Y du cytosol serait trophiquement disponible. Certes, ce concept de métaux trophiquement disponibles se vérifiait aussi dans le cas de prédateurs invertébrés (Seebaugh et al., 2006; Dubois et Hare, 2009). Cependant, hormis pour les métaux essentiels et le mercure, ce n'est pas habituellement le cas pour les poissons. Le transfert trophique des métaux vers les poissons apparait en général faible, avec des EA inférieures à 10% et cela malgré une propension en TAM très supérieure à 10% (Steen Redeker et al., 2007; Zhang et al., 2011). Ainsi nos résultats ne nous permettent pas de véritablement statuer sur la relation entre TAM et EA dans le cas de l'Y. La réalisation de nouveaux essais de nourrissage d'*O. mykiss* avec d'autres proies enrichies en Y pourrait confirmer cette relation. Il serait néanmoins nécessaire que les proies choisies présentent une propension en Y au moins supérieur à 10%. *C. riparius,* à la vue de son fractionnement subcellulaire en Y estimé dans le chapitre 2, serait une proie intéressante à exploiter.

Il est bien admis que le transfert trophique des métaux est effectivement dépendant du métal et de la proie considérée (Lapointe et al., 2009). Toutefois, il est aussi lié au pouvoir digestif du prédateur (Rainbow et al., 2011). Par conséquent, des expériences de nourrissage avec des daphnies enrichies en Y impliquant un autre prédateur d'eau douce que *O. mykiss*, comme *Danio rerio* ou *P. promelas,* pourraient aussi être réalisées dans le futur.

Un faible potentiel de transfert trophique

Au travers des EA et BMF mesurés, le chapitre 3 semble confirmer le faible potentiel de biomagnification de l'Y et des ETR. En effet, les quelques études réalisées à ce jour sur l'analyse des ETR le long de chaînes trophiques naturelles indiquaient une biodilution de ces éléments (Amyot et al., 2017; MacMillan et al., 2017). De plus, le chapitre 2 révélait que la majorité de l'Y accumulé par les consommateurs primaires (*D. magna* et *C. riparius*) se fixait

dans des composantes subcellulaires considérées comme trophiquement indisponibles (c.-à-d. dans les débris cellulaires et dans la fraction résistante à la soude). Par ailleurs, le chapitre 3 conclue que le muscle n'accumule que très peu d'ETR au regard des autres organes (foie, branchies et intestins). Ce constat déjà réalisé dans d'autres études analysant les ETR dans les tissus de poissons (Qiang et al., 1994; Hao et al., 1996) mais aussi de mammifères (MacMillan et al., 2017) indiquent également un faible risque de transfert de ces métaux pour l'homme par la consommation de poissons.

En conclusion, tous les résultats collectés à ce jour indiquent une très faible probabilité de biomagnification des ETR. Il pourrait néanmoins être intéressant de le confirmer, en réalisant de nouvelles études de l'accumulation des ETR le long de chaîne trophique d'écosystèmes différents de ceux déjà analysés pour les ETR dans la littérature.

Le foie : un organe essentiel pour la compréhension de la toxicité des ETR

L'accumulation de l'Y au sein des organes d'*O. mykiss* se distribuait dans l'ordre suivant muscle > foie > branchies > intestin. Néanmoins une élimination de plus de 75% de l'Y dans les branchies, les intestins et les muscles dès 120 heures de dépuration a été mesurée. À l'inverse, aucune dépuration de l'Y dans le foie n'a été observée durant cette période (une augmentation des concentrations en Y était même observée). Cet ordre d'accumulation est cohérent avec ce qui a déjà été observé dans d'autres organismes pour de nombreux métaux (Subotic et al., 2014). De la même manière, la dynamique de dépuration de l'Y dans le foie de *O. mykiss* estimée dans le chapitre 3 rejoint celle modélisée pour l'ensemble des métaux dans le foie des poissons par Jezierska et Witeska (2001).

L'absence d'élimination de l'Y dans le foie observé dans ce chapitre souligne l'importance de cet organe dans la prise en charge de l'Y par les organismes. En outre, les données du chapitre 2 indique qu'une majorité de l'Y s'accumulait dans les MSF du foie de *O. mykiss.* Cela suggère une toxicité importante pour cet organe et appuie encore la position clef de cet organe dans la compréhension des mécanismes de toxicité de l'Y et des ETR. Des études comparant le fractionnement subcellulaire de métaux entre différents organes d'un même organisme ont révélé des distributions significativement différentes (Cooper et al., 2013; Leonard et al., 2014). En conséquence, il serait intéressant, dans une nouvelle étude, de

comparer le fractionnement subcellulaire de l'Y dans le foie avec d'autres organes de *O. mykiss*.

Conclusion générale

Ce projet de thèse contribue à améliorer nos connaissances du risque induit par l'Y et les ETR sur les écosystèmes dulcicoles. Il met en évidence un danger accru pour les organismes benthiques et présente de nouvelles preuves du faible potentiel de biomagnification de ces métaux. Par ailleurs, ce projet souligne l'importance du foie, des granules et des membranes mitochondriales pour comprendre les mécanismes de toxicité et de détoxication de l'Y. Enfin, il démontre l'intérêt du fractionnement subcellulaire en écotoxicologie et donne des pistes pour perfectionner les données liées à cette analyse dans le futur.

Bibliographie

AEMQ, 2016. Consultations particulieres sur le projet de loi concernant la mise en oeuvre de la politique energetique 2030 et modifiant diverses dispositions legislatives.

Agathokleous, E., Kitao, M., Calabrese, E.J., 2018. The rare earth element (REE) lanthanum (La) induces hormesis in plants. Environ. Pollut. 238, 1044–1047. https://doi.org/10.1016/j.envpol.2018.02.068

Aide, M.T., Aide, C., 2012. Rare Earth Elements: their importance in understanding soil genesis. ISRN Soil Sci. 2012, 1–11. https://doi.org/10.5402/2012/783876

Alonso, E., Sherman, A.M., Wallington, T.J., Everson, M.P., Field, F.R., Roth, R., Kirchain, R.E., 2012. Evaluating rare earth element availability: a case with revolutionary demand from clean technologies. Environ. Sci. Technol. 46, 3406–14. https://doi.org/10.1021/es203518d

Amiard, J.C., Amiard-Triquet, C., Barka, S., Pellerin, J., Rainbow, P.S., 2006. Metallothioneins in aquatic invertebrates: Their role in metal detoxification and their use as biomarkers. Aquat. Toxicol. 76, 160–202. https://doi.org/10.1016/j.aquatox.2005.08.015

Amyot, M., Clayden, M.G., Macmillan, G.A., Perron, T., Arscott-Gauvin, A., 2017. Fate and trophic transfer of rare earth elements in temperate lake food webs. Environ. Sci. Technol. 51, 6009–6017. https://doi.org/10.1021/acs.est.7b00739

Arnot, J. a, Gobas, F.A., 2006. A review of bioconcentration factor (BCF) and bioaccumulation factor (BAF) assessments for organic chemicals in aquatic organisms. Environ. Rev. 14, 257–297. https://doi.org/10.1139/a06-005

Atibu, E.K., Devarajan, N., Laffite, A., Giuliani, G., Salumu, J.A., Muteb, R.C., Mulaji, C.K., Otamonga, J.P., Elongo, V., Mpiana, P.T., Poté, J., 2016. Assessment of trace metal and rare earth elements contamination in rivers around abandoned and active mine areas. The case of Lubumbashi River and Tshamilemba Canal, Katanga, Democratic

Republic of the Congo. Chemie der Erde - Geochemistry 76, 353–362. https://doi.org/10.1016/j.chemer.2016.08.004

Auffan, M., Bertin, D., Chaurand, P., Pailles, C., Dominici, C., Rose, J.Ô., Bottero, J.Y., Thiery, A., 2013. Role of molting on the biodistribution of CeO_2nanoparticles within *Daphnia pulex*. Water Res. 47, 3921–3930. https://doi.org/10.1016/j.watres.2012.11.063

Axelsson, M., Gentili, F., 2014. A single-step method for rapid extraction of total lipids from green microalgae. PLoS One 9, e89643. https://doi.org/10.1371/journal.pone.0089643

Ayedun, H., Arowolo, T.A., Gbadebo, A.M., Idowu, O.A., 2017. Evaluation of rare earth elements in groundwater of Lagos and Ogun States, Southwest Nigeria. Environ. Geochem. Health 39, 649–664. https://doi.org/10.1007/s10653-016-9839-8

Babula, P., Adam, V., Opatrilova, R., Zehnalek, J., Havel, L., Kizek, R., 2009. Uncommon heavy metals, metalloids and their plant toxicity: a review. In Organic Farming, Pest Control and Remediation of Soil Pollutants, pp. 275-317. Springer, Dordrecht.

Barry, M.J., Meehan, B.J., 2000. The acute and chronic toxicity of lanthanum to *Daphnia carinata*. Chemosphere 41, 1669–74.

Barst, B.D., Rosabal, M., Campbell, P.G.C., Muir, D.G.C., Wang, X., Köck, G., Drevnick, P.E., 2016. Subcellular distribution of trace elements and liver histology of landlocked Arctic char (*Salvelinus alpinus*) sampled along a mercury contamination gradient. Environ. Pollut. 212, 574–583. https://doi.org/10.1016/j.envpol.2016.03.003

Béchard, K.M., Gillis, P.L., Wood, C.M., 2008. Trophic transfer of Cd from larval chironomids (*Chironomus riparius*) exposed via sediment or waterborne routes, to zebrafish (*Danio rerio*): Tissue-specific and subcellular comparisons. Aquat. Toxicol. 90, 310–321. https://doi.org/10.1016/j.aquatox.2008.07.014

Bednarska, A.J., Świątek, Z., 2016. Subcellular partitioning of cadmium and zinc in mealworm beetle *Tenebrio molitor* larvae exposed to metal-contaminated flour. Ecotoxicol. Environ. Saf 133, 82–89.

Beedle, A.M., Hamid, J., Zamponi, G.W., 2002. Inhibition of transiently expressed low- and high-voltage-activated calcium channels by trivalent metal cations. J. Membr. Biol. 187, 225–238. https://doi.org/10.1007/s00232-001-0166-2

Berthet, J., De Duve, C., 1951. Tissue fractionation studies. 1. The existence of a mitochondria-linked, enzymically inactive form of acid phosphatase in rat-liver tissue. Biochem. J 50, 174.

Binnemans, K., Jones, P.T., Blanpain, B., Van Gerven, T., Yang, Y., Walton, A., Buchert, M., 2013. Recycling of rare earths: a critical review. J. Clean. Prod. 51, 1–22.

Blaise, C., Gagne, F., 2008. Ecotoxicity of selected nano-materials to aquatic organisms. Environ. Toxicol. 591–598. https://doi.org/10.1002/tox

Borgmann, U., Couillard, Y., Doyle, P., Dixon, D.G., 2005. Toxicity of sixty-three metals and metalloids to *Hyalella azteca* at two levels of water hardness. Environ. Toxicol. Chem. 24, 641–652. https://doi.org/10.1897/04-177r.1

Bosco-Santos, A., Luiz-Silva, W., Silva-Filho, E.V. da, Souza, M.D.C. de, Dantas, E.L., Navarro, M.S., 2017. Fractionation of rare earth and other trace elements in crabs, *Ucides cordatus*, from a subtropical mangrove affected by fertilizer industry. J. Environ. Sci. 54, 69–76. https://doi.org/10.1016/j.jes.2016.05.024

Bowles, K.C., Apte, S.C., Maher, W.A., Kawei, M., Smith, R., 2001. Bioaccumulation and biomagnification of mercury in Lake Murray, Papua New Guinea. Can. J. Fish. Aquat. Sci. 58, 888–897. https://doi.org/10.1139/f01-042

Bragigand, V., Berthet, B., 2003. Some methodological aspects of metallothionein evaluation. Comp. Biochem. Physiol., Part A Mol. Integr. Physiol 1341, 55–61.

Bray, D.F., Bagu, J., Koegler, P., 1993. Comparison of hexamethyldisilazane (HMDS), Peldri II, and critical-point drying methods for scanning electron microscopy of biological specimens. Microsc. Res. Tech 26, 489–495.

Brown, L., Rosabal, M., Sorais, M., Poirier, A., Widory, D., Verreault, J., 2018. Habitat use strategy influences the tissue signature of trace elements including rare earth elements

in an urban-adapted omnivorous bird. Environ. Res. 168, 261–269. https://doi.org/10.1016/j.envres.2018.10.004

Buchwalter, D.B., Cain, D.J., Martin, C.A., Xie, L., Luoma, S.N., Garland, T., 2008. Aquatic insect ecophysiological traits reveal phylogenetically based differences in dissolved cadmium susceptibility. Proc. Natl. Acad. Sci. U. S. A. 105, 8321–6. https://doi.org/10.1073/pnas.0801686105

Bustamante, P., Bertrand, M., Boucaud-Camou, E., Miramand, P., 2006. Subcellular distribution of Ag, Cd, Co, Cu, Fe, Mn, Pb, and Zn in the digestive gland of the common cuttlefish *Sepia officinales*. J. Shellfish Res. 25, 987–994.

Bustamante, P., Cosson, R.P., Gallien, I., Caurant, F., Miramand, P., 2002. Cadmium detoxification processes in the digestive gland of cephalopods in relation to accumulated cadmium concentrations. Mar. Environ. Res. 53, 227–241. https://doi.org/10.1016/S0141-1136(01)00108-8

Cain, D.J., Luoma, S.N., Wallace, W.G., 2004. Linking metal bioaccumulation of aquatic insects to their distribution patterns in a mining- impacted river. Environ. Toxicol. Chem. 23, 1463–1473. https://doi.org/10.1897/03-291

Calabrese, E.J., 2005. Toxicological awakenings: the rebirth of hormesis as a central pillar of toxicology. Toxicol. Appl. Pharmacol. 204, 1–8. https://doi.org/10.1016/j.taap.2004.11.015

Campana, O., Taylor, A.M., Blasco, J., Maher, W. a., Simpson, S.L., 2015. Importance of Subcellular metal partitioning and kinetics to predicting sublethal effects of copper in two deposit-feeding organisms. Environ. Sci. Technol. 49, 1806–1814. https://doi.org/10.1021/es505005y

Campbell, L.M., Fisk, A.T., Wang, X.W., Kock, G., Muir, D.C.G., 2005. Evidence for biomagnification of rubidium in freshwater and marine food webs. Can. J. Fish. Aquat. Sci. 62, 1161–1167.

Campbell, P.G.C., Giguere, A., Bonneris, E., Hare, L., 2005. Cadmium-handling strategies in two chronically exposed indigenous freshwater organisms - the yellow perch (*Perca flavescens*) and the floater mollusc (*Pyganodon grandis*). Aquat. Toxicol. 72, 83–97.

Cardon, P.-Y., Caron, A., Rosabal, M., Fortin, C., Amyot, M., 2018. Enzymatic validation of species-specific protocols for metal subcellular fractionation in freshwater animals. Limnol. Oceanogr. Methods. https://doi.org/10.1002/lom3.10265

Cardon, P.-Y., Triffault-Bouchet, G., Caron, A., Rosabal, M., Fortin, C., Amyot,. Toxicity and subcellular fractionation of yttrium in three freshwater organisms: *Daphnia magna* , *Chironomus riparius* and *Oncorhynchus mykiss*. Env. Sci Technol. To be submitted for publication

Casado-Martinez, M.C., Duncan, E., Smith, B.D., Maher, W. a., Rainbow, P.S., 2012a. Arsenic toxicity in a sediment-dwelling polychaete: Detoxification and arsenic metabolism. Ecotoxicology 21, 576–590. https://doi.org/10.1007/s10646-011-0818-7

Casado-Martinez, M.C., Duncan, E., Smith, B.D., Maher, W.A., Rainbow, P.S., 2012b. Arsenic toxicity in a sediment-dwelling polychaete: Detoxification and arsenic metabolism. Ecotoxicology 21, 576–590. https://doi.org/10.1007/s10646-011-0818-7

CEAEQ, 2011. Détermination de la toxicité létale CL_{50} (48 h) *Daphnia magna*. MA 500 - D.mag. 1.1, Rév. 1. ed. Ministère du Développement durable, de l'Environnment et des Parcs du Québec, Québec.

Cheung, M., Wang, W.-X., 2005. Influence of subcellular metal compartmentalization in different prey on the transfer of metals to a predatory gastropod. Mar. Ecol. Prog. Ser. 286, 155–166. https://doi.org/10.3354/meps286155

Cohen, E., Moussian, B., 2016. Extracellular composite matrices in arthropods, Extracellular composite matrices in arthropods. https://doi.org/10.1007/978-3-319-40740-1

Cooper, S., Bonneris, E., Michaud, A., Pinel-Alloul, B., Campbell, P.G.C., 2013. Influence of a step-change in metal exposure (Cd, Cu, Zn) on metal accumulation and subcellular partitioning in a freshwater bivalve, *Pyganodon grandis*: A long-term transplantation

experiment between lakes with contrasting ambient metal levels. Aquat. Toxicol. 132–133, 73–83. https://doi.org/10.1016/j.aquatox.2013.01.021

Couillard, Y., Campbell, P.G.C., Pellerin-Massicotte, J., Auclair, J.C., 1995. Field transplantation of a freshwater bivalve, *Pyganodon grandis*, across a metal contamination gradient. 1. Temporal changes in metallothionein and metal (Cd, Cu, and Zn) concentrations in soft tissues. Can. J. Fish. Aquat. Sci. 52, 703–715. https://doi.org/10.1139/f95-070

Croteau, A.M., Luoma, S.N., Stewart, A.R., Croteau, M., Survey, U.S.G., Road, M., Park, M., 2005. Trophic transfer of metals along freshwater food webs: Evidence of cadmium biomagnification in nature. Limnology 50, 1511–1519.

Cui, J., Zhang, Z., Bai, W., Zhang, L., He, X., Ma, Y., Liu, Y., Chai, Z., 2012. Effects of rare earth elements La and Yb on the morphological and functional development of zebrafish embryos. J. Environ. Sci. 24, 209–213. https://doi.org/10.1016/S1001-0742(11)60755-9

Dang, F., Rainbow, P.S., Wang, W.-X., 2012. Dietary toxicity of field-contaminated invertebrates to marine fish: Effects of metal doses and subcellular metal distribution. Aquat. Toxicol. 120–121, 1–10. https://doi.org/10.1016/j.aquatox.2012.04.007

de Bisthoven, L.J., Postma, J.F., Parren, P., Timmermans, K.R., Ollevier, F., 1998. Relations between heavy metals in aquatic sediments and in *Chironomus* larvae of Belgian lowland rivers and their morphological deformities. Can. J. Fish. Aquat. Sci. 55, 688–703. https://doi.org/10.1139/cjfas-55-3-688

De Duve, C., 1975. Exploring cell with a centrifuge. Science. 189, 186–194.

Dent, P.C., 2012. Rare earth elements and permanent magnets. J. Appl. Phys. 111, 1–7. https://doi.org/10.1063/1.3676616

Dubois, M., Hare, L., 2009a. Selenium assimilation and loss by an insect predator and its relationship to Se subcellular partitioning in two prey types. Environ. Pollut. 157, 772–7. https://doi.org/10.1016/j.envpol.2008.11.022

Dubois, M., Hare, L., 2009b. Subcellular distribution of cadmium in two aquatic invertebrates: Change over time and relationship to Cd assimilation and loss by a predatory insect. Environ. Sci. Technol. 43, 356–361. https://doi.org/10.1021/es801406r

Dumas, J., Hare, L., 2008. The internal distribution of nickel and thallium in two freshwater invertebrates and its relevance to trophic transfer. Environ. Sci. Technol. 42, 5144–5149. https://doi.org/10.1021/es800378j

Eaton, J.W., Quian, M., 2002. Molecular bases of cellular iron toxicity. Free Radic. Bio Med 32, 833–840.

EC, MDDEP, 2007. Critères pour l'évaluation de la qualité des sédiments au Québec et cadres d'application : prévention, dragage et restauration. Environnement Canada et ministère du Développement durable, de l'Environnement et des Parcs du Québec.

El-Akl, P., Smith, S., Wilkinson, K.J., 2015. Linking the chemical speciation of Ce to its bioavailability in water for a freshwater alga. Environ. Toxicol. Chem. 34, 1711-1719. https://doi.org/10.1002/etc.2991

Eliseeva, S. V., Bünzli, J.C.G., 2011. Rare earths: jewels for functional materials of the future. New J. Chem. 35, 1165–1176. https://doi.org/10.1039/c0nj00969e

Environnement Canada, 1997. Biological test method: test for survival and growth in sediment using larvae of freshwater midges (*Chironomus tentans* or *Chironomus riparius*).

Environnement Canada, 2011. Méthode d'essai biologique : essai de croissance et de survie sur des larves de tête-de-boule.

EPA, 1985. Methods for measuring the acute toxicity of effluents to freshwater and marine organisms, EPA/600/4-. ed. Cincinnati.

European Commission, 2003. Technical guidance document on risk assessment, Part II, in support of Commission Directive 93/67/EEC on Risk Assessment for new notified substances, Commission Regulation (EC) No 1488/94 on Risk Assessment for existing substances, Directive 98/8/EC of th. Ispra, Italy.

Evseeva, T., Geras'kin, S., Majstrenko, T., Brown, J., Belykh, E., 2010. Comparative estimation of ^{232}Th and stable Ce (III) toxicity and detoxification pathways in

freshwater alga *Chlorella vulgaris*. Chemosphere 81, 1320–1327. https://doi.org/10.1016/j.chemosphere.2010.08.028

Eyckmans, M., Blust, R., De Boeck, G., 2012. Subcellular differences in handling Cu excess in three freshwater fish species contributes greatly to their differences in sensitivity to Cu. Aquat. Toxicol. 118–119, 97–107. https://doi.org/10.1016/j.aquatox.2012.03.019

Ferrat, M., Weiss, D.J., Strekopytov, S., Dong, S., Chen, H., Najorka, J., Sun, Y., Gupta, S., 2011. Improved provenance tracing of Asian dust sources using rare earth elements and selected trace elements for palaeomonsoon studies on the eastern Tibetan Plateau. Geochim. Cosmochim. Acta 75, 6374–6399. https://doi.org/10.1016/j.gca.2011.08.025

Flik, G., Klaren, P.H.M., Schoenmakers, T.J.M., Bijvelds, M.J.C., 1996. Cellular calcium transport in fish: unique and universal mechanisms. Physiol. Zool. 69, 403–417.

Frelon, S., Mounicou, S., Lobinski, R., Gilbin, R., Simon, O., 2013. Subcellular fractionation and chemical speciation of uranium to elucidate its fate in gills and hepatopancreas of crayfish *Procambarus clarkii*. Chemosphere 91, 481–490. https://doi.org/10.1016/j.chemosphere.2012.12.008

Fuller, B.J., Rubinacci, A., Geboes, K., De Loecker, W., 1989. The bioenergetics of mitochondria after cryopreservation. Cryobiology 264, 333–340.

Fusconi, A., Repetto, O., Bona, E., Massa, N., Gallo, C., Dumas-Gaudot, E., Berta, G., 2006. Effects of cadmium on meristem activity and nucleus ploidy in roots of *Pisum sativum L*. Frisson seedlings. Environ. Exp. Bot. 58, 253–260. https://doi.org/10.1016/j.envexpbot.2005.09.008

Gao, Y., Zeng, F., Yi, A., Ping, S., Jing, L., 2003. Research of the entry of rare earth elements Eu^{3+} and La^{3+} into plant cell. Biol. Trace Elem. Res. 91, 253–265. https://doi.org/10.1385/BTER:91:3:253

Geffard, A., Sartelet, H., Garric, J., Biagianti-Risbourg, S., Delahaut, L., Geffard, O., 2010. Subcellular compartmentalization of cadmium, nickel, and lead in Gammarus fossarum: Comparison of methods. Chemosphere 78, 822–829. https://doi.org/10.1016/j.chemosphere.2009.11.051

Gibbs, P.E., Nott, J.A., Nicolaidou, A., Bebianno, M.J., 1998. The composition of phosphate granules in the digestive glands of marine prosobranch gastropods: Variation in relation to taxonomy. J. Molluscan Stud. 64, 423–433. https://doi.org/10.1093/mollus/64.4.423

Giguère, A., Campbell, P.G.C., Hare, L., Couture, P., 2006. Sub-cellular partitioning of cadmium, copper, nickel and zinc in indigenous yellow perch (*Perca flavescens*) sampled along a polymetallic gradient. Aquat. Toxicol. 77, 178–189. https://doi.org/10.1016/j.aquatox.2005.12.001

Giguère, A., Couillard, Y., Campbell, P.G.C., Perceval, O., Hare, L., Pinel-Alloul, B., Pellerin, J., 2003. Steady-state distribution of metals among metallothionein and other cytosolic ligands and links to cytotoxicity in bivalves living along a polymetallic gradient. Aquat. Toxicol. 64, 185–200. https://doi.org/10.1016/S0166-445X(03)00052-3

Gimbert, F., Geffard, A., Guédron, S., Dominik, J., Ferrari, B.J.D., 2016. Mercury tissue residue approach in *Chironomus riparius*: Involvement of toxicokinetics and comparison of subcellular fractionation methods. Aquat. Toxicol. 171, 1–8. https://doi.org/10.1016/j.aquatox.2015.11.027

Gnaiger, E., Kuznetsov, V., Schneeberger, S., Seiler, R., Brandacher, G., Steurer, W., Margreiter, R., 2000. Mitochondria in the cold, in: Berlin Heidelberg (Ed.), Life in the Cold. pp. 431–442.

González, V., Vignati, D. a. L., Pons, M.-N., Montarges-Pelletier, E., Bojic, C., Giamberini, L., 2015. Lanthanide ecotoxicity: First attempt to measure environmental risk for aquatic organisms. Environ. Pollut. 199, 139–147. https://doi.org/10.1016/j.envpol.2015.01.020

Goto, D., Wallace, W.G., 2009. Influences of prey- and predator-dependent processes on cadmium and methylmercury trophic transfer to mummichogs (*Fundulus heteroclitus*). Can. J. Fish. Aquat. Sci. 66, 836–846. https://doi.org/10.1139/F09-038

Graham, J.M., Rickwood, D., 1997. Homogenization of tissues and cells, in: Subcellular fractionation-a pratical approach. The Pratical Approach Series. Oxford Univ. Press, pp. 1–29.

Greenaway, B.Y.P., 1985. Calcium Balance and Moulting in the Crustacea. Biol. Rev. 60, 425–454. https://doi.org/10.1111/j.1469-185X.1985.tb00424.x

Greenwood, N.N., Earnshaw, A., 1997. Chemistry of the Elements 2nd Edition.

Gupta, C.K., Krishnamurthy, N., 2005. Extractive metallurgy of rare earths: Boca Raton, CRC Press. ed. Florida.

Gwenzi, W., Mangori, L., Danha, C., Chaukura, N., Dunjana, N., Sanganyado, E., 2018. Sources, behaviour, and environmental and human health risks of high-technology rare earth elements as emerging contaminants. Sci. Total Environ. 636, 299–313. https://doi.org/10.1016/j.scitotenv.2018.04.235

Hall, B.D., Bodaly, R.A., Fudge, R.J.P., Rudd, J.W.M., Rosenberg, D.M., 1997. Food as the dominant pathway of methylmercury uptake by fish. Water. Air. Soil Pollut. 100, 13–24. https://doi.org/10.1023/A:1018071406537

Handy, R.D., 1992. The assessment of episodic metal pollution. 2. The effects of cadmium and copper enriched diets on tissue contaminant analysis in rainbow trout (*Oncorhynchus mykiss*). Arch. Environ. Contam. Toxicol. 22, 82–87.

Hao, S., Xiaorong, W., Lemei, D., Zhong, L., Yijun, C., 1996. Bioconcentration and elimination of five LREEs in Carp. Chemosphere 33, 1475–1483.

Hatje, V., Bruland, K.W., Flegal, A.R., 2016. Increases in Anthropogenic Gadolinium Anomalies and Rare Earth Element Concentrations in San Francisco Bay over a 20 Year Record. Environ. Sci. Technol. 50, 4159–4168. https://doi.org/10.1021/acs.est.5b04322

He, M.L., Ranz, D., Rambeck, W. a, 2001. Study on the performance enhancing effect of rare earth elements in growing and fattening pigs. J. Anim. Physiol. Anim. Nutr. 85, 263–270.

He, M.L., Wehr, U., Rambeck, W. a., 2010. Effect of low doses of dietary rare earth elements on growth performance of broilers. J. Anim. Physiol. Anim. Nutr. 94, 86–92. https://doi.org/10.1111/j.1439-0396.2008.00884.x

Hedrick, J.B., 1995. The global rare-earth cycle. J. Alloys Compd. 225, 609–618. https://doi.org/10.1016/0925-8388(94)07134-9

Herrmann, H., Nolde, J., Berger, S., Heise, S., 2016. Aquatic ecotoxicity of lanthanum – A review and an attempt to derive water and sediment quality criteria. Ecotoxicol. Environ. Saf. 124, 213–238. https://doi.org/10.1016/j.ecoenv.2015.09.033

Hoecke, K. Van, Quik, J.T.K., Mankiewicz-boczek, J., Schamphelaere, K. a C. De, Elsaesser, A., Meeren, P. Van Der, Barnes, C., Mckerr, G., Howard, C.V., Meent, D. Van De, Rydzyn, K., Dawson, K. a, Salvati, A., Lesniak, A., Lynch, I., Silversmit, G., Samber, B. De, Vincze, L., Janssen, C.R., 2009. Fate and Effects of CeO_2 Nanoparticles in Aquatic Ecotoxicity Tests. Environ. Sci. Technol. 43, 4537–4546.

Hogstrand, C., Verbost, P.M., Bonga, S.E., Wood, C.M., 1996. Mechanisms of zinc uptake in gills of freshwater rainbow trout: interplay with calcium transport. Am. J. Physiol. 270, R1141-7.

Hopkin, S.P., 1990. Critical concentrations, pathways of detoxification and cellular ecotoxicology of metals in terrestrial arthropods. Funct. Ecol. 4, 321–327.

Hossain, A.H., Li, A., Brickwedde, A., Wilms, L., Caspers, M., Overkamp, K., Punt, P.J., 2016. Rewiring a secondary metabolite pathway towards itaconic acid production in *Aspergillus niger*. Microb. Cell Fact 151, 130.

Hu, Z., Richter, H., Sparovek, G., Schnug, E., 2004. Physiological and biochemical effects of rare earth elements on plants and their agricultural significance: A review. J. Plant Nutr. 27, 183–220. https://doi.org/10.1081/PLN-120027555

Hua, D., Wang, J., Yu, D., Liu, J., 2017. Lanthanum exerts acute toxicity and histopathological changes in gill and liver tissue of rare minnow (*Gobiocypris rarus*). Ecotoxicology 26, 1207–1215. https://doi.org/10.1007/s10646-017-1846-8

Huang, P., Li, J., Zhang, S., Chen, C., Han, Y., Liu, N., Xiao, Y., Wang, H., Zhang, M., Yu, Q., Liu, Y., Wang, W., 2011. Effects of lanthanum, cerium, and neodymium on the nuclei and mitochondria of hepatocytes: Accumulation and oxidative damage. Environ. Toxicol. Pharmacol. 31, 25–32. https://doi.org/10.1016/j.etap.2010.09.001

Humphries, M., 2013. Rare Earth Elements: The Global Supply Chain.

ISO 10229, 1994. Water quality - Determination of the prolonged toxicity of substances to freshwater fish - Method for evaluating the effects of substances on the growth rate of rainbow trout *Oncorhynchus mykiss*. Cei.

ISO 10706, 2000. Qualité de l'eau - Détermination de la toxicité à long terme de substances vis-à-vis de *Daphnia magna Straus* (Cladocera, Crustacea).

Jakubek, L.M., Marangoudakis, S., Raingo, J., Liu, X., Lipscombe, D., Hurt, R.H., 2009. The inhibition of neuronal calcium ion channels by trace levels of yttrium released from carbon nanotubes. Biomaterials 30, 6351–6357. https://doi.org/10.1016/j.biomaterials.2009.08.009

Jezierska, B., Witeska, M., 2001. Metal toxicity to fish 69. https://doi.org/10.1007/978-1-4020-4728-2

Jordens, A., Cheng, Y.P., Waters, K.E., 2013. A review of the beneficiation of rare earth element bearing minerals. Miner. Eng. 41, 97–114. https://doi.org/10.1016/j.mineng.2012.10.017

Kamunde, C., 2009. Early subcellular partitioning of cadmium in gill and liver of rainbow trout (*Oncorhynchus mykiss*) following low-to-near-lethal waterborne cadmium exposure. Aquat. Toxicol. 91, 291–301. https://doi.org/10.1016/j.aquatox.2008.10.013

Kamunde, C., MacPhail, R., 2008. Bioaccumulation and hepatic speciation of copper in rainbow trout (*Oncorhynchus mykiss*) during chronic waterborne copper exposure. Arch. Environ. Contam. Toxicol. 54, 493–503. https://doi.org/10.1007/s00244-007-9046-9

Kawagoe, M., Hirasawa, F., Shou, C.W., Liu, Y., Ueno, Y., Sugiyama, T., 2005. Orally administrated rare earth element cerium induces metallothionein synthesis and increases glutathione in the mouse liver. Life Sci. 77, 922–937. https://doi.org/10.1016/j.lfs.2005.02.004

Khan, F.R., Bury, N.R., Hogstrand, C., 2010. Cadmium bound to metal rich granules and exoskeleton from *Gammarus pulex* causes increased gut lipid peroxidation in zebrafish

following single dietary exposure. Aquat. Toxicol. 96, 124–129. https://doi.org/10.1016/j.aquatox.2009.10.010

Korotkov, S.M., Sobol', K. V., Shemarova, I. V., Furaev, V. V., Nesterov, V.P., 2016. Comparative study of Y^{3+} effect on calcium-dependent processes in frog cardiac muscle and mitochondria of rat cardiomyocytes. J. Evol. Biochem. Physiol. 52, 196–203. https://doi.org/10.1134/S0022093016030029

Kulaksiz, S., Bau, M., 2011. Anthropogenic gadolinium as a microcontaminant in tap water used as drinking water in urban areas and megacities. Appl. Geochemistry 26, 1877–1885. https://doi.org/10.1016/j.apgeochem.2011.06.011

Kulaksız, S., Bau, M., 2011. Rare earth elements in the Rhine River, Germany: first case of anthropogenic lanthanum as a dissolved microcontaminant in the hydrosphere. Environ. Int. 37, 973–9. https://doi.org/10.1016/j.envint.2011.02.018

Langston, W.J., Bebianno, M.J., Burt, G.R., 1998. Metal handling strategies in molluscs, in: Springer (Ed.), Metal Metabolism in Aquatic Envrionments. Boston, MA, pp. 219–283.

Lapointe, D., Gentes, S., Ponton, D.E., Hare, L., Couture, P., 2009. Influence of prey type on nickel and thallium assimilation, subcellular distribution and effects in juvenile fathead minnows (*Pimephales promelas*). Environ. Sci. Technol. 43, 8665–8670. https://doi.org/10.1021/es901929m

Lavoie, M., Bernier, J., Fortin, C., Campbell, P.G.C., 2009. Cell homogenization and subcellular fractionation in two phytoplanktonic algae: implications for the assessment of metal subcellular distributions. Limnol. Oceanogr.: Methods. 7, 277–286.

Leonard, E.M., Banerjee, U., D'Silva, J.J., Wood, C.M., 2014. Chronic nickel bioaccumulation and sub-cellular fractionation in two freshwater teleosts, the round goby and the rainbow trout, exposed simultaneously to waterborne and dietborne nickel. Aquat. Toxicol. 154, 141–153. https://doi.org/10.1016/j.aquatox.2014.04.028

Li, X., Chen, Z., Chen, Z., Zhang, Y., 2013. A human health risk assessment of rare earth elements in soil and vegetables from a mining area in Fujian Province, Southeast

China. Chemosphere 93, 1240–1246. https://doi.org/10.1016/j.chemosphere.2013.06.085

Liang, T., Li, K., Wang, L., 2014. State of rare earth elements in different environmental components in mining areas of China 1499–1513. https://doi.org/10.1007/s10661-013-3469-8

Lide, D.R., 2003. CRC Handbook of Chemistry and Physics. CRC Handb. Chem. Phys. 1264–1266. https://doi.org/10.1021/ja906434c

Lilley, R.M., Stitt, M., Mader, G., Heldt, H.W., 1982. Rapid fractionation of wheat leaf protoplasts using membrane filtration. Plant. Physiol. 70, 965–970.

Lin, J.T., Griffith, O.M., Corse, J.W., 1985. Subcellular fractionation of wheat leaf protoplasts by centrifugal elutriation. Anal. Biochem. 148, 10–14. https://doi.org/10.1016/0003-2697(85)90621-9

Liu, X.-J., Ni, I., Wang, W.-X., 2002. Trophic transfer of heavy metals from freshwater zooplankton *Daphnia magna* to zebrafish *Danio rerio*. Water Res. 36, 4563–4569.

Liu, X., Byrne, R.H., 1997. Rare earth and yttrium phosphate solubilities in aqueous solution. Geochim. Cosmochim. Acta 61, 1625–1633. https://doi.org/10.1016/S0016-7037(97)00037-9

Lobinger, P., Jarzina, H., Roesky, H.W., Singh, S., Kumar, S.S., Schmidt, H.G., Noltemeyer, M., Freyhardt, H.C., 2005. New synthetic approach to yttrium hydroxoacetates, structural characterization, and use as a precursor for coated conductors. Inorg. Chem. 44, 9192–9196. https://doi.org/10.1021/ic0505192

Lürling, M., Tolman, Y., 2010. Effects of lanthanum and lanthanum-modified clay on growth, survival and reproduction of *Daphnia magna*. Water Res. 44, 309–19. https://doi.org/10.1016/j.watres.2009.09.034

Ma, L., Dang, D.H., Wang, W., Evans, R.D., Wang, W.-X., 2018. Rare earth elements in the Pearl River Delta of China: Potential impacts of the REE industry on water, suspended particles and oysters. Environ. Pollut. https://doi.org/10.1016/j.envpol.2018.10.015

Ma, Y., Wang, J., Peng, C., Ding, Y., He, X., Zhang, P., Li, N., Lan, T., Wang, D., Zhang, Z., Sun, F., Liao, H., Zhang, Z., 2016. Toxicity of cerium and thorium on *Daphnia magna*. Ecotoxicol. Environ. Saf. 134, 226–232. https://doi.org/10.1016/j.ecoenv.2016.09.006

MacMillan, G.A., Chételat, J., Heath, J.P., Mickpegak, R., Amyot, M., 2017. Rare earth elements in freshwater, marine, and terrestrial ecosystems in the eastern Canadian Arctic. Environ. Sci. Process. Impacts 19, 1336–1345. https://doi.org/10.1039/C7EM00082K

Magnusson, G., 1963. The behavior of certain lanthanons in rats. Acta Pharmacol. Toxicol.. 2, 533–557.

Manunta, M., Izzo, L., Duncan, R., Jones, A.T., 2007. Establishment of subcellular fractionation techniques to monitor the intracellular fate of polymer therapeutics II. Identification of endosomal and lysosomal compartments in HepG2 cells combining single-step subcellular fractionation with fluorescent imag. J. Drug Target. 151, 37–50.

Marigómez, I., Soto, M., Cajaraville, M.P., Angulo, E., Giamberini, L., 2002. Cellular and subcellular distribution of metals in molluscs. Microsc. Res. Tech. 56, 358–392. https://doi.org/10.1002/jemt.10040

Marshall, W.S., 2002. Na^+, Cl^-, $Ca^{2+}$and Zn^{2+}transport by fish gills: Retrospective review and prospective synthesis. J. Exp. Zool. 293, 264–283. https://doi.org/10.1002/jez.10127

Martin, P., Wang, P., Robinson, A., Poole, L., Dragone, J., Smyth, M., Pratt, R., 2011. Comparison of dietary phosphate absorption after single doses of lanthanum carbonate and sevelamer carbonate in healthy volunteers: a balance study. Am. J. Kidney Dis. 57, 700–6. https://doi.org/10.1053/j.ajkd.2010.11.028

Mason, A.Z., Jenkins, K.D., 1995. Metal detoxification in aquatic organisms. Met. Speciat. Bioavailab. Aquat. Syst. 3, 479–578.

Mason, A.Z., Nott, J.A., 1981. The role of intracellular biomineralized granules in the regulation and detoxification of metals in gastropods with special reference to the marine prosobranch Littorina littorea. Aquat. Toxicol. 1, 239–256.

Massari, S., Ruberti, M., 2013. Rare earth elements as critical raw materials: Focus on international markets and future strategies. Resour. Policy 38, 36–43. https://doi.org/10.1016/j.resourpol.2012.07.001

Mayfield, D.B., Fairbrother, A., 2015. Chemosphere Examination of rare earth element concentration patterns in freshwater fish tissues. Chemosphere 120, 68–74. https://doi.org/10.1016/j.chemosphere.2014.06.010

McGeer, J.C., Brix, K. V., Skeaff, J.M., DeForest, D.K., Brigham, S.I., Adams, W.J., Green, A., 2003. Inverse Relationship Between Bioconcentration Factor and Exposure Concentration for Metals: Implications for Hazard Assessment of Metals in the Aquatic Environment. Environ. Toxicol. Chem. 22, 1017–1037.

MDDEFP, 2013. Critères de qualité de l'eau de surface, 3e édition. ed. ISBN 978-2-550-68533-3.

MDDELCC, 2016. Guide de caractérisation physico-chimique et toxicologique des sédiments.

MENVIQ, 1990b. Méthodologie de calcul des critères de qualité de l'eau pour les substances toxiques. Ministère de l'Environnement, Québec.

Merschel, G., Bau, M., 2015. Rare earth elements in the aragonitic shell of freshwater mussel Corbicula fluminea and the bioavailability of anthropogenic lanthanum, samarium and gadolinium in river water. Sci. Total Environ. 533, 91–101. https://doi.org/10.1016/j.scitotenv.2015.06.042

Misra, S., Peak, D., Chen, N., Hamilton, C., Niyogi, S., 2012. Tissue-specific accumulation and speciation of selenium in rainbow trout (*Oncorhynchus mykiss*) exposed to elevated dietary selenomethionine. Comp. Biochem. Physiol. - part C 155, 560–565. https://doi.org/10.1016/j.cbpc.2012.01.005

Morrison, W.M., Tang, R., 2012. China's rare earth industry and export regime: economic and trade implications for the United States.

Nassiri, Y., Rainbow, P.S., Amiard-Triquet, C., Rainglet, F., Smith, B.D., 2000. Trace-metal detoxification in the ventral caeca of *Orchestia gammarellus* (Crustacea: Amphipoda). Mar. Biol. 136, 477–484.

NF XP T90-339-1, 2004. Détermination de la toxicité des sédiments d'eau douce vis-à-vis de *Chironomus riparius*. Québec.

Ng, T., Smith, S., 2011. Review of aquatic effects of lanthanides and other uncommon elements. EC Contribution Agreement with the CNTC for 2010/2011.

Ng, T.Y.T., Pais, N.M., Wood, C.M., 2011. Mechanisms of waterborne Cu toxicity to the pond snail *Lymnaea stagnalis*: Physiology and Cu bioavailability. Ecotoxicol. Environ. Saf. 74, 1471–1479. https://doi.org/10.1016/j.ecoenv.2011.03.010

Ng, T.Y.T., Wood, C.M., 2008. Trophic transfer and dietary toxicity of Cd from the oligochaete to the rainbow trout. Aquat. Toxicol. 87, 47–59. https://doi.org/10.1016/j.aquatox.2008.01.003

Ni, I.H., Wang, W.-X., Tam, Y.K., 2000. Transfer of Cd, Cr and Zn from zooplankton prey to mudskipper *Periophthalmus cantonensis* and glassy Ambassis urotaenia fishes. Mar. Ecol. Prog. Ser. 194, 203–210. https://doi.org/10.3354/meps194203

NICNAS, 2001. Lanthanum Modified Clay report No:NA/899, 28 p.

Nieboer, E., Richardson, D.H.S., 1980. The replacement of the nondescript term "heavy metals" by a biologically and chemically significant classification of metal ions. Environ. Pollution. Ser. B, Chem. Phys. 1, 3–26. https://doi.org/10.1016/0143-148X(80)90017-8

Økelsrud, A., Lydersen, E., Fjeld, E., 2016. Biomagnification of mercury and selenium in two lakes in southern Norway. Sci. Total Environ. 566–567, 596–607. https://doi.org/10.1016/j.scitotenv.2016.05.109

Pan, K., Wang, W.X., 2009. Biodynamics to explain the difference of copper body concentrations in five marine bivalve species. Environ. Sci. Technol. 43, 2137–2143. https://doi.org/10.1021/es802888u

Paulick, H., Machacek, E., 2017. The global rare earth element exploration boom: An analysis of resources outside of China and discussion of development perspectives. Resour. Policy 52, 134–153. https://doi.org/10.1016/j.resourpol.2017.02.002

Penen, F., Isaure, M.P., Dobritzsch, D., Bertalan, I., Castillo-Michel, H., Proux, O., Gontier, E., Le Coustumer, P., Schaumlöffel, D., 2017. Pools of cadmium in *Chlamydomonas reinhardtii* revealed by chemical imaging and XAS spectroscopy. Metallomics 9, 910–923. https://doi.org/10.1039/c7mt00029d

Penen, F., Malherbe, J., Isaure, M.P., Dobritzsch, D., Bertalan, I., Gontier, E., Le Coustumer, P., Schaumlöffel, D., 2016. Chemical bioimaging for the subcellular localization of trace elements by high contrast TEM, TEM/X-EDS, and NanoSIMS. J. Trace Elem. Med. Biol. 37, 62–68. https://doi.org/10.1016/j.jtemb.2016.04.014

Perceval, O., Couillard, Y., Pinel-Alloul, B., Campbell, P.G.C., 2006. Linking changes in subcellular cadmium distribution to growth and mortality rates in transplanted freshwater bivalves (*Pyganodon grandis*). Aquat. Toxicol. 79, 87–98.

Pillai, C.K.S., Paul, W., Sharma, C.P., 2009. Chitin and chitosan polymers: Chemistry, solubility and fiber formation. Prog. Polym. Sci. 34, 641–678. https://doi.org/10.1016/j.progpolymsci.2009.04.001

Podgurskaya, O. V., Kavun, V.Y., 2006. Cadmium concentration and subcellular distribution in organs of the mussel *Crenomytilus grayanus* from upwelling regions of Okhotsk Sea and Sea of Japan. Arch. Environ. Contam. Toxicol. 51, 567–572. https://doi.org/10.1007/s00244-005-0151-3

Pouil, S., Warnau, M., Oberhänsli, F., Teyssié, J., Bustamante, P., Metian, M., 2016. Influence of food on the assimilation of essential elements (Co, Mn, and Zn) by turbot *Scophthalmus maximus*. Mar. Ecol. Prog. Ser. 550, 207–218. https://doi.org/10.3354/meps11716

Pouil, S., Warnau, M., Oberhänsli, F., Teyssié, J.L., Metian, M., 2015. Trophic transfer of ^{110}mAg in the turbot *Scophthalmus maximus* through natural prey and compounded feed. J. Environ. Radioact. 150, 189–194. https://doi.org/10.1016/j.jenvrad.2015.08.016

Poynton, H.C., Wintz, H., Vulpe, C.D., 2008. Progress in ecotoxicogenomics for environmental monitoring, mode of action, and toxicant identification. Adv. Exp. Biol. 2, 21–323. https://doi.org/10.1016/S1872-2423(08)00002-1

Qiang, T., Xiao-rong, W., Li-qing, T., Le-mei, D., 1994. Bioaccumulation of the rare earth elements lanthanum, gadolinium and yttrium in carp (*Cyprinus carpio*). Environ. Pollut. 85, 345–350. https://doi.org/10.1016/0269-7491(94)90057-4

Racine, K., 2016. Étude de la répartition subcellulaire des éléments du groupe platine et des terres rares chez l'algue verte *Chlamydomonas reinhardtii*. Université du Québec, Institut national de la recherche scientifique.

Rainbow, P.S., Amiard, J.C., Amiard-Triquet, C., Cheung, M.S., Zhang, L., Zhong, H., Wang, W.-X., 2007. Trophic transfer of trace metals: Subcellular compartmentalization in bivalve prey, assimilation by a gastropod predator and in vitro digestion simulations. Mar. Ecol. Prog. Ser. 348, 128–138. https://doi.org/10.3354/meps07086

Rainbow, P.S., Liu, F., Wang, W.-X., 2015. Metal accumulation and toxicity: The critical accumulated concentration of metabolically available zinc in an oyster model. Aquat. Toxicol. 162, 102–108. https://doi.org/10.1016/j.aquatox.2015.03.007

Rainbow, P.S., Luoma, S.N., Wang, W.-X., 2011. Trophically available metal - A variable feast. Environ. Pollut. 159, 2347–2349. https://doi.org/10.1016/j.envpol.2011.06.040

Rainbow, P.S., Smith, B.D., 2010. Trophic transfer of trace metals: Subcellular compartmentalisation in bivalve prey and comparative assimilation efficiencies of two invertebrate predators. J. Exp. Mar. Bio. Ecol. 390, 143–148. https://doi.org/10.1016/j.jembe.2010.05.002

Redling, K., 2006. Rare earth elements in agriculture with emphasis on animal husbandry. Institut für Physiologie, Physiologische Chemie und Tierernährung der Ludwig-Maximilians-Universität München

Ricciardi, A., Bourget, E., 1998. Weight-to-weight conversion factors for marine benthic macroinvertebrates. Mar. Ecol. Prog. Ser. 163, 245–251. https://doi.org/10.3354/Meps163245

Romero-Freire, A., Minguez, L., Pelletier, M., Cayer, A., Caillet, C., Devin, S., Gross, E.M., Guérold, F., Pain-Devin, S., Vignati, D.A.L., Giamberini, L., 2018. Assessment of baseline ecotoxicity of sediments from a prospective mining area enriched in light rare

earth elements. Sci. Total Environ. 612, 831–839. https://doi.org/10.1016/j.scitotenv.2017.08.128

Rosabal, M., Hare, L., Campbell, P.G.C., 2014. Assessment of a subcellular metal partitioning protocol for aquatic invertebrates: preservation, homogenization, and subcellular fractionation. Limnol. Oceanogr. Methods 12, 507–518. https://doi.org/10.4319/lom.2014.12.507

Rosabal, M., Hare, L., Campbell, P.G.C., 2012. Subcellular metal partitioning in larvae of the insect Chaoborus collected along an environmental metal exposure gradient (Cd, Cu, Ni and Zn). Aquat. Toxicol. 120–121, 67–78. https://doi.org/10.1016/j.aquatox.2012.05.001

Rosabal, M., Pierron, F., Couture, P., Baudrimont, M., Hare, L., Campbell, P.G.C., 2015. Subcellular partitioning of non-essential trace metals (Ag, As, Cd, Ni, Pb, and Tl) in livers of American (*Anguilla rostrata*) and European (*Anguilla anguilla*) yellow eels. Aquat. Toxicol. 160, 128–141. https://doi.org/10.1016/j.aquatox.2015.01.011

Rosenkrantz, M., Alam, T., Kim, K.S., Clark, B.J., Srere, P.A., Guarente, L.P., 1986. Mitochondrial and nonmitochondrial citrate synthases in *Saccharomyces cerevisiae* are encoded by distinct homologous genes. Mol. Cell. Biol 612, 4509–4515.

Sánchez-Marín, P., Beiras, R., 2017. Subcellular distribution and trophic transfer of Pb from bivalves to the common prawn *Palaemon serratus*. Ecotoxicol. Environ. Saf. 138, 253–259. https://doi.org/10.1016/j.ecoenv.2017.01.003

Sanders, L.M., Luiz-Silva, W., Machado, W., Sanders, C.J., Marotta, H., Enrich-Prast, A., Bosco-Santos, A., Boden, A., Silva-Filho, E. V., Santos, I.R., Patchineelam, S.R., 2013. Rare earth element and radionuclide distribution in surface sediments along an estuarine system affected by fertilizer industry contamination. Water. Air. Soil Pollut. 224. https://doi.org/10.1007/s11270-013-1742-7

Sappal, R., Burka, J., Dawson, S., Kamunde, C., 2009. Bioaccumulation and subcellular partitioning of zinc in rainbow trout (*Oncorhynchus mykiss*): Cross-talk between waterborne and dietary uptake. Aquat. Toxicol. 91, 281–290. https://doi.org/10.1016/j.aquatox.2008.10.007

Schaller, J., 2013. Invertebrate shredder as a factor controlling the fixation potential for metals/metalloids in organic matter during decay. Ecol. Eng. 53, 200–204.

Schulze, R., Buchert, M., 2016. Estimates of global REE recycling potentials from NdFeB magnet material. Resour. Conserv. Recycl. 113, 12–27. https://doi.org/10.1016/j.resconrec.2016.05.004

Seebaugh, D.R., Estephan, A., Wallace, W.G., 2006. Relationship between dietary cadmium absorption by grass shrimp (*Palaemonetes pugio*) and trophically available cadmium in amphipod (*Gammarus lawrencianus*) prey. Bull. Environ. Contam. Toxicol. 76, 16–23. https://doi.org/10.1007/s00128-005-0884-8

Seebaugh, D.R., Wallace, W.G., 2009. Assimilation and subcellular partitioning of elements by grass shrimp collected along an impact gradient. Aquat. Toxicol. 93, 107–115. https://doi.org/10.1016/j.aquatox.2009.04.010

Seib, P.F., Jones, A.T., Duncan, R., 2006. Establishment of subcellular fractionation techniques to monitor the intracellular fate of polymer therapeutics I. Differential centrifugation fractionation B16F10 cells and use to study the intracellular fate of HPMA copolymer–doxorubicin. J. Drug Target. 146, 375–390.

Simon, O., Camilleri, V., Grasset, G., Garnier-Laplace, J., 2005. Subcellular fraction associated to radionuclide analysis in various tissues: Validation of the technique by using light and electron observations applied on bivalves and uranium. Radioprotection 40S1, S199–S204.

Sneller, F.E.., Kalf, D.., Weltje, L., Van Wezel, A.., 2000. Maximum Permissible Concentrations and Negligible Concentrations for Rare Earth Elements (REEs). RIVM report 601, 66 p.

Stauber, J.L., 2000. Toxicity Testing of Modified Clay Leachates Using Freshwater. CSIRO Cent. Adv. Anal. Chem. Energy Technol. Report No.

Steen Redeker, E., van Campenhout, K., Bervoets, L., Reijnders, H., Blust, R., 2007. Subcellular distribution of Cd in the aquatic oligochaete *Tubifex tubifex*, implications

for trophic availability and toxicity. Environ. Pollut. 148, 166–175. https://doi.org/10.1016/j.envpol.2006.10.031

Subotic, S., Spasić, S., Visnjić-Jeftić, Z., Hegedis, A., Krpo-ćetković, J., Mićković, B., Skorić, S., Lenhardt, M., 2014. Heavy metal and trace element bioaccumulation in target tissues of four edible predatory fish species from Bovan Reservoir (Serbia). Ecotoxicol. Environ. Saf. 23, 1884–1891. https://doi.org/10.1016/j.ecoenv.2013.08.020

Tai, P., Zhao, Q., Su, D., Li, P., Stagnitti, F., 2010. Biological toxicity of lanthanide elements on algae. Chemosphere 80, 1031–5. https://doi.org/10.1016/j.chemosphere.2010.05.030

Tang, J., Johannesson, K.H., 2003. Speciation of rare earth elements in natural terrestrial waters: Assessing the role of dissolved organic matter from the modeling approach. Geochim. Cosmochim. Acta 67, 2321–2339. https://doi.org/10.1016/S0016-7037(02)01413-8

Taylor, A.M., Maher, W.A., 2012. Exposure-dose-response of *Anadara trapezia* to metal contaminated estuarine sediments. 1. Cadmium spiked sediments. Aquat. Toxicol. 109, 234–242. https://doi.org/10.1016/j.aquatox.2011.09.014

Thacker, P. a, 2013. Alternatives to antibiotics as growth promoters for use in swine production: a review. J. Anim. Sci. Biotechnol. 4, 35. https://doi.org/10.1186/2049-1891-4-35

United States Environmental Protection Agency, 2002. Short-term Methods for Estimating the Chronic Toxicity of Effluents and Receiving Waters to Freshwater Organisms Fourth Edition October 2002 1–350. https://doi.org/http://www.dep.state.fl.us/water/wastewater/docs/ctf.pdf

Van Campenhout, K., Bervoets, L., Redeker, E.S., Blust, R., 2009. A kinetic model for the relative contribution of waterborne and dietary cadmium and zinc in the common carp (*Cyprinus carpio*). Environ. Toxicol. Chem. 28, 209–219. https://doi.org/10.1897/08-136.1

Vukov, O., Smith, D.S., McGeer, J.C., 2016. Acute dysprosium toxicity to *Daphnia pulex* and *Hyalella azteca* and development of the biotic ligand approach. Aquat. Toxicol. 170, 142–151. https://doi.org/10.1016/j.aquatox.2015.10.016

Wadige, C.P.M., Taylor, A.M., Maher, W.A., Krikowa, F., 2014. Bioavailability and toxicity of zinc from contaminated freshwater sediments: linking exposure-dose–response relationships of the freshwater bivalve *Hyridella australis* to zinc-spiked sediments. Aquat. Toxicol. 156, 179–190.

Wallace, W.G., Lee, B.G., Luoma, S.N., 2003. Subcellular compartmentalization of Cd and Zn in two bivalves. I. Significance of metal-sensitive fractions (MSF) and biologically detoxified metal (BDM). Mar. Ecol. Prog. Ser. 249, 183–197. https://doi.org/10.3354/meps257125

Wallace, W.G., Lopez, G.R., 1996. Relationship between subcellular cadmium distribution in prey and cadmium trophic transfer to a predator. Estuaries 19, 923–930. https://doi.org/10.2307/1352308

Wallace, W.G., Luoma, S.N., 2003. Subcellular compartmentalization of Cd and Zn in two bivalves. II. Significance of trophically available metal (TAM). Mar. Ecol. Prog. Ser. 257, 125–137. https://doi.org/10.3354/meps257125

Wang, M.-J., Wang, W.-X., 2009. Cadmium in three marine phytoplankton: Accumulation, subcellular fate and thiol induction. Aquat. Toxicol. 95, 99–107. https://doi.org/10.1016/j.aquatox.2009.08.006

Wang, W.-X., Guan, R., 2010. Subcellular distribution of zinc in *Daphnia magna* and implication for toxicity. Environ. Toxicol. Chem. 29, 1841–1848. https://doi.org/10.1002/etc.229

Wang, W.-X., Qiu, J.W., Qian, P.Y., 1999. The trophic transfer of Cd, Cr, and Se in the barnacle *Balanus amphitrite* from planktonic food. Mar. Ecol. Prog. Ser. 187, 191–201. https://doi.org/10.3354/meps187191

Watson-leung, T., 2009. Phoslock TM Toxicity Testing with Three Sediment Dwelling Organisms (*Hyalella azteca*, *Hexagenia spp* . and *Chironomus dilutus*) and Two Water

Column Dwelling Organisms (Rainbow Trout and *Daphnia magna*). Technical Memorandum.

Weltje, L., 2002. Bioavailability of lanthanides to freshwater organisms: speciation, accumulation and toxicity, Delft Univ. ed. Delft university Press, Delft, The Netherlands.

Weltje, L., Heidenreich, H., Zhu, W., Wolterbeek, H.T., Korhammer, S., Goeij, J.J.M., Markert, B., 2002. Lanthanide concentrations in freshwater plants and molluscs, related to those in surface water, pore water and sediment. A case study in The Netherlands. Sci. Total Environ. 286, 191–214. https://doi.org/10.1016/S0048-9697(01)00978-0

Xie, F., Zhang, T.A., Dreisinger, D., Doyle, F., 2014. A critical review on solvent extraction of rare earths from aqueous solutions. Miner. Eng. 56, 10–28. https://doi.org/10.1016/j.mineng.2013.10.021

Xu, Y., Wang, W.-X., 2002. Exposure and potential food chain transfer factor of Cd, Se and Zn in marine fish *Lutjanus argentimaculatus*. Mar. Ecol. Prog. Ser. 238, 173–186. https://doi.org/10.3354/meps238173

Yang, L., Wang, X., Nie, H., Shao, L., Wang, G., Liu, Y., 2016. Residual levels of rare earth elements in freshwater and marine fish and their health risk assessment from Shandong, China. Mar. Pollut. Bull. 107, 393–397. https://doi.org/10.1016/j.marpolbul.2016.03.034

Yang, X., Yin, D., Sun, H., Wang, X., Dai, L., Chen, Y., Cao, M., 1999. Distribution and bioavailability of rare earth elements in aquatic microcosm. Chemosphere 39, 2443–2450.

Yang, X., Yin, D., Sun, H., Wang, X., Dai, L., Chen, Y., Cao, M., 1999. Distribution and Bioavailability of Rare Earth Elements. Chemosphere 39, 2443–2450. https://doi.org/10.1016/S0045-6535(99)00172-1

Yu, R., Wang, W., 2002. Trace metal assimilation and release budget in *Daphnia magna*. Limnol. Oceanogr. 47, 495–504. https://doi.org/10.4319/lo.2002.47.2.0495

Zhang, L., Campbell, L.M., Johnson, T.B., 2012. Seasonal variation in mercury and food web biomagnification in Lake Ontario, Canada. Environ. Pollut. 161, 178–184. https://doi.org/10.1016/j.envpol.2011.10.023

Zhang, L., Wang, W.-X., 2006. Significance of subcellular metal distribution in prey in influencing the trophic transfer of metals in a marine fish. Limnol. Oceanogr. 51, 2008–2017. https://doi.org/10.4319/lo.2006.51.5.2008

Zhang, W., Huang, L., Wang, W.X., 2011. Arsenic bioaccumulation in a marine juvenile fish *Terapon jarbua*. Aquat. Toxicol. 105, 582–588. https://doi.org/10.1016/j.aquatox.2011.08.